



# Primary structures materials Models for fire behavior

A. Palacios, R Tejerina (Airbus D&S), V. Biasi, G. Leplat (ONERA),  
M.L. Rodriguez (Embraer)

Future Sky Safety is a Joint Research Programme (JRP) on Safety, initiated by EREA, the association of European Research Establishments in Aeronautics. The Programme contains two streams of activities: 1) coordination of the safety research programmes of the EREA institutes and 2) collaborative research projects on European safety priorities.

This deliverable is produced by the Project P7 “Mitigating Risks of Fire, Smoke and Fumes”, and aims at improving characterization capabilities and understanding with respect to the fire and high temperature behaviour of primary structure CFRP materials. Modelling results for the primary structures composite materials are presented in this report.

---

<b>Programme Manager</b>	Michel Piers, NLR
<b>Operations Manager</b>	Lennaert Speijker, NLR
<b>Project Manager (P7)</b>	Eric Deletombe , ONERA

---

<b>Grant Agreement No.</b>	640597
<b>Document Identification</b>	D7.9
<b>Status</b>	Approved
<b>Version</b>	2.1
<b>Classification</b>	Public

**Project:** Mitigating risks of fire, smoke and fumes  
**Reference ID:** FSS\_P7\_AD&S\_D7.9  
**Classification** Public  
:



This page is intentionally left blank

## Contributing partners

Company	Name
ONERA DMPE/HEAT	V. Biasi
ONERA DMPE/HEAT	G. Leplat
Embraer	Maria Luis Vieira Rodrigues
AIRBUS DS	Alejandro Palacios Madrid
AIRBUS DS	Rubén Tejerina Hernanz

## Document Change Log

Version No.	Issue Date	Remarks
1.0	22-12-2017	First formal release
2.0	30-12-2017	Second formal release
2.1	02-07-2018	Third formal release (some textual changes)

## Approval status

Prepared by: <i>(name)</i>	Company	Role	Date
A. Palacios, R Tejerina	Airbus DS	Structural Integrity	02-07-2018
Checked by: <i>(name)</i>	Company	Role	Date
J. Berthe	ONERA	Quality Assurance	02-07-2018
Approved by: <i>(name)</i>	Company	Role	Date
E. Deletombe	ONERA	Project Manager (P7)	11-07-2018
L.J.P. Speijker	NLR	Operations Manager	24-07-2018

## ACRONYMS

Acronym	Definition
A/C	Aircraft
AC	Advisory Circular
AMC	Acceptable Means of Compliance
ADS	Airbus Defence & Space
APU	Auxiliary Power Unit
BLADE	Banc Laser de cAractérisation et de DEgradation
CAD	Computer Aided Design
CFAST	Consolidated Model of Fire and Smoke Transport
CFD	Computational Fluid Dynamics
CFRP	Carbon Fibre Reinforced Plastics
Cp	Specific Heat Capacity
CS	Certification Specification
EREA	Association of European Research Establishments in Aeronautics
FAA	Federal Aviation Administration
FAR	Federal Aviation Regulations
FDS	Fluid Dynamics Simulator
FE, FEA	Finite Element, Finite Element Analysis
FFS	Future Sky Safety
GIC	Strain energy release rate or Inter-laminar fracture toughness
GICC	Critical strain energy release rate in sliding shear mode
HETVAL	Heat generation subroutine
IR	Infrared
ISO	International Organization for Standardization
JRP	Joint Research Programme
Kts	knots
MDO	Multidisciplinary Optimisation
MoDeTheC	Model for Thermal Degradation of Composites
NDT	Non destructive Testing
NIST	National Institutes of Standards and Technology

<b>NLR</b>	Netherlands Aerospace Centre
<b>NPA</b>	Notice of Proposed Amendment
<b>ONERA</b>	Office National d'Etudes et de Recherches Aéronautiques
<b>P7</b>	FSS Project n°7
<b>PhD</b>	Doctor of Philosophy
<b>RT</b>	Room Temperature
<b>Tg</b>	Glass Transition Temperature
<b>TGA</b>	ThermoGravimetric Analysis
<b>UD</b>	Uni-directional
<b>WP</b>	Work-Package

## EXECUTIVE SUMMARY

### Problem Area

There is a need to enhance knowledge concerning the fire behavior and performance of CFRP primary structure composite materials, in order to better predict safety and survivability issues in case of fire incident or post-crash situation. Such predictions rely on physical models and numerical tools which need to be developed based on exhaustive characterization material process and a components validation for experimental testing. A comprehensive experimental database for a reference material to be shared by the European research community as a basis for material model development of the fire behavior and degradation of CFRP materials needs to be created. There is a need for understanding, characterizing and predicting the fire behavior of primary structure composite materials (epoxy resins, standard Carbon Fiber Reinforced Polymer (CFRP)). In particular, the T700GC/M21 material could be investigated, because a lot of published results already exist about its standard mechanical behavior which can be built upon. This allows assessment of state-of-the-art models and simulation tools according to sets of experimental data.

### Description of Work

A relevant requirement for certification and safety is the fire behavior of carbon fiber composites in large airframe areas, both in primary and secondary structures: carbon fiber composites present a worse behavior than metallic counterparts mainly due to the vulnerability of the resin component of the composite. Indeed the mechanical properties of the Carbon Fiber material decreased in a very significant way at high temperature and under fire conditions the material has an almost complete loss of these properties. In addition the very complex physical and chemical behavior of the resin of the material on these fire conditions preclude the use of prediction tools to advance the final material conditions and properties without complex and expensive tests.

By the simplification of this complex physical and chemical behavior applied to the normalized standard fire tests some and by the precise characterization of the material thermal properties evolution a thermal or thermomechanical model is possible to be established. The expertise in this field is mainly focused on using the finite element method for a simplified model elaboration giving relevance to conductive, convective and mechanical effects and simplifying the flame effect. Alternate approximations could be also valid and a state of the art of the current methods available in literature is presented. A determinant point of any thermal or thermomechanical model is the definition of the variation of thermal and mechanical properties in all the range within this fire tests, from 0 to 1000°C, and the characterization of the material. Conclusions and recommendations to improve material and structure behaviour submitted to fire, select the best material candidate and reducing testing and design costs are provided.

### Results & Conclusions

Structural thermal requirements for primary and secondary structures based on EASA regulation are stated. A study of the current bibliographic state of the art of thermal and thermomechanical simulations is included. An approach for the simulation of thermal and chemical behavior of specific tests is proposed.

A simplified methodology for fire testing prediction is proposed. This methodology is applicable to the prediction of standard fire test on composite loaded panels. This methodology relies on:

- Simplified thermal boundary conditions:
  - Flame model, based on the repetitivity of thermal hot face map on a standard fire test.
  - Convection model based on constant heat transfer coefficient dependent on the cold face flow speed.
- A thermal characterization on an intact panel and a degraded panel.
- Simplified assumption of a direct relation between thermal and mechanical degradation
- Simplified failure criteria based in cold face temperature map evolution through test.
- Confirmation, by dedicated and especially monitored test, of the adequacy of these assumptions for a typical composite configuration in a typical load range.
- Thermal (only) transient problem resolution to establish the cold face temperature map evolution
- Determination of the failure instant based in the failure criteria defined.
- Thermomechanical problem resolution, with the same assumptions, to evaluate impact of secondary effects that may impact on the problem (large deformations with impact on thermal contact between elements)

The objective of thermo-mechanical modelling is to understand the response and performance of a physical system including the effects of heat transfer processes convection and radiation combined with the effects of the loads applied. The use of thermo-mechanical modelling in order to obtain a couple simulation of the real problem is a key factor to predict the behavior of the composite material submitted to fire under real conditions. The analysis simulation results can provide an estimation of the degradation state of the composite materials submitted to fire and other boundary conditions. Analysis of simulation results supports the designer to take decisions related to with aircraft fire wall with loads applied and to define geometries and configurations suitable from point of view of its behavior under generalized fire.

It is therefore recommended to:

- i. Implement the **model** into suitable simulation **platform software** to carry out the Coupled-Simulation.
- ii. Generate a Thermo-Mechanical model by means of finite element method representative of the behavior of materials submitted to applied loads, temperature and degradation.
- iii. Work out and analyze problems with interaction thermal and mechanical, initial thermally uncoupled followed by coupled.

Establish a systematic procedure to perform correlations of the model through results obtained in laboratory tests.

## Applicability

Primary (and secondary) structure in fire zone (determined by actual civil Aircraft normative [Ref1])

*This page is intentionally left blank*

## TABLE OF CONTENTS

Acronyms	3
Executive Summary	5
Table of Contents	8
List of Figures	9
List of Tables	14
<b>1 INTRODUCTION</b>	<b>15</b>
1.1. The Programme	15
1.2. Project context	15
1.3. Research objectives	15
1.4. Structure of the document	15
<b>2 REQUIREMENTS (ADS)</b>	<b>17</b>
2.1. Applicable regulation	17
2.2. Practical fire substantiation	17
2.2.1. Substantiation by flame test	18
2.2.2. Thermal Behaviour	19
2.2.3. Mechanical Behaviour	20
<b>3 SIMULATION tools TO PREDICT FIRE BEHAVIOUR AND STRUCTURAL EFFECTS</b>	<b>21</b>
3.1. Degradation Mechanisms and Flame Behavior Characterization	22
3.2. Flame and Heat	23
3.2.1. Thermomechanical Effects	24
3.2.2. Thermal Conductivity Effects	27
3.2.3. Morphology Changes	31
3.3. Simulation Approaches for Fire Modelling	32
3.3.1. Finite Elements Modelling	33
3.3.2. Computational Fluid Dynamics	37
3.3.3. Multidisciplinary MDO-like Approaches	41
<b>4 MODELLING AND SIMULATION OF THE THERMAL AND CHEMICAL BEHAVIOUR OF THE T700GC/M21 EXPOSED TO HIGH ENERGY LASER BEAM</b>	<b>43</b>
4.1. Introduction to the MoDeTheC solver	43
4.1.1. Homogenization laws of material properties	44
4.1.2. Chemical reactions	45
4.1.3. Conservation laws	46

4.1.4.	Numerical methods	46
4.2.	Thermo-chemical properties of homogenized T700GC/M21	47
4.2.1.	Kinetic model of decomposition reactions	47
4.2.2.	Thermo-physical properties	48
4.3.	MoDeTheC simulations of the BLADE facility	53
4.3.1.	Model definition of the BLADE facility	53
4.3.2.	Impinging flux at 53.7kW/m2	56
4.3.3.	Impinging flux at 76.2kW/m2	60
4.3.4.	Impinging flux at 101.2kW/m2	65
<b>5 PROCEDURE FOR THE SIMULATION OF COMPOSITES MATERIALS SUBMITTED TO FIRE AND HIGH TEMPERATURE (ADS):</b>		<b>72</b>
5.1.	General procedure definition to simulate simplified thermal, mechanical and coupled problems	72
5.2.	Procedure described in stages to obtain a simulation of thermomechanical problem of a composite material submitted to fire conditions	75
5.3.	General considerations	86
5.3.1.	Boundary conditions simulation	88
5.3.2.	Standard flame model	89
5.3.3.	Experimental forced convection correlations.	90
5.3.4.	Practical application: M21/T700G panel simulation submitted to fire.	90
5.4.	Thermal and Mechanical Model	91
5.4.1.	Coupled Model	93
5.4.2.	Coupled Model Inputs	96
5.4.3.	Coupled Model Results	97
5.4.4.	Failure Criterion Definition	99
5.5.	Future tasks	101
<b>6 CONCLUSIONS AND RECOMMENDATIONS</b>		<b>103</b>
6.1.	Conclusions	103
6.2.	Recommendations	104
<b>7 References</b>		<b>105</b>
<b>8 ANNEXES</b>		<b>108</b>
8.1.1.	Annex I: Standard FAR/CS25 requirements	108
8.1.2.	Annex II: Standard AC20-135 (FAA) requirements	110
8.1.3.	Annex III: ISO 2685	114

## LIST OF FIGURES

FIGURE 1 FIRE ZONES NACELLE AND HTP .....	17
FIGURE 2 FIRE ZONE: ENGINE NACELLE FAN COWL .....	18
FIGURE 3 FLAME TEST ON A HINGE FITTING .....	18
FIGURE 4 FIRE ZONE: AUXILIARY POWER UNIT COMPARTMENT .....	19
FIGURE 5 MECHANICAL PROPERTIES FOR SEVERAL COMPOSITE MATERIALS: RESIDUAL FLEXURAL STRENGTH AND EVOLUTION OF TENSILE STRENGTH [REF 14] .....	20
FIGURE 6 SCHEMATIC REPRESENTATION OF COMPOSITE STRUCTURE SCALES [REF 19] .....	21
FIGURE 7 EXAMPLE OF A COMBUSTION PROCESS AND SECONDARY PRODUCTS GENERATION. ....	22
FIGURE 8 KINETIC PARAMETERS FROM THE DECOMPOSITION OF A CFRP MATERIAL [4]. ....	25
FIGURE 9 GASES VOLUME FRACTION OBTAINED FROM DECOMPOSITION OF A CFRP MATERIAL (ABOVE) AND RESPECTIVE SPECIFIC HEAT CAPACITY THE GASES AS FUNCTION OF THE TEMPERATURE (BELOW) [REF 22] .....	25
FIGURE 10 REPRESENTATION OF CFRP DEGRADATION THROUGH REMAINING MASS TOGETHER WITH GAS CONCENTRATIONS EVOLUTION, ALONG TIME AND TEMPERATURE EVOLUTION [REF 23] .....	26
FIGURE 11 THERMAL CONDUCTIVITY DURING HEATING (LEFT) AND SPECIFIC HEAT AND HEAT OF DECOMPOSITION DURING HEATING (RIGHT) [4]. ....	27
FIGURE 12 THERMAL CONDUCTIVITY IN-PLANE (LEFT) AND THROUGH THICKNESS (RIGHT) [REF 22]. ....	28
FIGURE 13 TEMPERATURE PROFILE IN UD AND ISO CFRP THICKNESS AND REAR FACE [REF 23] .....	28
FIGURE 14 HEAT FLUX MAPPING ON A CFRP FACE FOR 116kW/M <sup>2</sup> (LEFT) AND 182kW/M <sup>2</sup> (RIGHT) [REF 23] .....	29
FIGURE 15 IMAGES OF THE COUPONS AFTER 420 S OF TEST DURATION AND THE CALCULATION OF THE DECOMPOSITION DEGREE IN 3D [REF 24] .....	29
FIGURE 16 THERMAL BOUNDARY (AND ELECTRICAL) CONDITIONS IMPOSED IN LIGHTNING STRIKE FE SIMULATIONS [REF 20] .....	30
FIGURE 17 CFRP THROUGH THICKNESS DECOMPOSITION ALONG TIME AND DEPTH [5]. ....	31
FIGURE 18 FIRE MODELING APPROACHES [7]. ....	32
FIGURE 19 EXAMPLE OF GAS DENSITY AND VELOCITY AFTER IGNITION – GAS DIFFUSION [REF 26] .....	38
FIGURE 20 EXAMPLE OF CALORIC CHAMBER AFTER COMBUSTION HAS INITIATED – HEAT TRANSFER (OR MASS LOSS) EVOLUTION DURING THE WHOLE COMBUSTION PROCESS [REF 26] .....	38
FIGURE 21 EXAMPLE OF GAS DENSITY AND VELOCITY AFTER IGNITION – GAS DIFFUSION [REF 26] .....	39
FIGURE 22 EXAMPLE OF COMBUSTION FLUID DYNAMICS AND TEMPERATURE PROFILES – COMBUSTION BETWEEN THE FLAME, RESIN AND RESIN DEGRADATION RESULTANT GASES [REF 26] .....	39
FIGURE 23 : SCHEME OF A REPRESENTATIVE ELEMENTARY VOLUME WITH MULTI-SPECIES COMPOSITION	43
FIGURE 24 - 3 REACTIONS THERMO-CHEMICAL MECHANISM OF T700GC/M21 .....	47
FIGURE 25 - RELATIVE MASS LOSS RECONSTRUCTION AT 2, 5 AND 10K/min IN AIR ATMOSPHERE USING A 3-STAGE-MODEL .....	48
FIGURE 26 – MASS LOSS RATE RECONSTRUCTION AT 2, 5 AND 10K/min IN AIR ATMOSPHERE USING A 3- STAGE-MODEL .....	48
FIGURE 27 - RECONSTRUCTION OF THERMAL CONDUCTIVITY IN MAIN CARTESIAN COORDINATES AND HEAT CAPACITY AS A FUNCTION OF TEMPERATURE OF THE T700GC/M21 UD IN THE VIRGIN STATE .....	49
FIGURE 28 - RECONSTRUCTION OF THERMAL CONDUCTIVITY IN MAIN CARTESIAN COORDINATES AND HEAT CAPACITY AS A FUNCTION OF TEMPERATURE OF THE T700GC/M21 UD IN THE CHARRED STATE.....	50
FIGURE 29 – RECONSTRUCTION OF THE THERMAL CONDUCTIVITY USING A MORI-TANAKA OPTIMIZATION AS A FUNCTION OF TEMPERATURE OF THE T700GC/M21 UD IN THE VIRGIN STATE .....	52

FIGURE 30 – RECONSTRUCTION OF THE THERMAL CONDUCTIVITY USING A MORI-TANAKA OPTIMIZATION AS A FUNCTION OF TEMPERATURE OF THE T700GC/M21 UD IN THE CHARRED STATE.....52  
 FIGURE 31 – RECONSTRUCTION OF THE THERMAL CONDUCTIVITY USING A MORI-TANAKA OPTIMIZATION AS A FUNCTION OF TEMPERATURE FOR EACH SOLID SPECIES.....53  
 FIGURE 32 - ILLUSTRATION OF THE BLADE FACILITY: SETUP AND INSTRUMENTATION .....54  
 FIGURE 33 - PRINCIPLE OF THE EXPERIMENTS: THERMAL CHARACTERIZATION AND LASER-INDUCED DECOMPOSITION OF CHARRING MATERIALS.....54  
 FIGURE 34 : MoDeTheC MODEL OF THE BLADE DOMAIN.....55  
 FIGURE 35 : 2D MESH OF THE BLADE CONFIGURATION.....55  
 FIGURE 36 - TEMPERATURE FIELDS AT DIFFERENT TIMES FROM THE T700GC/M21 ISO SIMULATION EXPOSED TO A 53.7 kW/m<sup>2</sup> LASER BEAM .....56  
 FIGURE 37 - TEMPERATURE EVOLUTION AT DIFFERENT POSITIONS ALONG THE FRONT SURFACE FROM THE T700GC/M21 ISO SIMULATION EXPOSED TO A 53.7 kW/m<sup>2</sup> LASER BEAM .....57  
 FIGURE 38 - TEMPERATURE EVOLUTION AT DIFFERENT POSITIONS ALONG THE BACK SURFACE FROM THE T700GC/M21 ISO SIMULATION EXPOSED TO A 53.7 kW/m<sup>2</sup> LASER BEAM AND COMPARED TO EXPERIMENTAL MEASUREMENTS.....57  
 FIGURE 39 – FINAL PYROLYSIS EVOLUTION FUNCTION FIELD OF THE T700GC/M21 ISO SIMULATION EXPOSED TO A 53.7 kW/m<sup>2</sup> LASER BEAM .....58  
 FIGURE 40 : – FINAL CHAR OXIDATION EVOLUTION FUNCTION FIELD OF THE T700GC/M21 ISO SIMULATION EXPOSED TO A 53.7 kW/m<sup>2</sup> LASER BEAM .....58  
 FIGURE 41 : INTERNAL PRESSURE FIELDS AT DIFFERENT MOMENTS FROM THE T700GC/M21 ISO SIMULATION EXPOSED TO A 53.7 kW/m<sup>2</sup> LASER BEAM .....59  
 FIGURE 42 : INTERNAL PRESSURE EVOLUTION AT DIFFERENT POSITIONS ALONG THE MID-PLANE FROM THE T700GC/M21 ISO SIMULATION EXPOSED TO A 53.7 kW/m<sup>2</sup> LASER BEAM .....60  
 FIGURE 43 - TEMPERATURE FIELDS AT DIFFERENT MOMENTS FROM THE T700GC/M21 ISO SIMULATION EXPOSED TO A 76.2kW/m<sup>2</sup> LASER BEAM .....61  
 FIGURE 44 - TEMPERATURE EVOLUTION AT DIFFERENT POSITIONS ALONG THE FRONT SURFACE FROM THE T700GC/M21 ISO SIMULATION EXPOSED TO A 76.2 kW/m<sup>2</sup> LASER BEAM .....62  
 FIGURE 45 - TEMPERATURE EVOLUTION AT DIFFERENT POSITIONS ALONG THE BACK SURFACE FROM THE T700GC/M21 ISO SIMULATION EXPOSED TO A 76.2 kW/m<sup>2</sup> LASER BEAM AND COMPARED TO EXPERIMENTAL MEASURES .....62  
 FIGURE 46 – FINAL PYROLYSIS EVOLUTION FUNCTION FIELD OF THE T700GC/M21 ISO SIMULATION EXPOSED TO A 76.2 kW/m<sup>2</sup> LASER BEAM .....63  
 FIGURE 47 : – FINAL CHAR OXIDATION EVOLUTION FUNCTION FIELD OF THE T700GC/M21 ISO SIMULATION EXPOSED TO A 76.2 kW/m<sup>2</sup> LASER BEAM .....63  
 FIGURE 48 : INTERNAL PRESSURE FIELDS AT DIFFERENT MOMENTS FROM THE T700GC/M21 ISO SIMULATION EXPOSED TO A 76.2 kW/m<sup>2</sup> LASER BEAM .....64  
 FIGURE 49 : INTERNAL PRESSURE EVOLUTION AT DIFFERENT POSITIONS ALONG THE MID-PLANE FROM THE T700GC/M21 ISO SIMULATION EXPOSED TO A 76.2 kW/m<sup>2</sup> LASER BEAM .....65  
 FIGURE 50 - TEMPERATURE FIELDS AT DIFFERENT MOMENTS FROM THE T700GC/M21 ISO SIMULATION EXPOSED TO A 101.2 kW/m<sup>2</sup> LASER BEAM .....66  
 FIGURE 51 - TEMPERATURE EVOLUTION AT DIFFERENT POSITIONS ALONG THE FRONT SURFACE FROM THE T700GC/M21 ISO SIMULATION EXPOSED TO A 101.2 kW/m<sup>2</sup> LASER BEAM .....67

FIGURE 52 - TEMPERATURE EVOLUTION AT DIFFERENT POSITIONS ALONG THE BACK SURFACE FROM THE T700GC/M21 ISO SIMULATION EXPOSED TO A 101.2 kW/m <sup>2</sup> LASER BEAM AND COMPARED TO EXPERIMENTAL MEASURES .....	67
FIGURE 53 – FINAL PYROLYSIS EVOLUTION FUNCTION FIELD OF THE T700GC/M21 ISO SIMULATION EXPOSED TO A 101.2 kW/m <sup>2</sup> LASER BEAM .....	68
FIGURE 54 : – FINAL CHAR OXIDATION EVOLUTION FUNCTION FIELD OF THE T700GC/M21 ISO SIMULATION EXPOSED TO A 101.2 kW/m <sup>2</sup> LASER BEAM .....	68
FIGURE 55 : RELATIVE MASS LOSS ALONG TIME OF THE T700GC/M21 ISO SIMULATION EXPOSED TO A 53.7 kW/m <sup>2</sup> LASER BEAM.....	69
FIGURE 56 : INTERNAL PRESSURE FIELDS AT DIFFERENT MOMENTS FROM THE T700GC/M21 ISO SIMULATION EXPOSED TO A 101.2 kW/m <sup>2</sup> LASER BEAM .....	70
FIGURE 57 : INTERNAL PRESSURE EVOLUTION AT DIFFERENT POSITIONS ALONG THE MID-PLANE FROM THE T700GC/M21 ISO SIMULATION EXPOSED TO A 101.2 kW/m <sup>2</sup> LASER BEAM .....	71
FIGURE 58 PROCESS SCHEME .....	74
FIGURE 59 FIRST STAGE OF THE SIMULATION PROCEDURE .....	75
FIGURE 60 TEMPERATURE DISTRIBUTION ON BOTH SIDES OF A COMPOSITE PANEL UNDER FIRE .....	77
FIGURE 61 FIRE TEST LAB .....	77
FIGURE 62 SECOND STAGE OF THE SIMULATION PROCEDURE .....	78
FIGURE 63 ADAPTED FLASH METHOD .....	78
FIGURE 64 THIRD STAGE OF THE SIMULATION PROCEDURE .....	79
FIGURE 65 DIFFERENT DEGRADATION AREAS.....	80
FIGURE 66 STANDARD ISO 2685 FLAME.....	80
FIGURE 67 FOURTH STAGE OF THE SIMULATION PROCEDURE.....	81
FFIGURE 68 HOT FACE MAP DUE TO FLAME HYPOTHESIS .....	81
FIGURE 69 FLAME POWER AND TEMPERATURE CONTROL AT CERTIFIED FIRE LABORATORY TEST .....	81
FFIGURE 70 THERMAL PROPERTIES.....	83
FIGURE 71 FIFTH STAGE OF THE SIMULATION PROCEDURE.....	84
FIGURE 72 TYPICAL FITTING-MONOLITHIC COMPOSITE HILOK JOINT IN COMPOSITE .....	84
FIGURE 73 SIMPLIFIED SPECIMEN CONFIGURATIONS FOR FIRE TEST .....	86
FIGURE 74 TYPICAL MESH SIZE ON A TEST PANEL.....	87
FIGURE 75 TYPICAL MESH SIZE ON A TEST PANEL: FITTING DETAIL.....	88
FIGURE 76 THROUGH THICKNESS TEMPERATURE DISTRIBUTION AT 36SEC FROM FLAME INITIATION (SIMULATION) .....	89
FIGURE 77 HOT FACE SIMULATION AT 5SEC FLAME INITIATION.....	89
FIGURE 78 CROSS SECTION TEMPERATURE DISTRIBUTION AT DIFFERENT TEST TIME (SIMULATION).....	91
FIGURE 79 DISPLACEMENT AT TEST TIME 1SEC (THERMOMECHANICAL SIMULATION) .....	93
FIGURE 80 DISPLACEMENT AT TEST TIME 1SEC (THERMOMECHANICAL SIMULATION) .....	93
FIGURE 81 HILOK MESH (THERMOMECHANICAL SIMULATION) .....	94
FIGURE 82 LOCAL COUNTERSUNK FASTENER COMPOSITE MESH (THERMOMECHANICAL SIMULATION).....	94
FIGURE 83 LOCAL COUNTERSUNK FASTENER COMPOSITE MESH (THERMOMECHANICAL SIMULATION).....	95
FIGURE 84 LOCAL COUNTERSUNK FASTENER COMPOSITE MESH (THERMOMECHANICAL SIMULATION).....	95
FIGURE 85 M21/T700G THERMAL PROPERTIES .....	96
FIGURE 86 M21/T700G PANEL DISPLACEMENTS (20 SEC FROM FLAME INIT) (THERMOMECHANICAL SIMULATION) .....	97



FIGURE 87 M21/T700G PANEL THERMAL MAP (20 SEC FROM FLAME INIT) (THERMOMECHANICAL SIMULATION) LOCAL TEMPERATURE PEAK AT COLD FACE .....98

FIGURE 88 M21/T700G PANEL DISPLACEMENT MAP (20 SEC FROM FLAME INIT) (THERMOMECHANICAL SIMULATION) .....98

FIGURE 89 M21/T700G PANEL VON MISSES STRESS MAP (20 SEC FROM FLAME INIT) (THERMOMECHANICAL SIMULATION) LOCAL TEMPERATURE PEAK AT COLD FACE. ....99

FIGURE 90 M21/T700G PANEL: TEMPERATURE DISTRIBUTION DETAIL (20 SEC FROM FLAME INIT) (THERMOMECHANICAL SIMULATION).....100

FIGURE 91 M21/T700G PANEL: TEMPERATURE DISTRIBUTION DETAIL (20 SEC FROM FLAME INIT) (THERMOMECHANICAL SIMULATION).....100

## LIST OF TABLES

TABLE 1 – ARRHENIUS PARAMETERS OF THE 3 REACTIONS THERMO-CHEMICAL MECHANISM OF T700GC/M21 .....	47
TABLE 2 - THERMO-PHYSICAL AND OPTICAL PROPERTIES OF THE T700GC/M21 UD IN THE VIRGIN STATE .....	49
TABLE 3 - THERMO-PHYSICAL AND OPTICAL PROPERTIES OF THE T700GC/M21 UD IN THE CHARRED STATE .....	49
TABLE 4 - THERMO-PHYSICAL AND OPTICAL PROPERTIES OF THE “CARBON FIBRES” SPECIES .....	50
TABLE 5 - THERMO-PHYSICAL AND OPTICAL PROPERTIES OF THE “EPOXY RESIN” SPECIES .....	50
TABLE 6 - THERMO-PHYSICAL AND OPTICAL PROPERTIES OF THE “CHAR” SPECIES .....	50

# 1 INTRODUCTION

## 1.1. The Programme

Horizon 2020 is the biggest EU Research and Innovation platform ever with nearly €80 billion of funding available over 7 years (2014 to 2020) – in addition to the private investment that this money will attract. Within this frame, EREA, the association of European Research Establishments in Aeronautics has proposed Future Sky program: a Joint Research Initiative in which development and integration of aviation technologies is taken to the European level. Future Sky is based on the alignment of national institutional research for aviation by setting up joint research programs: the first one to be launched in 2015 was the Future Sky Safety programme (<http://www.futuresky.eu/projects/safety>), because safety is a transverse domain of common interest to all stakeholders and with reduced competitive aspects. Four themes and seven projects (5 have already started) were identified (Runway Excursions, Total System Risk Assessment, Human Performance Envelope, Organizational Accidents, and Fire Smoke and Fumes). The work presented in this document belongs to the P7 project “Mitigating Risks of Fire, Smoke and Fumes”.

## 1.2. Project context

This document is part of WP7.1 of P7 “Mitigating the risks of fire, smoke and fumes” activity of Future Sky Safety project. The objective of WP7.1 is to enhance knowledge concerning the fire behavior and performance of CFRP primary structure composite materials, in order to better predict safety and survivability issues in case of fire incident or post-crash situation. Such predictions rely on physical models and numerical tools which need to be developed based on exhaustive characterization material process and a components validation for experimental testing. The objective of WP7.1 is to produce a comprehensive experimental database for a reference material to be shared by the European research community as a basis for material model development of the fire behavior and degradation of CFRP materials. The T700GC/M21 material has been proposed to be used in this WP7.1 because a lot of published results already exist about its standard mechanical behavior which the project can build on. Partners’ state-of-the-art models and simulation tools will be assessed according to this comprehensive set of experimental data.

The enhanced knowledge, on the one hand, will support WP7.2 along its works to improve materials solutions to better mitigate risks of fire, smoke and fumes in the cabin environment and, on the second hand, will be possibly enriched by WP7.3 proposing new measurement techniques of the on board air quality and possible contamination.

## 1.3. Research objectives

The final objective of this study is obtain a calibrated numerical model based on the application of finite elements techniques which represents a properly behavior of the composites materials submitted to loads either thermic or mechanical.

## 1.4. Structure of the document

Following this Introduction, Section 2 contains the main study requirements based on the applicable EASA Certification Specifications. Section 3 summarizes simulation tools to predict fire behavior and structural effects. Section 4 contains the modelling and simulation results of the thermal and chemical behavior of the T700GC/M21 material exposed to high energy laser beam. Section 5 gives the procedure established for the simulation of composite materials submitted to fire and high temperatures. The conclusions and recommendations are contained in Section 6. Finally, the Appendices contain the standard FAR/CS25 requirements and compliance method for fire protection, the AC20-135 (FAA) test methods, standards and criteria for protection against fire, and the ISO 2685 standard for resistance to fire in designated fire zones.

## 2 REQUIREMENTS (ADS)

### 2.1. Applicable regulation

The behavior of aircraft structure against fire is regulated by CS/FAR25 and specific normative which is summarized in the following list:

**FAR/CS 25** requirements:

- FAR/CS 25.867 Fire protection: other components
- FAR/CS 25.1181 Designated fire zones: regions included
- FAR/CS 25.1182 Nacelle areas behind firewalls, and engine pod attaching structures containing flammable fluid lines
- FAR/CS 25.1191 Firewalls
- FAR/CS 25.1193 Cowling and nacelle skin
- AMC 25.1181 Designated Fire Zones
- AMC 25.1193 Engine cowling and nacelle skin, APU compartment external skin

**ISO2685** (International Standard): Conditions and Methods for Fire testing used for certification under

EASA CS 25 (reference in AMC 25.1181)

**AC20-135** (FAA):

In spite of being a FAA document, it is used as a guideline in certification under EASA CS 25

**Others** (Advisory material):

JAA Notice of Proposed Amendment (NPA) E-266

### 2.2. Practical fire substantiation

Special importance has the objective of the project is related with the areas susceptible of being affected by a fire event. CS and AMC 25.1181 define two zones as fire zones:

- Designated fire zone: powerplant components inside firewall and APU compartment.
- "2D zone": Surfaces behind nacelles within one nacelle diameter of the nacelle centerline. In the event of external flames from Engine Designated fire zone, fire may be released from the engine nacelle and be directed rearwards to this zone

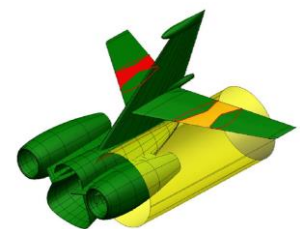
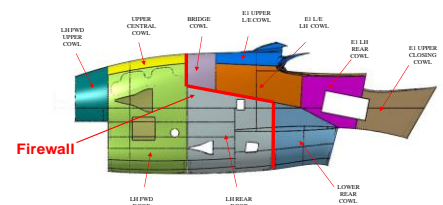


**Figure 1 Fire zones Nacelle and HTP**

**Firewall** (CS25.1191) design must be fireproof and constructed so that no hazardous quantity of air fluid or flame can pass and conveniently sealed and corrosion-protected.

**Nacelle** must be constructed and supported so that it can resist any vibration, inertia, and air load to which it may be subjected in operation.

An airplane must have fireproof skin (CS 25.1193) in areas subject to flame if a fire starts in the engine power or accessory sections.

Engine accessory section, each part of the accessory section cowling subject to flame in case of fire in the engine power section of the power plant must be fireproof and same properties as firewalls. Fireproof also is requested to cowling components subject to high temperatures due to its nearness to exhaust system parts or exhaust gas impingement.

This means elements mainly affected by a fire event may be access doors, cowlings, fixed nacelle, APU Access doors, etc.

The use of the composites on the external cowling of nacelles and engines compartment is an extensive practice in the aeronautic field.

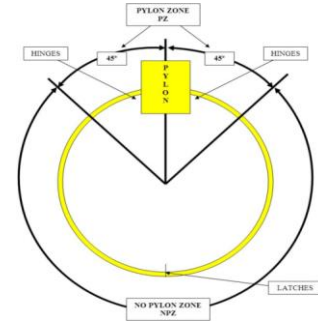


**Figure 2 Fire zone: Engine Nacelle Fan cowl**

Two grades of thermal/fire are defined:

- Fire-resistant

Grade designating components, equipment and structures capable of withstanding the application of heat by a standard flame for 5 minutes

- Fireproof

Grade designating components, equipment and structures capable of withstanding the application of heat by a standard flame for 15 minutes

### 2.2.1. Substantiation by flame test

The application of the current normative stated in previous section to a structural element can be substantiated by specific fire exposure tests defined in ISO 2685. EADS CASA has extensive experience in the application of this standard and test:

#### Fire duration

- 15 min for Fireproof
- 5 min for Fire-resistant

#### Ventilation (airflow)

- In-flight: min a/c airspeed (100 kts usually)
- On-ground: None

#### Load

- Normal maneuvers (usually max load of Fatigue envelope)



**Figure 3 Flame test on a hinge fitting**

Note: when loads are coming from enforced displacement benefit can be taken to reduce load at 5 min

#### Vibration

- Amplitude: +/-0.4 mm, normal to the skin surface
- Frequency: 50 Hz during the first 5 minutes (engine running)  
+ 15 Hz during the following 10 minutes (windmilling) for in-flight conditions

#### Pass/Fail criteria

- No flame penetration and no backside ignition
- Loads withstood throughout the test period. No detaching of structure. Deformation within acceptable limits



**Figure 4 Fire zone: Auxiliary Power Unit compartment**

#### 2.2.2. Thermal Behaviour

In order to adequately understand the event of fire over a structure, the thermal behavior and characterization is required to predict temperature distribution achieved in each place of the structure.

During a fire event over a composite structure thermal properties vary as degradation of matrix increases, and therefore this characterization must be performed through the different states of degradation of the composite.

In order to develop a thermomechanical model a prior thermal properties characterization is required apart from mechanical characterization.

EADS CASA has developed an internal characterization procedure validated through fire tests in order to obtain emissivity, conductivity, specific heat and in-plane diffusivity. Material involved in the program should be characterized following this procedure at Getafe facilities. The range to be characterized should cover from RT to 1100°C. In order to carry out the determination of the thermal parameters of the panels, before and after the heating, by the part of Airbus D&S are required at least two samples of a size approximated of 300x300 mm so as to perform this thermal characterization properly.

### 2.2.3. Mechanical Behaviour

Fire can seriously degrade mechanical properties and structural integrity of a composite structure, causing creeping, buckling, thermal deformation, collapse or some other failure. Laminate failure under tension loading is controlled by fiber resistance whereas under compression or shearing (interlaminar or in plane) the failure is controlled by the resin behavior. The main effort of characterization of the fire resistant properties of composites should be focused on the characterization of load states influenced by this resin softening and common in loaded composite structures.

Typical composite structures load introductions is performed through fittings (normally metallic) or bolted (inserts in case of sandwich) joints. Both types are normally controlled by the local resistance of the bolted joint: the deterioration of the load-bearing and pull-out properties in composites at elevated temperature or in fire are the most common failure responsible.

The residual mechanical properties of thermally degraded composites following fire are not as well understood. After a fire is extinguished, it is important to know the residual properties of a burnt composite at room temperature in order to determine the mechanical integrity and safety of a fire-damaged structure. From Ref 1 residual bending and tensile properties is obtained:

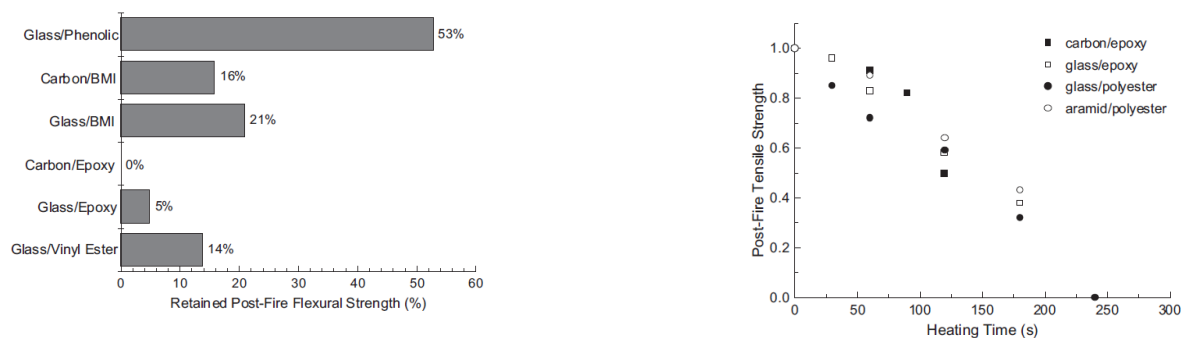


**Figure 5 Mechanical Properties for several composite materials: residual flexural strength and evolution of tensile strength [Ref 14]**

In order to develop a thermomechanical model once known all thermal properties characterization, a mechanical characterization is required. The range to be characterized should cover from RT to 1100°C.

This mechanical characterization should determine both stiffness and allowable evolution with temperature and degree of degradation. Characterization should address both, especially those properties related to matrix behavior:

- a) Stiffness
  - Bending
- b) Allowable:
  - Composite Joints properties: shear bearing, fastener pullout
  - Compression,
  - Bending

### 3 SIMULATION TOOLS TO PREDICT FIRE BEHAVIOUR AND STRUCTURAL EFFECTS

When looking at aircraft composites implementation, aviation authorities are very strict and cautious, and regulations expect the manufacturer to demonstrate that critical and crucial structures are airworthy. Product development and material's validation leads to build an extensive list of tests that must be performed to validate structure's properties. Today, mechanical plus flammability testing have been the main focus for structural safety verification.

Composites application within primary structures, near potential flame or heat affected areas raised the interest in predicting flame and heat effect on composite's structures, direct or indirectly. Mechanical properties are currently estimated taking into consideration worst case scenarios where structures perform as projected under harsh conditions (e.g. low and high temperatures operation, with high level of humidity) simulating worst degrading contexts; harsh flammability tests are performed against flammable materials.

Due to its properties such as toughness, chemical, mechanical and electrical resistance, epoxy resins are widely used in aeronautic industries where advantages of these resins counter balance their price. Compared to metallic structural materials, the low density and increased strength and stiffness in the required directions are considerable advantages of composites. Their main drawback is, however, their flammability.

As safety regulations are strict with aircraft safety demands, demands for flame resistant composites which can satisfy mechanical and fire requirements need to be taken into account in each and every structure that is mechanically demanded during a flight. Simulation tools are required to predict structure mechanical resistance in case of a fire. Materials behavior shall be determined and mirrored to a bigger scale.

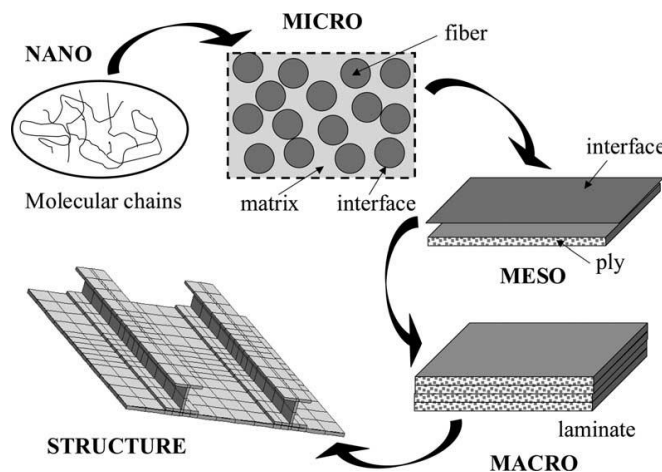


**Figure 6 Schematic representation of composite structure scales [Ref 19].**

Investigations on the dimension of fire hazard on aircraft CFRP structures are being performed for more than 10 years, as well as on metals, generally driven by accidental fire events. Nowadays, it

is seen that flame and/or flammability prediction/simulation could be a great advance for aircraft manufacturers and a greater comfort for aviation regulators.

When discussion how far can we go on simulation tools for CFRP structural behavior when a fire is occurring, we can be as precise as simulating the behavior of the shearing forces within the structure, and thus the adhesion between the polymer and the reinforcing fibers. Alternatively, simulation should be performed taking in account some assumptions and, as a result, a few accountable boundary conditions. For that, it is necessary to collect properties from the systems as much accurate as possible.

### 3.1. Degradation Mechanisms and Flame Behavior Characterization

Numerical simulation and test methods that are largely used in fire safety engineering for metallic structures are not completely applicable to CFRP structures and it is necessary to search for better applicable methods. An important starting point is to characterize these materials kinetics. For this purpose, it is also found important that novel test benches are equipped with a complete set of instrumentation designed to investigate the fire behavior of materials from heat fluxes, mass losses, gases generation, through thickness structure changes qualitative and quantitatively (and compliant with the ISO2685:1998 aeronautical certification test).

Temperature profile on the front on the back of the fire, structural mass loss, quantity and quality of released gases, would be ideally measured and as a function of time. In fact a few studies already identified that CFRP degrade in phases which are quite different in between. In a first moment it is important to address all the changes that are occurring at a structure surface until it starts affecting the structure through its thickness and before material ignition if (it is the case). Once the material ignites and/or the resin's pyrolysis starts in great speed through thickness it is important to monitor the front and the back mass, thermal and gaseous phase wise.

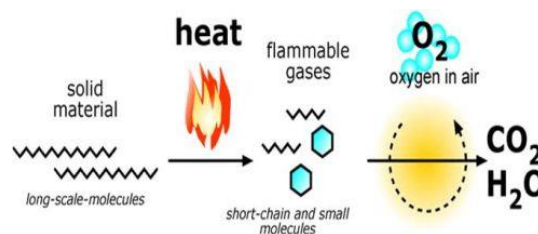


**Figure 7 Example of a combustion process and secondary products generation.**

It is fundamental that tests are developed to represent the interaction flame – material since it is the only way to enhance aeronautic industry and certification entities knowledge and confidence on CFRP fire behavior crashworthy wise.

Physical, thermal and chemical phenomena occurring during a fire tests shall be characterized in order to develop multiscale and multidisciplinary simulation tools that will simulate flame behavior within time and structure decomposition and the decomposition of the structure itself – including thermal expansion (inducing apparition of cracks), thermal decomposition of the resin, internal pressure phenomenon, gas migration through the material and thermal delamination. [Ref 19] [Ref 20] [Ref 21] [Ref 22][Ref 23] .

Important stages:

1. Characterization of the decomposition degree through decomposition kinetic parameters characterization
2. Characterize of the flame behavior with structural decomposition evolution, taking into account flame interaction with the structure
3. Simulate structural behavior during its thermomechanical and thermochemical degradation process

Experimental results reported in literature corroborate with the need to get physical (density), chemical (kinetic parameters) and thermal (heat capacity and thermal conductivity) parameters of composite laminates as necessary to get suitable models. Attention shall be taken to laminates stacking sequence and fibre selected as lamina properties are not sufficient as thermomechanical properties are totally different between fabrics and unidirectional laminates [Ref 19] [Ref 20] [Ref 21] [Ref 22][Ref 23]

Characterization of the heat fluxes of the flame need to be performed, and the ability of the test bench to give acceptable and fast response will be checked on titanium coupons. Measurement of temperature dependent-thermophysical composite properties as the anisotropic thermal conductivity and the specific heat capacity is not easy especially for high temperatures bigger than 200°C (characterization methods are being studied in order to calculate transverse thermal conductivities –  $\lambda T$  – and isobaric specific heat capacities) [Ref 19] [Ref 20] [Ref 21] [Ref 22][Ref 23]

### 3.2. Flame and Heat

Composite materials, above from its high mechanical performance, are constituted by more than 50% of resin. Resins are made of long polymeric chains which start to degrade or melt over a certain temperature limit (e.g.  $T_g$ ) depending on the type of resin. Resin's behavior to flame and fire effects promotes aging and mechanical properties degradation. There are many different aging mechanisms which vary considerably depending on the polymer, on the aging conditions such as the temperature and oxygen pressure, as well as on the reference state (curing cycle, cooling rate), and with the structure of the materials (geometry).

Temperature has the capacity of transforming a carbon fibre reinforced polymer (CFRP) substrate into something less such as a burned out structure with a carbon net left behind. Depending on fire characteristics and on the substrate behavior to that particular flame, fire may lead the substrate to degrade, to oxidize, to over polymerize, which involves weight losses, density variation (which might increase or decrease, depending on the phase), skin shrinkage and consequent into matrix fragilization. Several approaches to understand the interaction between flame and CFRP structures are being generated, the majority hitting the same: flame behavior has a dynamic interaction with these materials at the surface and through its thickness a physical, chemical, thermal and combustion way [Ref 19] .

There are flame driven physical changes reflecting in molecular rearrangements and chemical changes with irreversible structure changes in a macromolecular level such as thermal oxidation, chain ruptures, post-crosslinking, etc.. At the fire temperatures the majority of the thermochemical

processes include: carbon post-crosslinking, carbon chain's rupture, oxidation reactions and gases generation. Post-crosslinking reactions lead to an increase in the crosslinking density and on structure fragilization. Simultaneously carbon chain thermolysis decreases the crosslinking density. In a first moment, structures will feel degradation effects through surface such as surface etching on the region being hit by the flame but, quickly, flame effects will be felt on the surrounding areas and through its thickness. Mechanical properties degradation will be guided by different thermochemical degradation phases, which will be reflected on ultimate properties degradation and, when near its burnout phase, stress-strain capacity will collapse [Ref 19] .

Characteristic phenomena occurring during CFRP degradation:

- Thermal conductivity and combustion
- Thermomechanical degradation
- Thermochemical degradation

The path to simulate material's decomposition and degradation needs the material's kinetic model: Decomposition leads to material's degradation through a progressive mass loss and gases generation; degradation does not occur in just one stage and that should have nuance along material's decomposition; CFRP materials do not degrade linearly [Ref 22][Ref 23] [Ref 24] .

The overall aim is to get the apparent properties in each state of material as function of the temperature and time which include fibre, resin and gases evolution together with the flame as part of the context, to get the decomposition degree estimation and an equivalent homogenization predictive modelling tool.

### 3.2.1. Thermomechanical Effects

Experimental investigations of CFRP composites shows that, at accelerated aging, its degradation presents a two-step trend regarding due to mechanical properties evolution with heat and pyrolysis. A first stage is identified as the consolidation phase where some improvements in tensile mechanical properties can be identified. This phenomenon is observed since the polymeric matrix post-cures and its atomic structure wins more crosslinks. At a second stage, temperature no longer enhances the matrix significantly decreasing its mechanical properties as it starts to be pyrolysed while the crosslinks are being broken. When the matrix and fiber-matrix interface starts to degrade the matrix passes from a viscoelastic behavior to a fragile cracked substrate [Ref 21]

From the application of several physic-chemical, thermal diffusivity and gases characterization techniques information such as gases composition and quantity, activation energy and crosslinking order can be taken. For example, data such as specific heat capacity is important to estimate the decomposition degree and decomposition degree/remaining mass and thermal conductivity for heat transfer and degradation degree calculation [Ref 22].

Mechanical properties until a certain point provide a linear relationship between CFRP's mass loss and mechanical strength; once the thermo-oxidative processes starts to happen it starts to change the materials structure irreversibility decreasing its strength properties. The thermo-oxidative processes incites the appearance of combustible gases [Ref 21]

Reaction		Step 1	Step 2	Unit
<i>n<sup>th</sup></i> order decomposition				
Activation energy	$E_n$	58.7107	146.6740	(kJ/mol)
Frequency	$\text{Log } A$	0.8585	8.7268	(1/s)
Order	$n$	1.1125	2.0825	(-)
Contribution	Fraction	0.5540	0.9479	(-)
Autocatalysis				
Constant	$\text{log}K_{\text{cat}}$	-	0.8744	(-)

Figure 8 Kinetic parameters from the decomposition of a CFRP material [4].

NO and SO<sub>2</sub> result from the degradation of the resin and the hardener and CO<sub>2</sub> and H<sub>2</sub>O result from the combustion reaction between the flammable pyrolysis gases and the oxygen in the flame and will feed its combustion [Ref 22].

Gases	H <sub>2</sub> O	CO <sub>2</sub>	CO	SO <sub>2</sub>	CH <sub>4</sub>	NH <sub>3</sub>
Volume fraction ( $V_i$ ) (-)	0.675	0.213	0.038	0.039	0.019	0.01

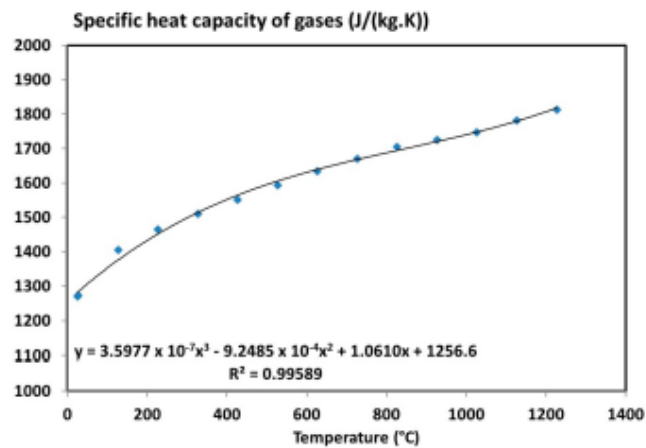
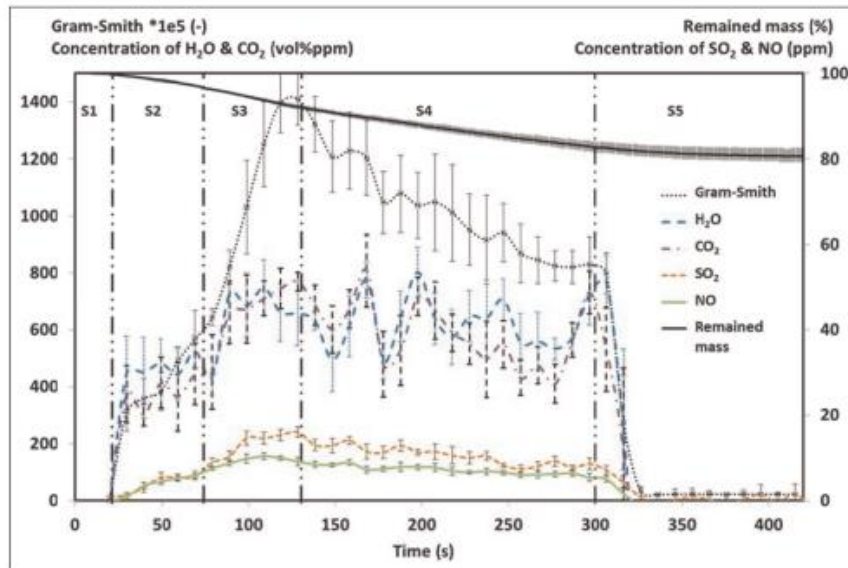


Figure 9 Gases volume fraction obtained from decomposition of a CFRP material (above) and respective specific heat capacity the gases as function of the temperature (below) [Ref 22]

It is important to refer that, due to the diffusion controlled gases and/or oxidative mechanism the rate of degradation will be dependent on the stacking sequence and on how permeable it is. Thermo-oxidation of the composite may occur on the fire front face or on the adjacent areas, being more catastrophic where fire is incident as the gases generated will enhance the flame combustion [Ref 21]

On the surrounding areas the damage might be on the skin which may not affect the mechanical properties if the load is transmitted by its inner plies. Nevertheless, studies show that CFRP materials under an oxidative-aging environment at 177<sup>0</sup> C suffer a decrease on its GIIC and increase on its GIC and increase on its. These phenomena are associated to delamination and transverse cracking thermal generation, i.e. to matrix thermal degradation. Also, thermal aging influences not only static material strength but fatigue behavior as well.

Thermomechanical and thermochemical decomposition processes can be split into five steps as characterized on the figure below [Ref 21] [Ref 23]



**Figure 10 Representation of CFRP degradation through remaining mass together with gas concentrations evolution, along time and temperature evolution [Ref 23] .**

On a first stage CFRP (S1) materials will suffer superficial etching where the flame is incident with little mass losses. On a second stage (S2) is when it is evident that thermal degradation starts damaging truly the material presenting a higher degree of mass loss and gases start to be released. The third stage (S3) is where gases concentration increases mostly and it is verified that mass loss starts its accelerated process while these combustible gases start to burn – combustion is started – and it goes through stage four (S4) with higher mass losses as intensity and gas combustion increases. S4 is a long stage represented by 170 seconds of duration which will culminate in a fifth stage (S5) where the small amounts of gases keeping the flame at the fire face will be kept until the point that it is all extinguished. In the end, CFRP presents around 20% of mass loss [Ref 23]

Extra considerations:

- The heat flux of the flame is lower on the border of the plate and, therefore, resin located on those areas has a potential of be less degraded than at the center [Ref 23]
- It is identified that fibers are not oxidized when its surface roughness is observed while virgin and half-degraded materials showed the same mass fraction of fibre with different mass fraction of resin and of carbonaceous residues [Ref 22].
- Half-degraded and degraded samples show a much lower thermal diffusivity at low temperature [Ref 22].
- The degraded sample show a weaker dependence to the temperature and the thermal diffusivity increases slightly above 300°C due to structural changes and radiation increase within the sample [Ref 22].

- The thermal diffusivity of the virgin material decreases linearly up to 350°C and then the slope of the curve become steeper with the formation of cracks and thermal delaminations [Ref 22]
- At high temperatures (>400°C), the virgin sample has 2–3 times lower thermal diffusivity than the burnt material which can be explained by the different thicknesses of the material and decomposition state [Ref 22]
- The degradation can be considered to be linear until 150°C and polynomial for the degraded state; it is also stated in other studies that thermal conductivity of degraded material varies with a third power of temperature [Ref 22]
- Tension load-bearing performance is faster deteriorated with increasing fibre offset angle having a substantial adverse impact on the fire performance [Ref 22]
- Areas adjacent to the flame which are irradiated by the flame are thermomechanically degraded; ultimate strength and modulus decrease with aging time and temperature [Ref 22]
- Compressive strength and modulus degradation are greater for perforated laminates due to accelerated oxygen diffusion [Ref 23]

### 3.2.2. Thermal Conductivity Effects

Many studies are being performed on lightning strike effects focused on understanding current flows in continuous CFRP composites and how is the structure affected. Similarly to lightning strike thermal effects structure damage is proportional to its conduction path. It is widely understood that thermal conductivity will be provided by the carbon fibre which is reinforcing a polymeric matrix. Through thickness and in-plane conductivities, as well as materials specific heat while is being degraded evolves dynamically and will strongly affect thermomechanical effects – see figures below [Ref 22]

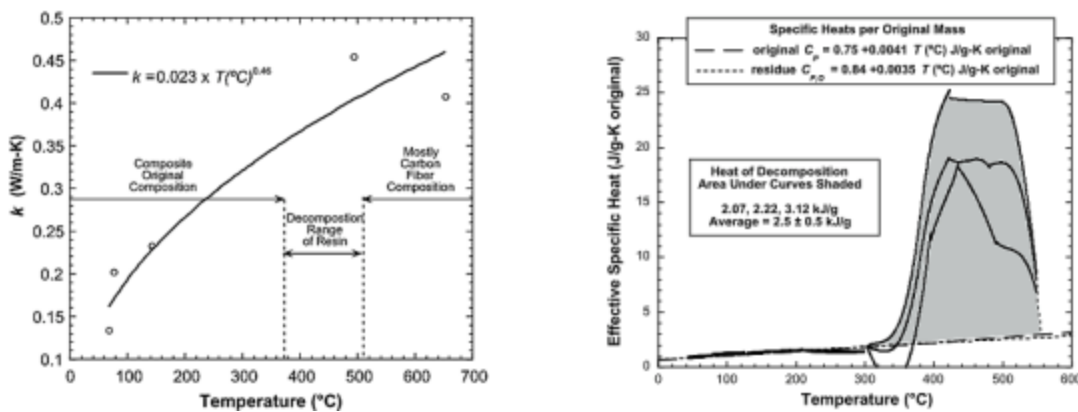


Figure 11 Thermal conductivity during heating (left) and specific heat and heat of decomposition during heating (right) [4].

CFRP plies present orthotropic thermal and electric properties, thermal and electrical conductivities higher in-plane and lower through-thickness directions – figures below [Ref 20]

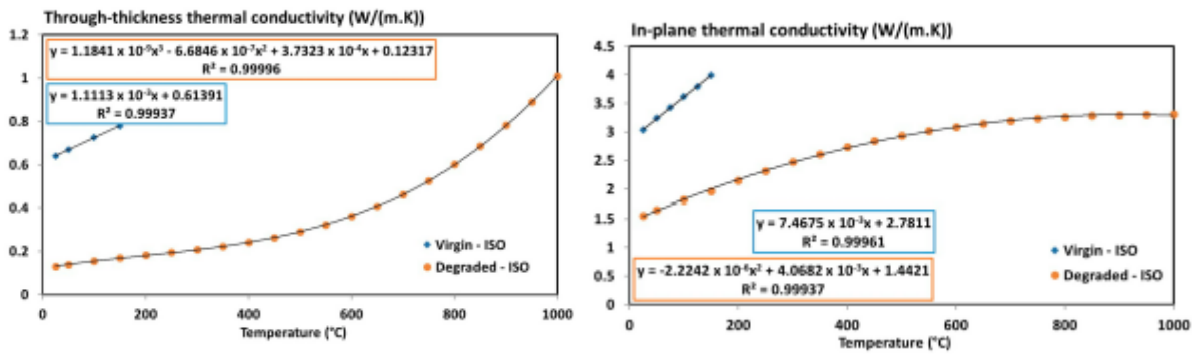


Figure 12 Thermal conductivity in-plane (left) and through thickness (right) [Ref 22].

CFRP stacking sequence and type of fibre applied has also a great influence on how and how fast these structures degrade. On figure below is shown that UD and ISO stacking sequences present completely different behavior. As it can be observed, a unidirectional laminate configuration provides bigger fire resistance in plane and through the material's thickness [Ref 23]

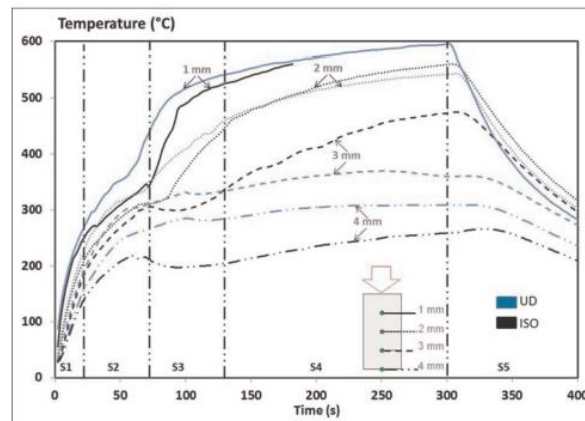
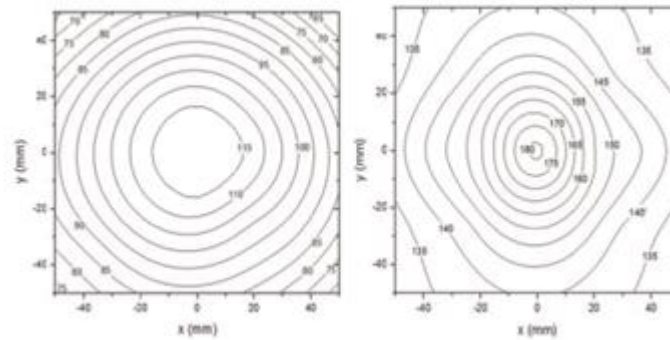


Figure 13 Temperature profile in UD and ISO CFRP thickness and rear face [Ref 23]

Tranchard et al. relates these phenomena to the fact that UD has higher thermal conductivity than ISO stacking in-plane and, therefore, it explains why UD temperatures are higher at 1mm thick. When analyzing through thickness temperature profiles at 2 and 3mm it is observed that the tendency changes as UD's present lower porosity and, therefore, UD inter-ply for thermal conductivity is poorer than when applying oriented stacking [Ref 23]

The back side of the sample behaves differently from the fire front and inner plies. Tranchard et al while studying all degradation mechanisms happening in composite structures identified that during composite degradation delamination occurs, decreasing through thickness heat conduction and temperature measured at 4mm. As UD has higher stability under these circumstances, it presented less delamination effects than ISO and, therefore, higher temperature profiles [Ref 23]

In isothermal experiments it was also found that the weight loss varies according to structure and flame location, and therefore degradation effects anisotropic. Flame characteristics will generate a different interaction, shape, heat flux and consequent thermal conduction with the substrate [Ref 23]



**Figure 14 Heat flux mapping on a CFRP face for 116kW/m<sup>2</sup> (left) and 182kW/m<sup>2</sup> (right) [Ref 23]**

Regarding flame location, the substrate will degrade differently. The figure below shows how the heat is conducted along the fibers and how the damage is expanded along the surface showing that the front of decomposition doesn't affect the material in z direction evenly. The border of the exposed area shows that is greatly affected in contrary to the corner that is being less decomposed [Ref 24].

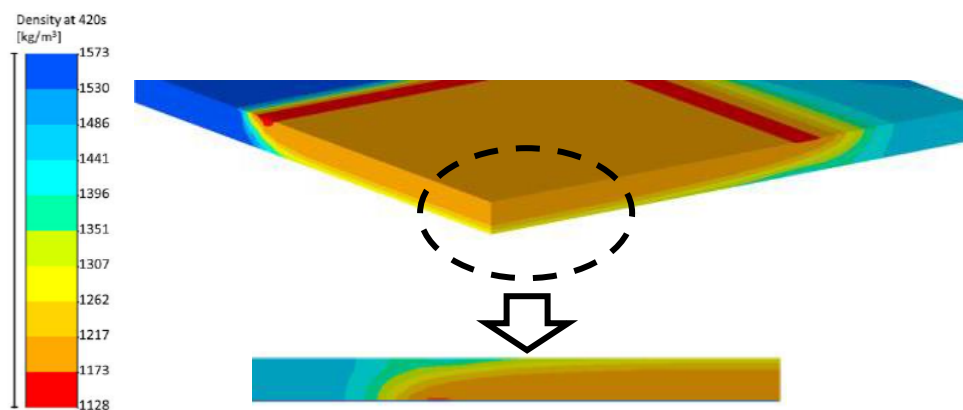


**Figure 15 Images of the coupons after 420 s of test duration and the calculation of the decomposition degree in 3D [Ref 24]**

Adjacent areas are also affected by fire, in this case by flame radiation and convection and, dependently on the location of the flame in the structure, will instigate more or less appetite to irreversible degradation. Thermal radiation is also the heat transfer mechanism identified during (and immediately) after a lightning strike which can be determined by the CFRP surface emissivity. Considering that a fire is always a turbulent fluid convection conditions could be also considered to account for simultaneous heat diffusion and advection [Ref 20]

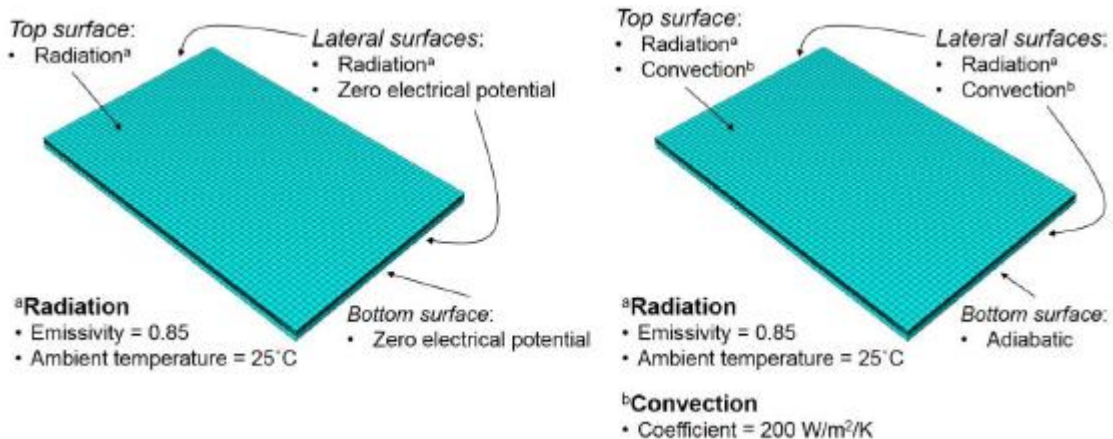


**Figure 16 Thermal boundary (and electrical) conditions imposed in lightning strike FE simulations [Ref 20]**

Extra considerations:

- Temperatures for the UD composite are higher than for the ISO composite in the thickness of the material by the fact that the thermal conductivity is higher for the UD stacking compared to the ISO stacking [5].
- Stacking does not influence the heat capacity at low temperature but decreases thermal conductivity perpendicular to the fibre direction because of lower porosity inter-ply for an UD than for an oriented stacking [5].
- Heat transfer in horizontal direction is more independent from the decomposition degree [Ref 23].
- Stiff carbon fibers hinder intumescence and no charred layer is formed leading to an improved heat and oxygen transport, as well as more intense burning [Ref 22].
- In-plane thermal diffusivity is 10 times higher than through plane and differences are found between the virgin and half-degraded structures [Ref 22].
- Anisotropic behavior with an In-Plane thermal conductivity 11 times higher than the through-thickness thermal conductivity before 500°C and six times higher after 500°C [Ref 22].
- Thermal conductivity tensor determined previously has to be multiplied by the ratio 2.1/3.35 in through-thickness direction and divided by its ratio in longitudinal direction [Ref 22].
- The thermal degradation is considered as endothermic, and the migration of evolved gases through the degraded part into the impacted face has a cooling effect depending on the heat capacity of released gases [Ref 22].

For UD CFRP type layouts, areas adjacent to the flame which are irradiated by the flame have its mechanical properties dependent on the fiber-matrix properties; quasi-isotropic laminates have its own dependent on the long term properties of the matrix [Ref 22].

Composite lay-up clearly changes the thermal conductivity of material. As reported in section 'Post-fire testing analysis', the amount of through-thickness delamination cracking seems to be dependent on the ply lay-up.

### 3.2.3. Morphology Changes

We can see flame effects as indirect precursors to internal morphological changes while CFRP starts to degrade. Material's progressive thermal degradation generates fiber-matrix disbonds, thermally generated delaminations, matrix post-crosslinking or pyrolysis which generates morphological changes through the structure volume. Under isothermal aging conditions, thermal oxidation and etching can be considered surface aging [Ref 23]

Figure below represents the effects along a fire incidence providing information on both CFRP faces, showing progressive degradation mechanisms which start to affect the front surface in the beginning of the degradation process [Ref 23]

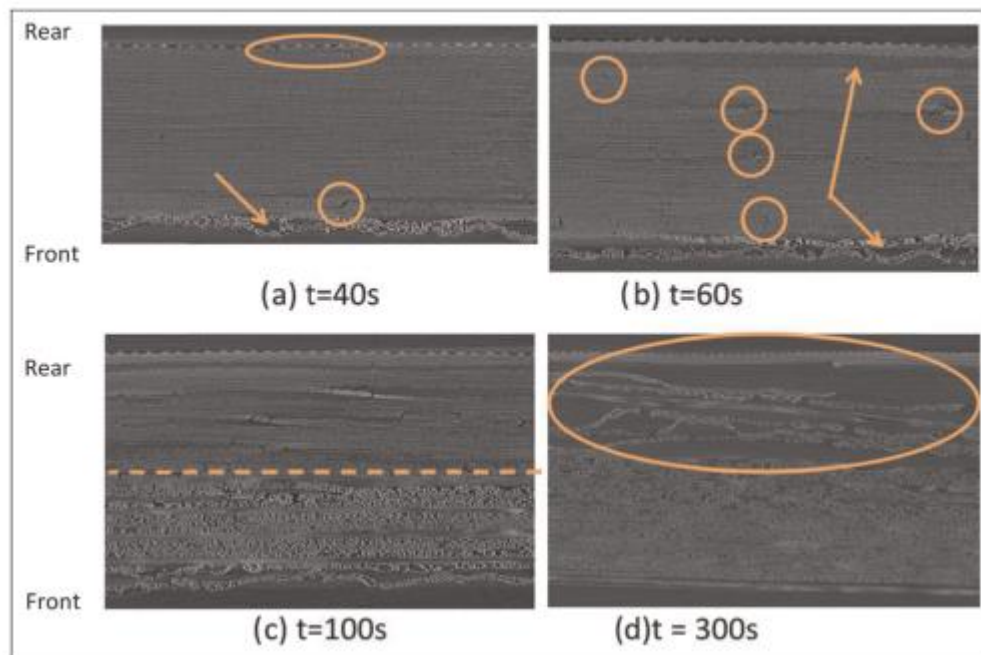


**Figure 17 CFRP through thickness decomposition along time and depth [5].**

On figure above in a) it is evidenced a fire front surface that is losing mass leaving behind resin cracks and the first plies start to present cracks; a layer of decomposed material starts to form in the front of the fire. Figure b) shows an evolution of the decomposition by presenting resin cracks through the thickness of the CFRP, in areas that are still untouched by the flame; the rear front that is still away from the fire starts to be affected by the heat; it is also evident that the fire front decomposed layer continues to grow. In c), after 100 seconds the material feels a quick and harsh degradation due to resin's pyrolysis, fiber debonding and through thickness thermal delaminations. In d) as the material continuously loses its resistance to the fire front with the resin continuous pyrolysis process, the rear face is no longer protected and starts to degrade its properties suffering from harsh delamination effects [5]. As a result laminates progressively delaminates layer by layer, evolved gases migrate from one side to the other and the material naturally expands [Ref 23]

Extra considerations:

- On CFRP materials fibre damage/degradation is not relevant to be accounted for as its degradation temperature is high; it is normally considered that only the matrix of the composite is subject to aging [4].
- Stiff carbon fibers hinder intumescence and, therefore, no appropriate charred layer is formed [Ref 22]
- After 100 seconds of exposing a CFRP material to a fire it is predictable that half of the material has lost its mechanical properties since it has been affected by harsh thermal degradation [Ref 22].
- After 60 seconds a CFRP substrate starts to suffer from thermal fibre–resin debonding and thermal delamination [Ref 23]
- Temperature profile and the mass loss as well as to identify and quantify the evolved gases released during a single propane fire test are important [Ref 23]
- Weight loss varies according to structure geometry and flame location, and therefore degradation effects and resultant anisotropic morphologic changes will be presented differently [Ref 24] .

### 3.3. Simulation Approaches for Fire Modelling

Thermomechanical models including material related kinetic models plot temperature versus weight loss in oxidative atmospheres at high temperatures and under thermomechanical cyclic stresses due to temperature variations; these phenomena all at the same time accelerate the damage process. In CFRP materials direct oxidation mechanism it has been neglected considering that in the flame front oxygenation will be almost zero. Nevertheless, on the areas around the fire front it might be taken into account as it will be a degradation acceleration factor. On the surrounding areas it is also important to predict viscoelastic thermomechanical behavior in a multiscale/ macroscopic model. In addition to thermomechanical stresses, flame surroundings suffer from physical and chemical aging effects which degrade the material physically and alter the residual performance of the structure [1].

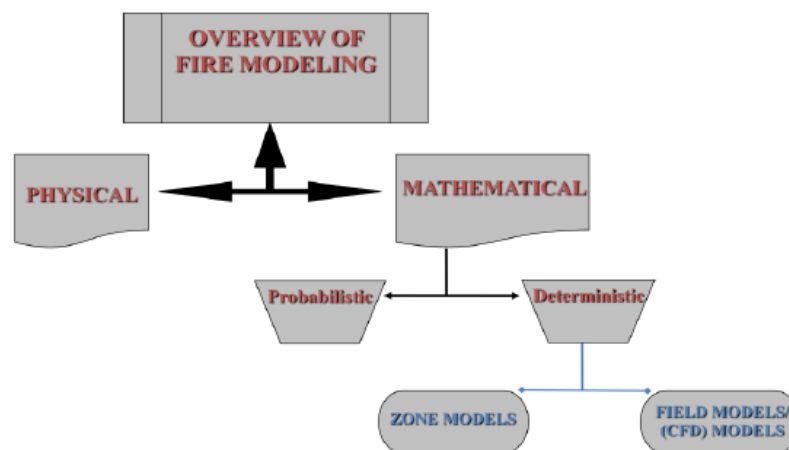


**Figure 18 Fire modeling approaches [7].**

Hand calculations can be made, as well as zone models and computation fluid dynamic models, depending on the degree of precision and complexity aimed for. Simulation can utilize mathematical

equations that can go from simple equations to complicated differential equations; the respective experimental correlation is also fundamental to characterize all the effects involved [Ref 25].

The majority of the studies found were normally related to the thermal and electric damage of CFRP structures provoked by lightning strike incidence rather than by fire. The ones related with fire events in aerostructures are scarce and normally for building industry. Only one stream line of studies performed was identified with potential of going straight to the point. A few others will be mentioned in order to understand what kind of approaches are being made and that could be applicable to simulate CFRP structures behavior while being degraded by fire.

Studies focused on CFRP degradation simulation for lightning strike situations will be taken into account as they are at a certain point equivalent.

### 3.3.1. Finite Elements Modelling

Finite element (FE) models have been developed and explored to simulate thermal damage in carbon/epoxy composites when a CFRP structure is attacked by a Lightning strike. For that purpose it was identified to have a good degree of accuracy.

The same way structural behavior is simulated and predicted by FE simulation tools driven by boundary conditions, it is also possible to simulate fire behavior by extrapolating known phenomenon's. In order to get to that point, it is fundamental that the fire effects in composites structures are known. Many studies are being performed in this area to understand and later map thermomechanical and thermochemical effects on mechanical-chemical properties on composite materials.

For example fatigue strength can be modeled through Arrhenius equation as well predicting changes on CFRP viscoelastic properties materials during degradation. Together with thermodynamic models, numerical models such as decomposition kinetic models are being developed using least-squares fitting procedures based on thermogravimetric curves.

A few case studies will be described below by numbered examples.

#### 3.3.1.1. Cases

#### 3.3.1.2. Example 1 – Fire exposure, study published in 2017 [Ref 24]

General characteristics:

- Three-dimensional thermochemical models which predict temperature profile, mass loss and decomposition front for CFRP (epoxy resin based) exposed to fire conditions.
- Takes into account the energy accumulation by the solid material, anisotropic heat conduction, thermal decomposition of the material, gas mass flow into the composite and internal pressure.
- The thermophysical properties defined as temperature dependent are used as input for the physical model.

- The model includes: multi-step decomposition kinetic modelling, temperature-dependent inputs as a function of the decomposition degree and near-surface empirical interactions between the CFRP and the gases resultant from the CFRP decomposition.

#### Capability:

- Simulation of mass/mass loss (though its overestimated)
- Time-to-ignition (rough) prediction
- Simulation of temperature/heat flux profiles (though is overestimated)
- Predicting the final state of the material such as emissivity and final thermal properties (without interactions)
- Simulation including a decomposition model built up to account for two (competitive) reactions – autocatalytic reaction and classical nth-order reaction

#### Improvements:

- Temperature estimation and measurement at the rear face
- Boundary conditions at the front face
- Thermo-optical properties characterization (to know what's the influence of radiation, e.g.)
- Flame heat flux simulated all together through CFD modeling and to accurately predict temperatures profiles as well as flame heat fluxes through a structure
- Model materials through thickness fire behavior which is non uniform/non-symmetric
- Change of heating rates included in the model, as it changes through thickness along decomposition (a pure conductive model it's not applicable; it is necessary to exchange to a current model)
- Include out-gassing and positive feedback and fire modelling for precise thermal response and mass loss simulation

#### Comments:

- The three-dimensional thermochemical model revealed capability of predicting material's behavior under fire, predicting mass losses and decomposition front phenomena when the carbon fibre/epoxy composite is directly impacted by a propane flame
- Interactions such as positive feedback, out-gassing, fire modeling were identified as necessary for future works to correctly predict direct material consumption, real incident heat fluxes and combustible gases reactions and avoid overestimation;
- It has been demonstrated that the lack of implementation of the delamination phenomena in the models is not necessarily responsible for the lack of accuracy of numerical predictions;
- The predicted time-to-ignition and the implementation in the model of the boundary condition at the exposed face have to be improved;
- The determination of the heat flux at the exposed surface was considered unsatisfying;
- The heat flux at the exposed face was overestimated, which caused an overestimation of temperature profiles in the beginning of the decomposition;
- Determination of the flame boundary condition has to be revisited using, for example, a joined thermochemical model and a CFD approach;

**Project:** Mitigating risks of fire, smoke and fumes  
**Reference ID:** FSS\_P7\_ADS\_D7.9  
**Classification:** Public



The model showed its capability to predict the fire behaviour of CFRP for fire safety engineering considering that it overestimated degradation effects.

### 3.3.1.3. Example 2 – Lightning strike exposure, study published in 2017 [Ref 20]

#### General characteristics:

- Matrix thermal decomposition associated with the time/temperature profile in order to simulate CFRP thermal damage development, considering that matrix suffers irreversible thermal damage
- Spatial and temporal temperature and matrix decomposition evolution simulation (for lightning strikes)
- Incorporation of material property changes as temperature increases progresses modelling
- Considered that thermal conductivities were isotropic
- Considered that through-thickness very high conductivities
- Electrical currents flows through thickness once the previous ply is ablated (to ensure ensures realistic current flows reaching inner plies)
- Simulation numerical modelling aims to embrace a moving boundary condition.
- Laminate discretization by three-dimensional linear brick continuum elements application (in-plane dimensions of 2.5x2.5 mm<sup>2</sup>)  
Radiation boundary condition was included during simulation for the exposed top and lateral surfaces
- For the simulations, it was considered a surface emissivity of 0.85, ambient temperature of 25°C
- For longer nonlinear heat transfer analyses, it was included a convection boundary condition to include heat diffusion and advection effects
- Unit-cell simplified model to represent a plain woven unit-cell through the combinations of several UD laminas
- Heat generation subroutine (HETVAL) included to simulate thermal decomposition with lightning strike currents and specially and temporally varying temperatures (applied two different ones that were used for epoxy matrix decomposition within affected temperatures)
- Arrhenius kinetic equation was included to characterize matrix thermal decomposition
- Quadratic approximation used to predict matrix decomposition degree within affected temperatures
- Thermal radiation is one of dominant heat transfer mechanisms during and immediately after lightning strike to composites.

#### Capability:

- Realistic current flows to reach the next inner ply
- The composite convection coefficient was assumed to be that of carbon dioxide (CO<sub>2</sub>, 200 W/m<sup>2</sup>/K)
- Three peak currents and respective thermal damage correctly simulated
- Thermal conductivities correctly simulated – capable of predicting thermal conductivity of complex CFRP structures by utilizing simplified unit-cell models

#### Improvements:

- Degree of matrix thermal decomposition defined between normalized values – zero (undamaged) and one (fully damaged) – and based on highest temperatures at each location
- Matrix thermal damage defined as independent of incidence time at any temperature, within the decomposition range
- Matrix decomposition assumed to vary linearly ( $m = 1$ ) or quadratically ( $m = 2$ ), within the decomposition range; this quadratic approximation limits decomposition reaction rates on increasing temperature estimation

Comments:

- The model was developed to FE model lightning strike effects on a CFRP structures;
- Applicable to predict matrix thermal decomposition on highest local temperatures;
- Matrix thermal decomposition defined to be in a normalized range of  $0 \leq D \leq 1$  and assumed to vary either linearly or quadratically in the given temperature ranges showed to be very limited as leads to quadratic damage estimation while applying Arrhenius kinetic equation approach;
- The FE model showed that the size, shape, depth, and intensity of predicted matrix thermal decomposition were strongly dependent on the order of the approximation and dependent on the thermal decomposition temperature range selected;
- This approach is limited to characterize thermal degradation simulation after lightning incidence and does not consider many other effects resultant from the flame and surface interaction;
- This approach can be applied on the surrounding areas of a fire which will be affected by the heat irradiated from the flame and conducted along the fibers;
- More investigation is required to better characterize optimal matrix thermal decomposition temperature range for a given composite, as well as the correct damage-temperature relationship;
- If the fire and the flame are considered as known variables and thermomechanical effects are possible to analyze, it can be applicable;
- From a spatial- and temporal - varying local temperature and the corresponding matrix point of view, this method enables to simulate decomposition resulting from applied electrical currents simulating lightning strikes.

Other studies lie also on studying only thermal conductivities of the plain woven and UD stacked composites under different temperatures, applying multi-scale finite element analyses (FEA) were used to investigate the thermal conductive behaviors.

### 3.3.2. Computational Fluid Dynamics

CFD tools enable simulation of intrinsic properties to fluid flows as flow patterns, pressure alterations, temperature distribution/flow and variations in fluid composition in a system. It also enables simulating qualitative and quantitative surface (not only) qualitative substances' in plot and animation forms. Data from all parameters and variables from equations and extra terms could be extracted and plotted against several other parameters/variables. CFD tools application would

enable to account for fire-substrate interactions and through thickness materials evolutive phenomena – e.g. reacting flows, anisotropic and phased heat flows, etc.

Tranchard et al. and other studies refer to the importance of dynamic simulation on the overall degradation covering phenomenon happening from the surface to the back of the CFRP being consumed by a fire. It was identified that, since the flame and flame interaction with the material is dynamic and generates flame and sub products exchanges, CFD tools coupled with FE could benefit these simulations [Ref 24]

Computer fire modeling has been applied in to design and analyze fire protection and evaluate its effects on people and/or buildings as it allows fire dynamics simulation in enclosed environment. Several studies have performed in this subject and this type of tools is being applied today for fire protection prevention and prediction in building and cabin interior [Ref 25]

Some examples of interesting fluids simulations that could provide a deeper and complementary understanding to FE multiscale and multidisciplinary studies are shown below.

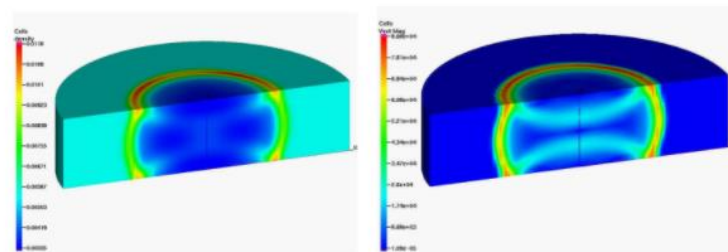


**Figure 19** Example of gas density and velocity after ignition – gas diffusion [Ref 26]

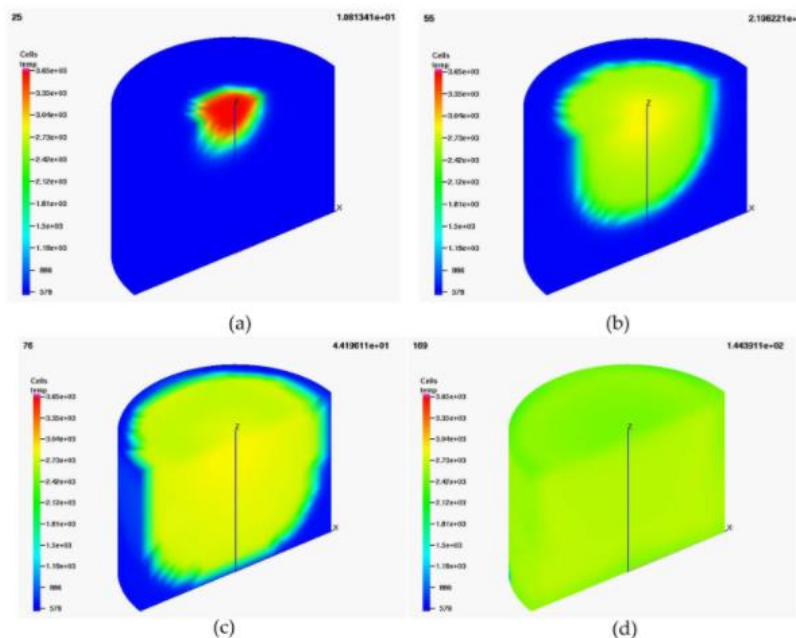


**Figure 20** Example of calorimetric chamber after combustion has initiated – heat transfer (or mass loss) evolution during the whole combustion process [Ref 26]

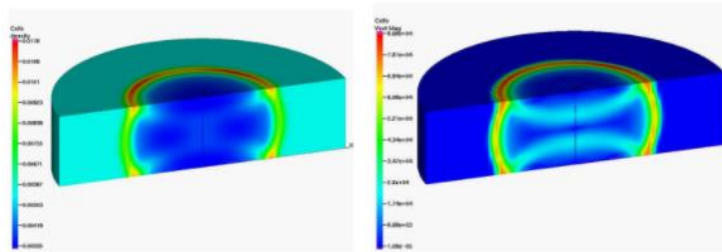


**Figure 21** Example of gas density and velocity after ignition – gas diffusion [Ref 26]

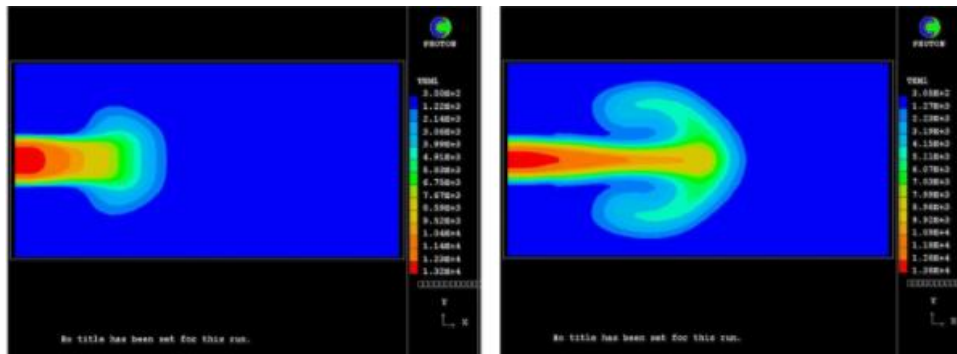


**Figure 22** Example of combustion fluid dynamics and temperature profiles – combustion between the flame, resin and resin degradation resultant gases [Ref 26]

A few software tools available will be described below as follows.

#### 3.3.2.1. SMARTFIRE, application study [Ref 27]

This study focused on applying SMARTFIRE CFD fire simulation software to investigate Swissair Flight 111 In-Flight Fire, a Fluid Dynamics Simulator (FDS) developed by University of Greenwich (<http://fseq.gre.ac.uk>). The SMARTFIRE was used to predict the behaviour of airflow as well as the spread of fire and smoke within SR 111 for cause and origin determination. This study identified that this CFD based fire analysis could be a cost effective approach to investigate complex flow/fire scenarios and, when coupled with targeted controlled experiments, delivers quality data and allows CFD fire simulation to be a powerful tool in aircraft accident investigation and perhaps in aircraft development.

The study included features specially developed for this project such as: a) face patches to facilitate integrating new boundary and surface burning condition, b) output file formats to monitor locations and fire spread tracking information and c) FEMGV mesh import filter. It was also utilized complementary software solutions such as RHINO to extract geometries from CAD, FEMGV to develop computational meshes and MayaVi to create three-dimensional visualizations. Mesh cells were created reduced in dimension assigned various properties such as material properties, ignition sites as well as ignition criteria, between others; also attention was given to boundary conditions, airflow patterns, ambient external temperature, when adapting the models (e.g. simulations were performed to guarantee that the airflow pattern could be observed in the model, similarly to what would be expected from an actual aircraft when flying).

#### Possible outputs:

- Flow pattern (velocity vectors)
- Temperature and smoke (line of filled contours) mapping
- 3D data
- Transient data at various locations gathering a total of 32 monitoring data locations

Fire and smoke spread scenarios were accessed to see what the associated outcomes would be; recognizing that before having the correct route to predict possible scenarios data would be required through extensive laboratory characterization – materials heat release rate, material properties, fire spread rate (depending on the fire conditions and dynamics with the substrate), behaviour of these materials when, between others. Thus it is important to understand the problem in study and apply it to the simulation platform; the software itself is recognized to be limited in a sense, and cannot be used straight from the shelf. It was also highlighted that it is important to ensure that key components that will have great influence on the nature of the predictions must be well represented (not depending on their size or shape).

#### 3.3.2.2. CFAST, software short introduction [Ref 28] [Ref 29]

CFAST is the Consolidated model for Fire Growth and Smoke Transport Modeling software developed by the by the Building & Fire Research Laboratory at the National Institutes of Standards and Technology NIST, ([www.nist.gov/el/fire-research-division-73300/product-services/consolidated-fire-and-smoke-transport-model-cfast](http://www.nist.gov/el/fire-research-division-73300/product-services/consolidated-fire-and-smoke-transport-model-cfast)) which is a (two) zoned fire model. Being a zoned modelling code it means that the code is lumped-parameter and each case is divided into two lumped-parameter volumes, in an upper and a lower layer. The last version identified is 4.0.1 since it has been firstly released in 1990.

CFAST is used to calculate distribution of smoke, fire gases and temperature throughout compartments of buildings during a fire as it accounts for smoke, heat and mass transport, within multileveled structures. It provides three-dimensional animations with the results of the CFAST simulation for specific fire's temperatures, various gases concentrations, smoke growth and movement.

#### Possible outputs:

- Mass transfer
- Heat Transfer

Heat and mass transfer can be calculated but concentration of gas species not. Specifying rates of pyrolysis, rates in which gaseous fuel is released by the burning object and consumed by the flame can enrich the code; combustion will be simulated as well proportionally to the oxygen available. Transport of combustion products can be also accounted for.

#### 3.3.2.3. FDS, software short introduction [Ref 29][Ref 30]

FDS is a computational fluid dynamics code that was primarily developed by the Building & Fire Research Laboratory at the National Institutes of Standards and Technology NIST, and it aimed calculating fire-driven flows in enclosures and in the ambient conditions, using a Fortran compiler.

During the years this software have been gaining features and version 6.0 already provides mixture-fraction based combustion and sophisticated radiation modeling.

FDS solves a modified form of Navier-Stokes which allows solving transient flows quickly, for a large number of nodes (especially when compared with other CFD codes) and it can generate direct solutions. It can account for turbulence, combustion (mixture-fraction concept), and heat transfer phenomena (radiation, surface heat transference, and a sprinkler) and tailored boundary conditions.

### 3.3.3. Multidisciplinary MDO-like Approaches

Future research should focus on developing more high level parametric processes for common analyses, such as FEA coupled with CFD and make these tools available for product design, for structural optimization and fire prediction and prevention. Accidents demonstrate that when intense fire starts the resin in the composites will burn and create a self-sustaining fire, as it has been proven during this literature review. It is important to define what boundary conditions are applicable and which CFRP structures can operate to accomplish every airworthiness requirement; new composite materials shall be developed based on the knowledge gained while studying thermal decomposition and flammability of polymers. Added to the thermochemical and thermochemical effects would be also relevant to characterize the influence of variable flames in different contexts, and within different flight conditions, allowing to predict incident heat fluxes but also changes on it through interactions at the boundary-layer gases [Ref 31] [Ref 32] [Ref 33]

Current status:

- Fire tests lack harmonization between ISO2685:1998 and FAR25.856(b) 2003 in terms of sources, method of calibration, test configurations and requirements definition (e.g. fire zones vs. burn through resistances) [15]
- Lack of reproducibility of the same fire test performed by different laboratories [Ref 33]
- Lack of information regarding the fire behavior of composite materials for aircraft [Ref 33]
- Currently the method leads to a pass or fail result [Ref 33]

A multidisciplinary approach could be developed, preferably an evolutive and integrated tool that simulates reliable and dynamic interactions between flame and structure, recognizes and quantifies sub products that are generated and its influence during the combustion of the materials, along its exposure. This approach could integrate CFD and FE modeling tools to generate:

- A) Dynamic modeling of the part degradation, the physical, thermal and chemical phenomena from abrading, as the thermal expansion inducing the apparition of cracks, the thermal degradation of the resin, the internal pressure phenomenon, the gas migration through the material and the thermal delamination - looking at interactions at the direct interface with the fire, through thickness behind the fire and gases being generated,

and

- B) Dynamic modeling of the flame, per location, structure position and shape, per combustion stage, including heat release and irradiation on the surroundings to the part.

A proposal is described below for an MDO like integrated simulation approach:

- Simulation of the whole thermomechanical and thermochemical process (from the front surface to the rear face, per staking configuration)
  - Dynamic degradation by thermal etching and resin pyrolysis
  - Dynamic degradation by thermal delamination and equivalent thermo defects propagation
  - Dynamic degradation by gases generation (qualitative and quantitative)
- Simulation of the whole combustion process (from ignition to combustion stagnation)
  - Dynamic heat transfer in-plane and through thickness by fibre conduction, flame irradiation
  - Dynamic combustion with the surface
  - Dynamic heat and gas flow through thickness
  - Account for the flame enhancing effect: thermal degradation generates gases which, in a certain stage, will enhance the flame and the combustion process
  - Account for the flame cooling effect: decomposition leads to thermal delaminations to occurs; when it happens it generates a sudden decrease in the temperature on the fire front

## 4 MODELLING AND SIMULATION OF THE THERMAL AND CHEMICAL BEHAVIOUR OF THE T700GC/M21 EXPOSED TO HIGH ENERGY LASER BEAM

### 4.1. Introduction to the MoDeTheC solver

Within the frame of the WP7.1, ONERA has been running numerical simulations with the solver named MoDeTheC developed for thermal decomposition of aeronautical composite materials. The development of the MoDeTheC solver was initiated by Valentin Biasi during his PhD thesis [Ref 16] and is still under active development. MoDeTheC is a 2D finite volume solver for unstructured meshes and is based on a multi-species and multi-reactions approach.

In this solver, a decomposing composite material is represented as a mix of different solid and gas species. Solid species are usually fibres or matrix both either at the virgin or charred state, or in a simpler representation, the whole virgin solid phase and the charred phase, as shown in the [Figure 23](#). The gas phase is considered as a mixture of several gases. The generalized pyrolysis model proposed by Lautenberger *et al.* [Ref 17] is taken as a basis, where a composite material is modelled by a set of  $I$  species including  $J$  gaseous species. The subscript  $i$  is used to refer to any species and the subscript  $j$  is used to refer only to a gaseous species. Moreover, a set of  $R$  chemical reactions is defined, describing the decomposition mechanism.

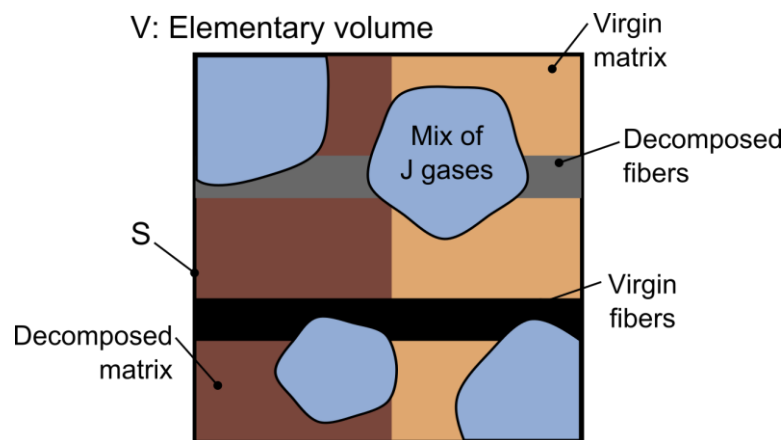


Figure 23 : Scheme of a representative elementary volume with multi-species composition

The present work focuses on thermo-chemical features of decomposing composite materials. The delamination phenomena and all other mechanical damages are presently ignored. Decomposition gases are assumed as inert and ideal, and no liquid species (oil, tar) is considered. Every  $i$  species is modelled as a continuum, in order to apply volume averaging operations. Finally, the local thermal equilibrium is assumed due to the separation between the microscopic scale (pores and fibres size) and the macroscopic scale (composite thickness).

#### 4.1.1. Homogenization laws of material properties

$\varphi_i$  and  $Y_i$  denote respectively the volume fraction and the mass fraction of each  $i$  species.  $\rho_i$  denotes the absolute density (mass of  $i$  divided by volume of  $i$ ) and not the bulk density (mass of  $i$  divided by total volume, which could be expressed as  $\rho Y_i$ ). Absolute density of each solid species is assumed constant ( $\rho_i = \rho_{i0}$  if  $i$  is solid). The weighted density is given by the relation:

$$\rho = \sum_{i=1}^I \rho_i \varphi_i \quad (1)$$

The porosity  $\varphi_g$  is calculated as the volume fraction of the whole gas phase:

$$\varphi_g = \sum_{j=1}^J \varphi_j \quad (2)$$

The molar mass  $M$  of the gaseous phase is given by the relation:

$$M = \frac{1}{\varphi_g} \sum_{j=1}^J \varphi_j M_j \quad (3)$$

The surface emissivity  $\varepsilon$  and absorptivity  $\alpha$  depends only on relative volume fractions of the  $I - J$  solid species:

$$\varepsilon = \frac{1}{\varphi_s} \sum_{i=1}^{I-J} \varphi_i \varepsilon_i \quad (4)$$

$$\alpha = \frac{1}{\varphi_s} \sum_{i=1}^{I-J} \varphi_i \alpha_i \quad (5)$$

with  $\varphi_s$  the volume fraction of the solid phase. The heat capacity of the material  $C_p$  depends on mass fractions and heat capacity of each species, as :

$$C_p = \sum_{i=1}^I C_{p_i} Y_i \quad (6)$$

The equivalent sensible enthalpy of the whole material  $h$  depends on sensible enthalpies  $h_i$  of all  $I$  species weighted respectively by mass fractions. Each  $h_i$  is calculated by integration of specific heat capacity from the initial temperature  $T_0$  to the current temperature  $T$ :

$$h_i(T) = \int_{T_0}^T C_{p_i}(\tau) d\tau \quad \text{and} \quad h(T) = \int_{T_0}^T C_p(\tau) d\tau \quad (7)$$

An ideal gas law is used to calculate the internal pressure as  $P = \rho_g (r_g / M) T$ . A Darcy's law is used to model the transport of gases within the porous medium with  $\mu_g$  the gas dynamic viscosity and  $\overline{\overline{K_p}}$  the permeability, as:

$$\vec{v}_g = - \frac{\overline{\overline{K_p}}}{\mu_g} \vec{\nabla} P \quad (8)$$

$\overline{\overline{K_p}}$  is a second order tensor, due to the anisotropic structure of the medium, and follows a Kozeny-Carman law modelling the decomposition effects by an ideal fibres network:

$$\overline{K_P} = \overline{K_{P0}} \frac{\varphi_g^3}{1-\varphi_g} \quad (9)$$

depending only of the porosity and the initial permeability tensor  $\overline{K_{P0}}$ .

#### 4.1.2. Chemical reactions

A set of  $R$  chemical reactions is considered to model pyrolysis or oxidation transformations. It is assumed that only solid species can react. The general form of the  $k$  reaction is expressed as:



where  $R_k$  is a solid reactant,  $P_k$  is a solid product and  $G_{lk}$  is a gas product (in the set of  $L$  gas products emitted in the  $k$  reaction).  $\nu$  is used to denote stoichiometric mass coefficients. The heat of reaction  $Q_k$  is introduced to express the generated or consumed heat in the  $k$  reaction for each consumed quantity of  $R_k$ . The reaction growth of  $k$  is given by the function  $\alpha_k$ :

$$\alpha_k = 1 - \frac{\varphi_i \rho_i}{(\varphi_i \rho_i)_0} \quad (11)$$

Terms with the subscript "0" correspond to quantities at the initial state (before any reaction begins). This function evolves from 0 at the initial state to 1 when the decomposition reaction is completed. The latter is expressed as a remaining mass ratio of  $R_k$  and is driven by an Arrhenius' law:

$$\frac{\partial \alpha_k}{\partial t} = A_k \cdot \exp\left(\frac{-E_{A_k}}{RT}\right) (1 - \alpha_k)^{n_k} \quad (12)$$

where  $A_k$ ,  $E_{A_k}$  and  $n_k$  are the Arrhenius' parameters for the  $k$  reaction. The mass reaction rate  $\dot{\omega}_{ik}$  (mass loss of  $i = R_k$  per volume unit) is linked to  $\alpha_k$  by the expression:

$$\dot{\omega}_{ik} = -(\varphi_i \rho_i)_0 \frac{\partial \alpha_k}{\partial t} \quad \text{if } i \text{ is a reactant} \quad (13)$$

$$\dot{\omega}_{ik} = \frac{\nu_{lk}}{\nu_{Rk}} \dot{\omega}_{Rk} \quad \text{if } i \text{ is a product} \quad (14)$$

The total mass source term of the  $i$  species (formation and destruction) is the sum of all reaction growth rates  $\dot{\omega}_{ik}$  where  $i$  takes part in the set of  $R$  reactions:

$$\dot{\omega}_i = \sum_{k=1}^R \dot{\omega}_{ik} \quad (15)$$

Another noticeable term is  $\dot{\omega}Q$  referring to the total heat source produced or consumed by the whole  $R$  reactions:

$$\dot{\omega}Q = \sum_{k=1}^R \dot{\omega}_{ik} Q_k \quad (16)$$

where  $Q_k$  is the heat of reaction in  $k$ .

#### 4.1.3. Conservation laws

Heat and mass conservation laws are written for every component at the microscopic scale and a volume averaging method is applied on a representative elementary volume to assess homogenized equations. This section presents the averaged local equations resulting from this procedure. The mass conservation law of each  $i$  solid species is expressed as:

$$\frac{\partial \varphi_i \rho_i}{\partial t} = \dot{\omega}_i \quad (17)$$

where the right hand side term is the mass source term resulting from decomposition reactions. Concerning gas species, a Darcy's law is used to drive the gas phase, as:

$$\frac{\partial \varphi_j \rho_j}{\partial t} + \vec{\nabla} \cdot \left( \frac{Y_j}{Y_g} \rho_g \vec{v}_g \right) = \dot{\omega}_j \quad (18)$$

The mass variations result from gas production as well as bulk gas transport. The mass source term  $\dot{\omega}_i$ , due to decomposition reactions, causes an increase of internal pressure and as a consequence of velocity field driving the gas phase from high pressure zones to lower pressure zones.

The local thermal equilibrium is assumed within the material. As a result there is no local temperature difference between all species. Kinetic energy and pressure work are ignored in the energy conservation. The resulting heat conservation equation for all species is:

$$\frac{\partial \rho h}{\partial t} + \vec{\nabla} \cdot (h_g \vec{v}_g) = \vec{\nabla} \cdot (\bar{k} \vec{\nabla} T) + \dot{\omega}Q \quad (19)$$

In this conservation equation, the left hand side represents the internal energy variation. The first right hand side term is the contribution of conduction fluxes. The last term  $\dot{\omega}Q$  is the energy source term, contribution of all heat released or consumed by all reactions.

#### 4.1.4. Numerical methods

The MoDeTheC solver is developed using a finite volume formulation to discretize the conservation equations developed in the previous section onto unstructured meshes for 2D (planar or axisymmetric) geometries. 3D capabilities are under current developments.

A first order operator-splitting is used to integrate numerically the equations over time. The system is split into two main operators with on one side the advective terms of the heat and mass conservation equations, and on the other side the diffusive and reactive terms.

The time integration of the advective system is performed using an Euler explicit scheme with a CFL criterion to limit the time step. The evaluation of advective fluxes is made using a first order upwind scheme. Gas velocity fields are interpolated at face centres with a least square method.

The time integration of the diffusive-reactive system is performed using an implicit  $\theta$ -scheme. Since Arrhenius-based source terms can cause instability issues due to non-linearity and short characteristic time scales, sub-time steps are used to limit reaction growth rate variations.

## 4.2. Thermo-chemical properties of homogenized T700GC/M21

### 4.2.1. Kinetic model of decomposition reactions

The chosen kinetic model for MoDeTheC simulations is detailed in the D7.7 report and considers 3 reactions with the following mechanism **Figure 24**:

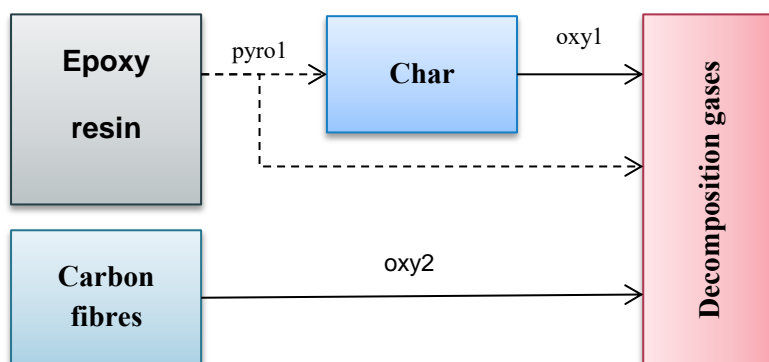


**Figure 24 - 3 reactions thermo-chemical mechanism of T700GC/M21**

The pyrolysis *pyro1* transforms the virgin epoxy resin in char and decomposition gases. The second reaction, named *oxy1*, models the decomposition of the *char* into volatiles and the third reaction, named *oxy2*, models the decomposition of the carbon fibres into volatiles. Gaseous species are not detailed and considered as *decomposition gases* for each reaction. The chemical mechanism is modelled using Arrhenius equations and parameters of *oxy1* and *oxy2* are detailed in the following table:

Reaction	$\nu$	$A$	$E_A$	$n$
<b>pyro1</b>	0.41	2.87e12	1.87e5	1.40
<b>oxy1</b>	-	6.70e4	1.21e5	0.85
<b>oxy2</b>	-	2.78e2	1.18e5	0.28

**Table 1 – Arrhenius parameters of the 3 reactions thermo-chemical mechanism of T700GC/M21**

Figure 25 and Figure 26 show the reconstruction of the numerical values of  $m/m_0$  and  $MLR$  in solid lines compared to experimental values in dashed lines.

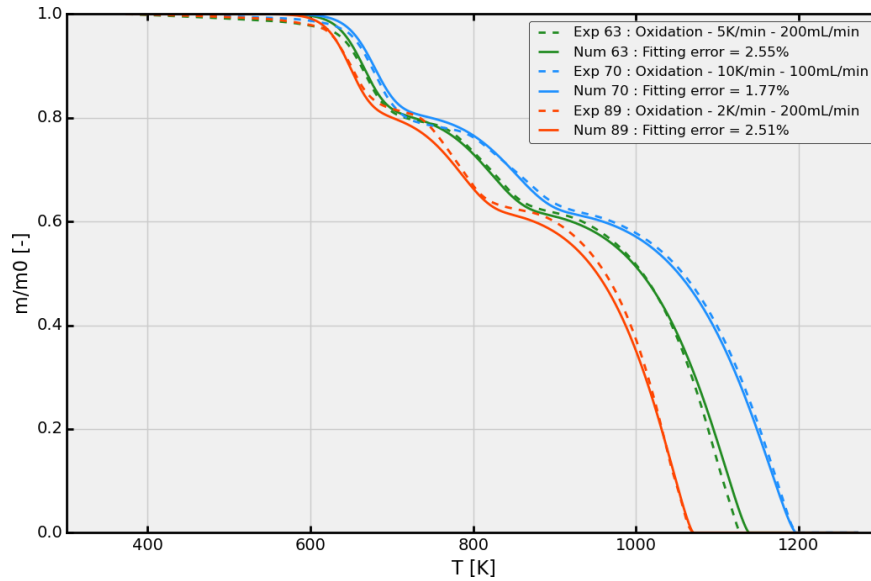


Figure 25 - Relative mass loss reconstruction at 2, 5 and 10K/min in air atmosphere using a 3-stage-model

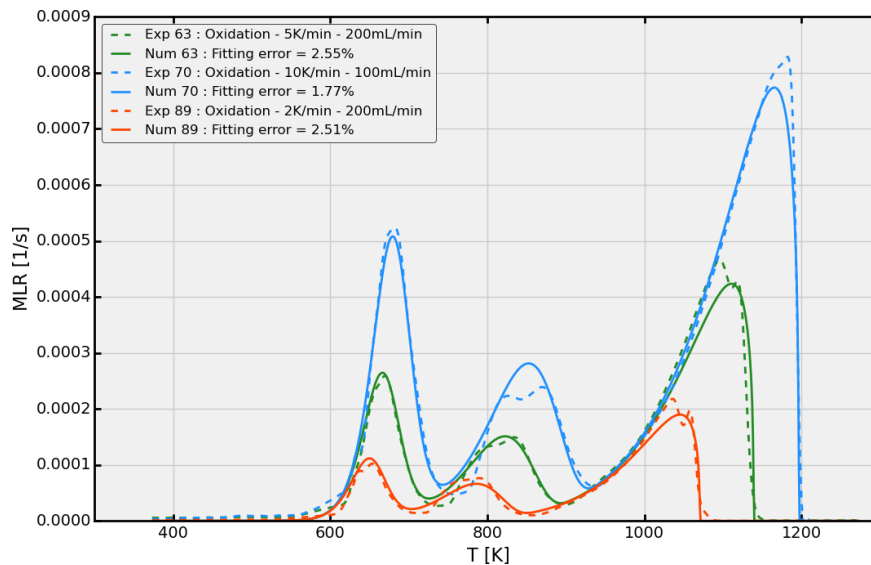


Figure 26 – Mass Loss Rate reconstruction at 2, 5 and 10K/min in air atmosphere using a 3-stage-model

#### 4.2.2. Thermo-physical properties

The Table 2 summarizes the thermo-physical properties of the T700GC/M21 in an unidirectional stacking sequence, characterized in the D7.4, as a function of temperature in the virgin state.

<b>Density</b>	1580	[kg/m3]
<b>Porosity</b>	0.003	[-]
<b>C<sub>p</sub></b>	-504.83 + 4.80 · T [K]	[J/kg/K]

$k_{xx}$	-0.68	+	2.22E-02	.T [K]	[W/m/K]
$k_{yy}$	0.29	+	1.77E-03	.T [K]	[W/m/K]
$k_{zz}$	0.10	+	1.52E-03	.T [K]	[W/m/K]
$\epsilon$	0.884				[-]
$\alpha$	0.904				[-]

Table 2 - Thermo-physical and optical properties of the T700GC/M21 UD in the virgin state

The Figure 27 plots the values of thermal conductivity in main Cartesian coordinates and heat capacity as a function of temperature of the T700GC/M21 in the virgin state. As these properties were characterized up to 373K, values are saturated above in solid line to limit extrapolations plotted in dashed lines for higher temperatures.

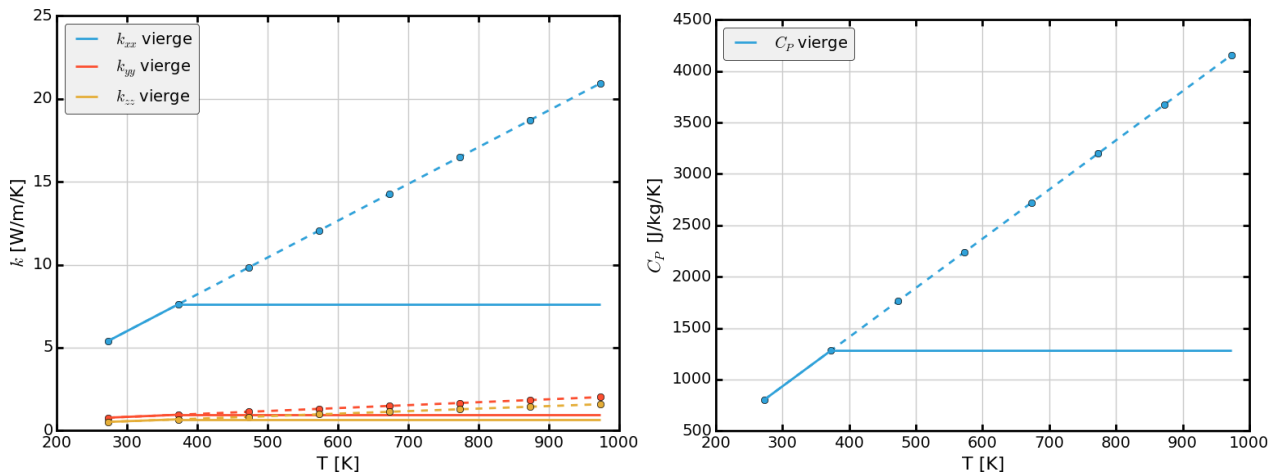


Figure 27 - Reconstruction of thermal conductivity in main Cartesian coordinates and heat capacity as a function of temperature of the T700GC/M21 UD in the virgin state

The Table 3 summarizes the thermo-physical properties of the T700GC/M21 in an unidirectional stacking sequence, characterized in the D7.7, as a function of temperature in the charred state.

Density	1317				[kg/m3]
Porosity	0.19				[-]
$C_p$	-613.43	+	5.3750	.T [K]	[J/kg/K]
$k_{xx}$	-2.76	+	2.92E-02	.T [K]	[W/m/K]
$k_{yy}$	-0.05	+	1.98E-03	.T [K]	[W/m/K]
$k_{zz}$	0.10	+	0.0	.T [K]	[W/m/K]
$\epsilon$	0.895				[-]
$\alpha$	0.93				[-]

Table 3 - Thermo-physical and optical properties of the T700GC/M21 UD in the charred state

The Figure 28 shows the values of thermal conductivity in main Cartesian coordinates and heat capacity as a function of temperature of the T700GC/M21 in the charred state. As these properties were characterized up to 373K, values are saturated above in solid line to limit extrapolations plotted in dashed lines for higher temperatures.

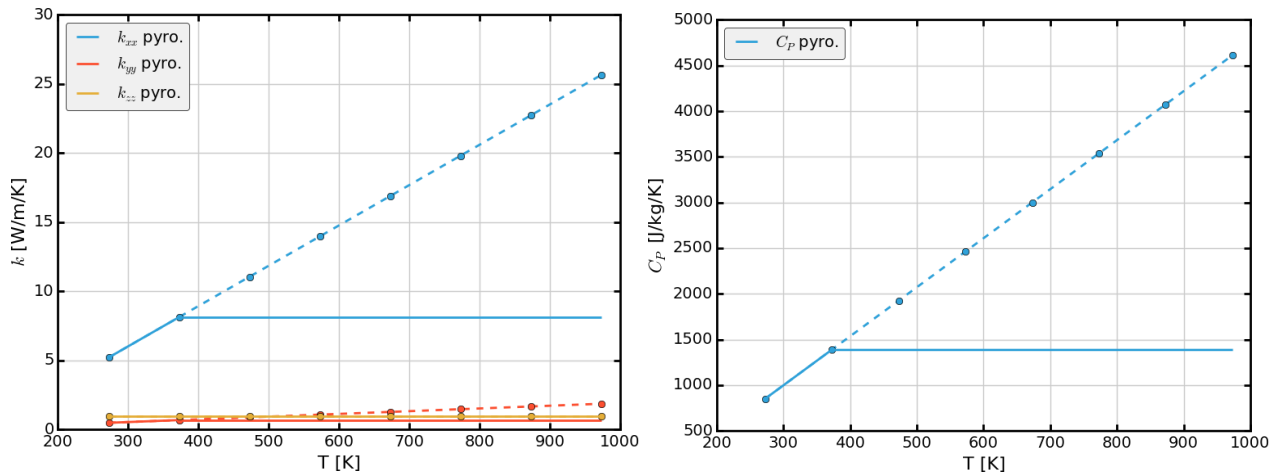


**Figure 28 - Reconstruction of thermal conductivity in main Cartesian coordinates and heat capacity as a function of temperature of the T700GC/M21 UD in the charred state**

From characterizations obtained on the homogenized material and species definition obtained in the TGA analysis, it was necessary to define properties for each species of the model, as a *carbon fibres/epoxy resin/char/decomposition gases* model was proposed. From the properties definition developed in the section 4.1.1, it is possible to evaluate properties of each solid species. **Table 4**, **Table 5** and **Table 6** exhibit the density, heat capacity and optical properties of the solid species.

<b>Density</b>	1800				[kg/m3]
$C_P$	-363.2	+	4.38	.T [K]	[J/kg/K]
$\epsilon$	0.884				[-]
$\alpha$	0.904				[-]

**Table 4 - Thermo-physical and optical properties of the “carbon fibres” species**

<b>Density</b>	1306.9				[kg/m3]
$C_P$	-756.62	+	5.54	.T [K]	[J/kg/K]
$\epsilon$	0.884				[-]
$\alpha$	0.904				[-]

**Table 5 - Thermo-physical and optical properties of the “epoxy resin” species**

<b>Density</b>	1231.9				[kg/m3]
$C_P$	-1440.88	+	8.67	.T [K]	[J/kg/K]
$\epsilon$	0.92				[-]
$\alpha$	0.99				[-]

**Table 6 - Thermo-physical and optical properties of the “char” species**

A Mori-Tanaka homogenization method was proposed to model the evolution of the thermal conductivity as a function of temperature and decomposition state. The Mori-Tanaka model is initially developed to homogenize the elastic mechanical properties of a material composed of a continuous phase, denoted  $\sigma$ , and ellipsoidal inclusions. This formulation is extended to a multi-

species model, where each phase (continuous or dispersal) of this mixture is indexed  $p$ . The expression of the apparent thermal conductivity  $\bar{k}$  is expressed as:

$$\bar{k} = \left( \sum_{p=1}^P \varphi_p k_p \bar{A}_p \right) \left( \sum_{p=1}^P \varphi_p \bar{A}_p \right)^{-1} \quad (20)$$

where  $k_p$  is the thermal conductivity of the  $p$  species and  $\varphi_p$  his volume fraction. The matrix  $\bar{A}_p$  is expressed as:

$$\bar{A}_p = \left( \bar{I} - \bar{S}_p \cdot \frac{k_o - k_p}{k_o} \right)^{-1} \quad (21)$$

where  $k_o$  is the thermal conductivity of the continuous phase.  $\bar{I}$  is the identity matrix and  $\bar{S}_p$  is the Eshelby tensor of  $p$ . If ellipsoidal inclusions can be identified as special cases (sphere, cylinder, plane), the Eshelby tensors turn into elementary matrices 0.

An optimization was performed to determine the inclusion shapes and the thermal conductivity of each species from the characterizations on the virgin and charred materials. The best compromise is a model with the resin as the continuous phase, infinite cylinders for the carbon fibres and planes in the ply direction for the char and the decomposition gases. The cylindrical inclusions for the fibres as well as the continuous phase model for the virgin resin are relevant because of the unidirectional stacking sequence is mixed with a cohesive resin in interlaminar interfaces. In addition, the plane-type inclusions for the gas and the char represent the thermal effects of the decohesions.

The Figure 29 and the Figure 30 show the evolution of characterized thermal conductivity of the virgin and the charred materials (solid lines) between 295 K and 373 K, compared with homogenized values obtained by the Mori-Tanaka model (dashed lines).

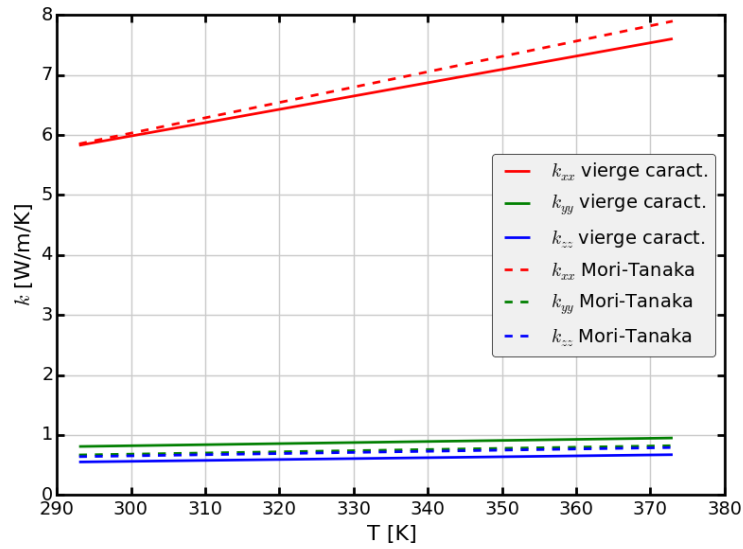


Figure 29 – Reconstruction of the thermal conductivity using a Mori-Tanaka optimization as a function of temperature of the T700GC/M21 UD in the virgin state

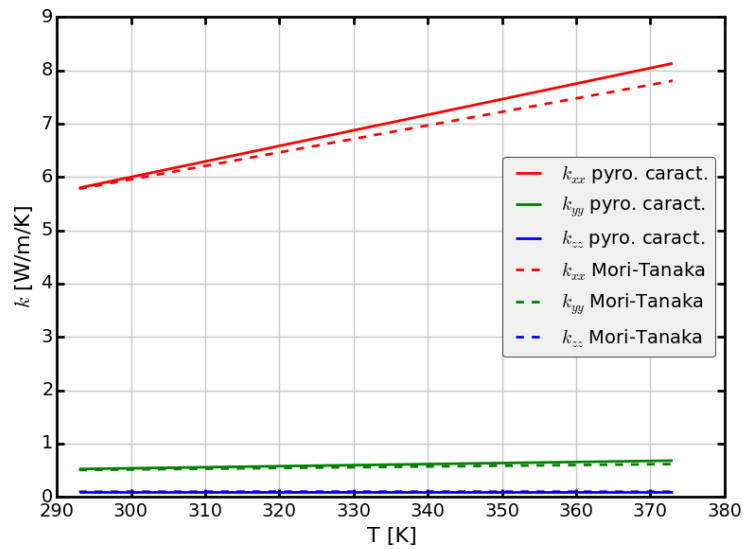


Figure 30 – Reconstruction of the thermal conductivity using a Mori-Tanaka optimization as a function of temperature of the T700GC/M21 UD in the charred state

The Figure 31 shows the thermal conductivity of each solid species as a function of temperature.

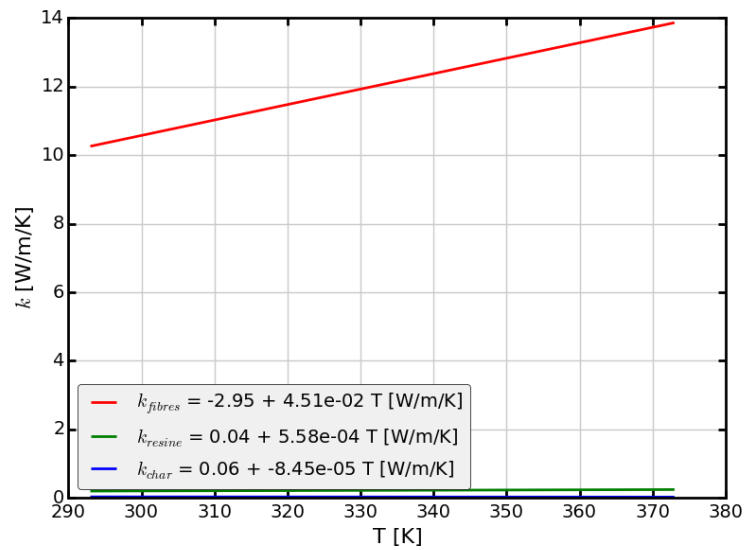


Figure 31 – Reconstruction of the thermal conductivity using a Mori-Tanaka optimization as a function of temperature for each solid species

$\bar{k}$  and  $C_p$  properties were saturated at  $T_{sat} = 373 K$  because extrapolated values evolve in a too large range for high temperatures. Detailed characterizations in this section were performed on an UD stacking sequence but MoDeTheC simulations are 2D axisymmetric and represent an isotropic stacking sequence. The transverse conductivity  $k_{zz}$  is not affected by this change but the radial conductivity  $k_{rr}$  is calculated according to the in-plane conductivity values:

$$k_{rr} = \frac{k_{xx} + k_{yy}}{2} \quad (22)$$

As no thermo-physical characterization of the decomposition gas phase was performed and as these properties have little effects on the thermal behaviour, thermo-physical properties of the decomposition gas phase is taken from [Ref 16], since the studied material is very similar.

### 4.3. MoDeTheC simulations of the BLADE facility

#### 4.3.1. Model definition of the BLADE facility

The BLADE facility named from the French "Banc Laser de cAractérisation et de DEgradation" (characterization and decomposition laser set-up) and presented in Figure 32, is devoted, first, to the characterization of thermo-physical properties of anisotropic materials and second, to the analysis of the thermal response during decomposition of charring materials.

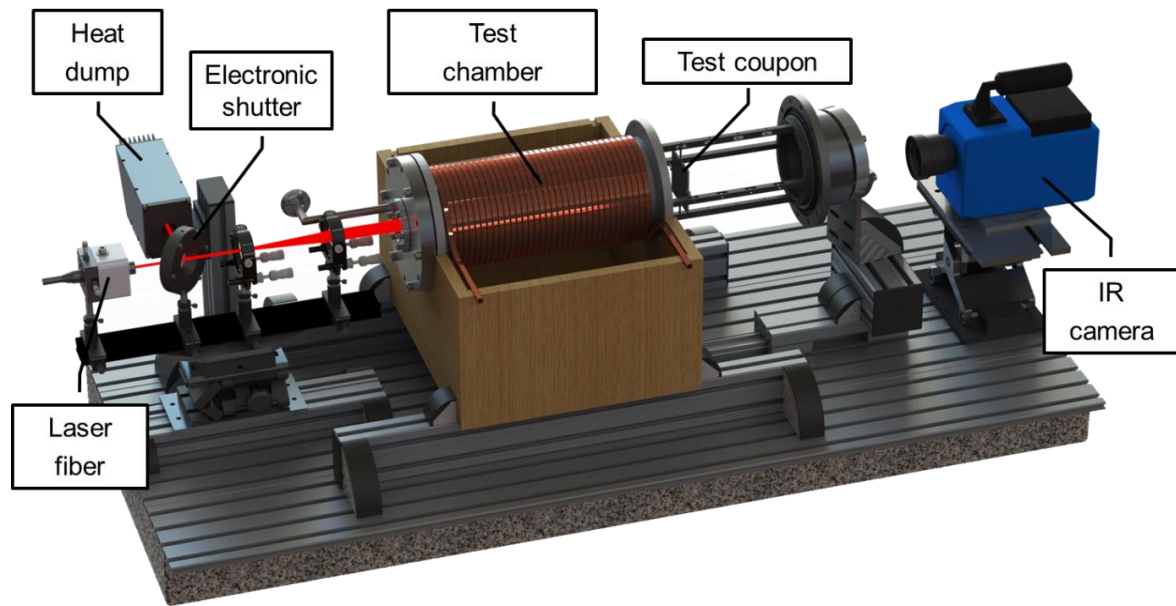


**Figure 32 - Illustration of the BLADE facility: setup and instrumentation**

Even if the apparatus is original, its principle is simple (Figure 33). A square-shaped ( $80 \times 80 \text{ mm}^2$ ) test coupon is located within an air-filled pressure- and temperature-regulated test chamber. The specimen holder consists of 4 small nylon screws for the coupon to stand up straight with minimum contact and thermal loss by conduction. A continuous laser is used to heat up the front side of the test coupon. The laser generates a Gaussian monochromatic beam at the wavelength of  $\lambda = 1080 \text{ nm}$ , collimated at  $\varnothing = 21.8 \text{ mm}$  at  $1/e^2$  and with a maximum power of  $50 \text{ W}$ . The exposure time is accurately controlled with an electronic reflective shutter the diaphragm of which either directs the beam towards a heat dump or opens to heat the coupon up. The transient temperature at the back (unheated) side of the test coupon is measured using quantitative infrared thermography from the test coupon at the initial cold temperature, then during the heating phase up to the cooling phase when the shutter diaphragm is closed and the laser switched off.

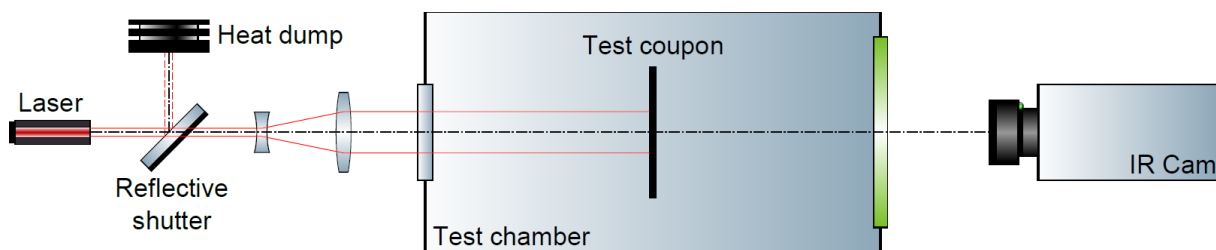


**Figure 33 - Principle of the experiments: thermal characterization and laser-induced decomposition of charring materials**

Within the test chamber, the temperature regulation of the test coupon is governed only by radiation. The inner surface of the test chamber is coated with a high emissivity black paint to maximize the

exchanges. Moreover, the internal pressure is decreased by a vacuum pump that runs continuously during the experiments. The nominal value is set down to 5 *mBar* (500 *Pa*) which is low enough to avoid any convective heat transfer and prevent volatiles from flaming. Indeed, the determination of the convective heat transfer coefficient would have been very difficult even in a simple geometrical configuration.

A 2D axisymmetric model was adopted in this study. Figure 34 represents the computational domain as well as the boundaries in the BLADE configuration. The geometry represents the half-plane of the median section of the coupon. The domain is composed of 4 limits: the axis, the free OUTER boundary, the upper TOP boundary exposed to the laser ( $y = 2.28 \text{ mm}$ ) and the lower free BOTTOM boundary ( $y = 0 \text{ mm}$ ). The axis is processed as a symmetry condition. It is assumed that the external pressure is known and constant during the degradation for all boundaries to model the condition imposed by the use of a vacuum pump which regulates the test chamber at a pressure  $P_0 = 500 \text{ Pa}$ . In the initial state, the whole domain is at  $T_0 = 295 \text{ K}$  and  $P_0 = 500 \text{ Pa}$ . All convective transfers are neglected and the radiative transfers are considered between the composite coupons at the surface temperature of the material and the internal walls of the test chamber, at a constant and uniform temperature  $T_0 = 295 \text{ K}$ .

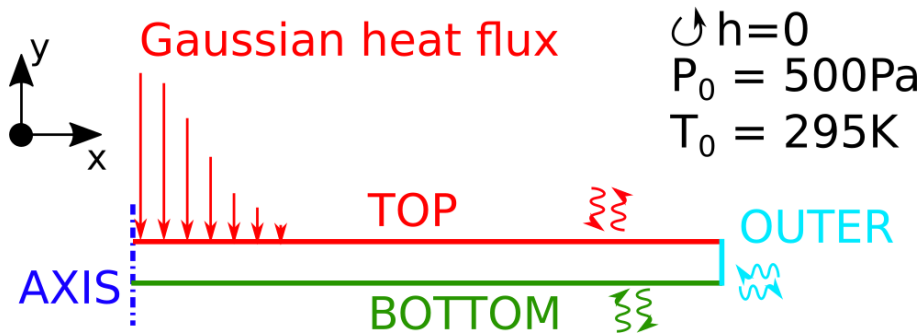


Figure 34 : MoDeTheC model of the BLADE domain

The domain is discretized according to a 2D mesh (cf. Figure 35) in quadrangles of  $50 \times 24$  cells, with a refinement in the  $x$ -direction in the zones close to the axis.

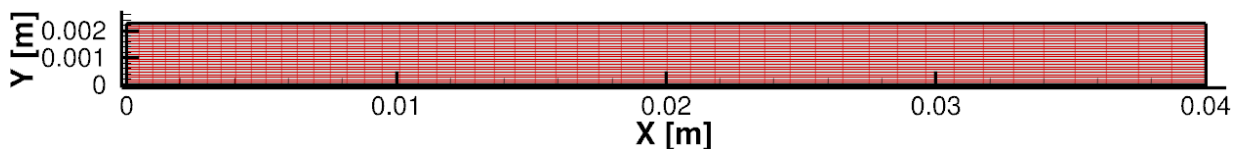
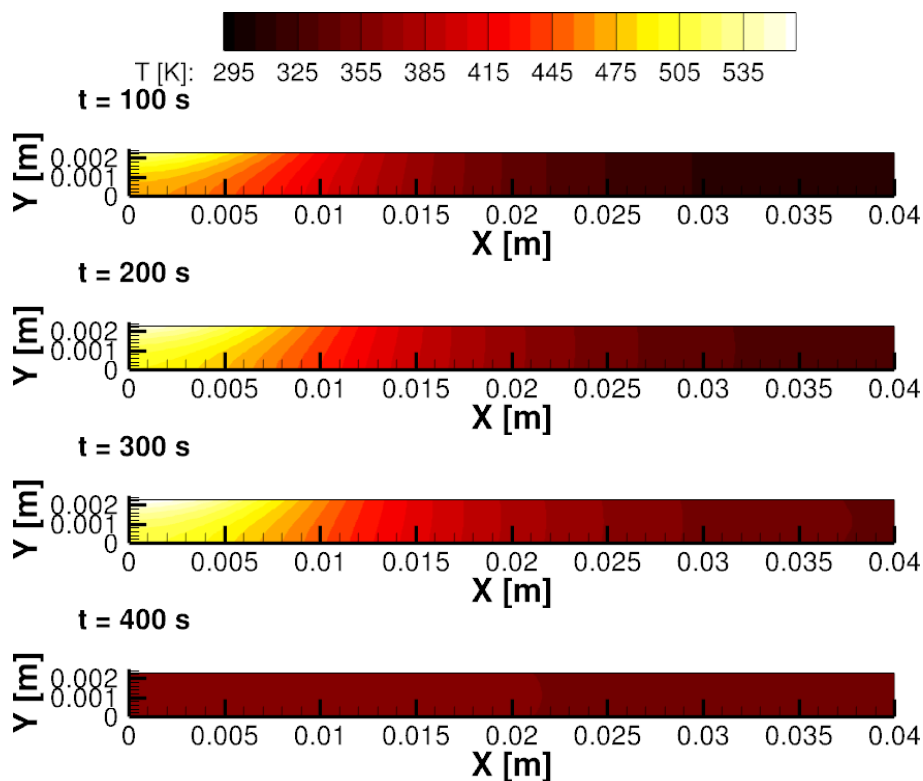


Figure 35 : 2D mesh of the BLADE configuration

### 4.3.2. Impinging flux at 53.7kW/m<sup>2</sup>

#### 4.3.2.1. Temperature evolution

Figure 36 shows the temperature fields extracted from the simulation of the T700GC/M21 decomposition exposed to a 53.7 kW/m<sup>2</sup> laser flux at different times during the 300 s exposure. From  $t = 300$  s, the material is no longer heated and the temperature quickly homogenizes, as shown by the field at  $t = 400$  s.



**Figure 36 - Temperature fields at different times from the T700GC/M21 ISO simulation exposed to a 53.7 kW/m<sup>2</sup> laser beam**

Figure 37 exhibits the evolution of the temperature along the front surface as a function of time at different locations spaced each 5 mm from the centre. The maximum temperature on the front face is 566 K at  $t = 300$  s. Figure 38 shows the evolution of the temperature along the back surface as a function of time and at different locations, and compared to the temperature measurements detailed in the D7.7 report. Comparisons to experimental measurements show a very good agreement in the first instants regardless of the position on the profile of the back surface. The maximum deviation is observed at the centre of the back surface at  $t = 300$  s and is equal to 11 K. The cooling phase is well reproduced with a rapid homogenization of the temperature and a maximum deviation between measurements and simulations of 13 K approximately.

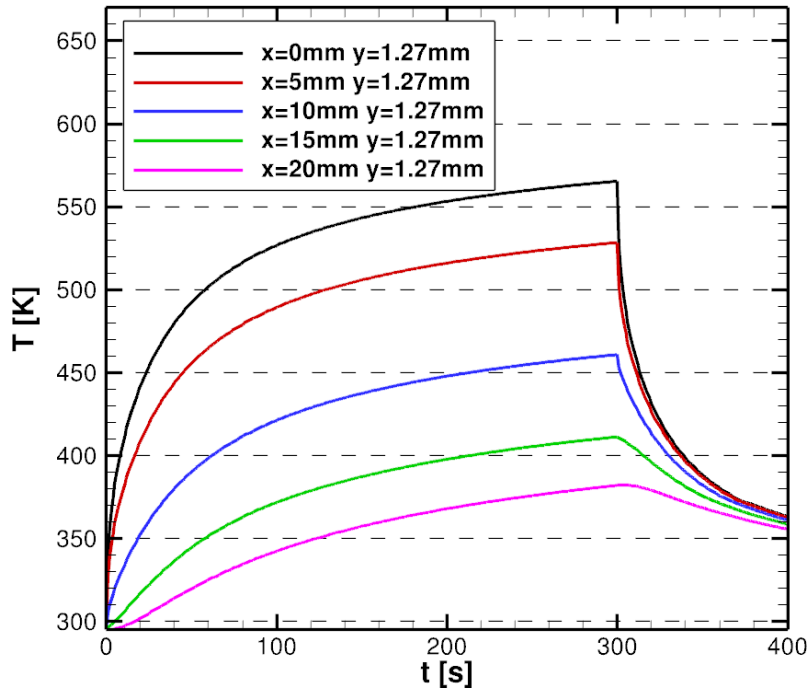


Figure 37 - Temperature evolution at different positions along the front surface from the T700GC/M21 ISO simulation exposed to a  $53.7 \text{ kW/m}^2$  laser beam

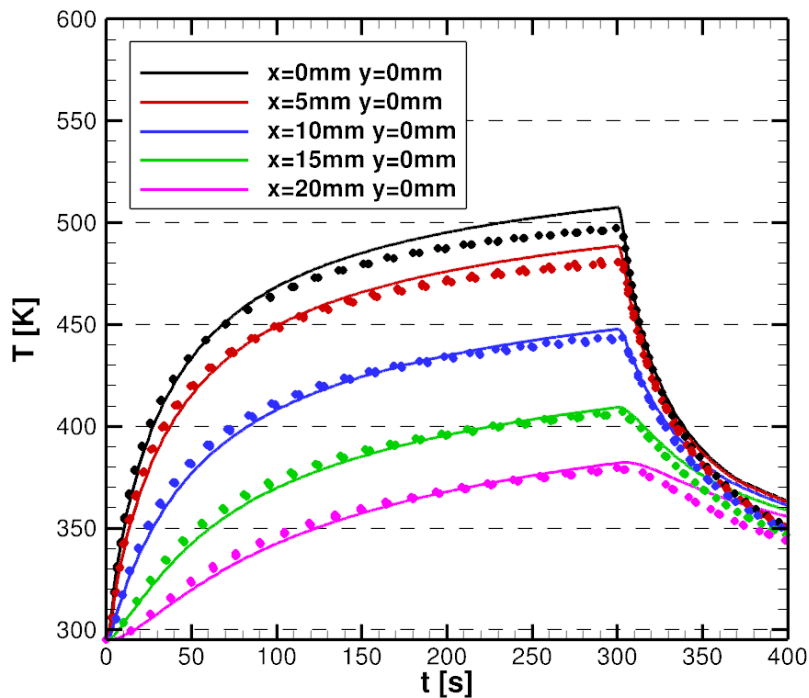


Figure 38 - Temperature evolution at different positions along the back surface from the T700GC/M21 ISO simulation exposed to a  $53.7 \text{ kW/m}^2$  laser beam and compared to experimental measurements

### 4.3.2.2. Decomposition growth rate

Figure 39 shows the  $\alpha_{pyro}$  field at the end of the simulation for the  $53.7 \text{ kW/m}^2$  laser flux test case, and also an iso-contour  $\alpha_{pyro} = 0.2$ , which was identified by Mouritz et al. [Ref 18] as an empirical threshold for the visible char.

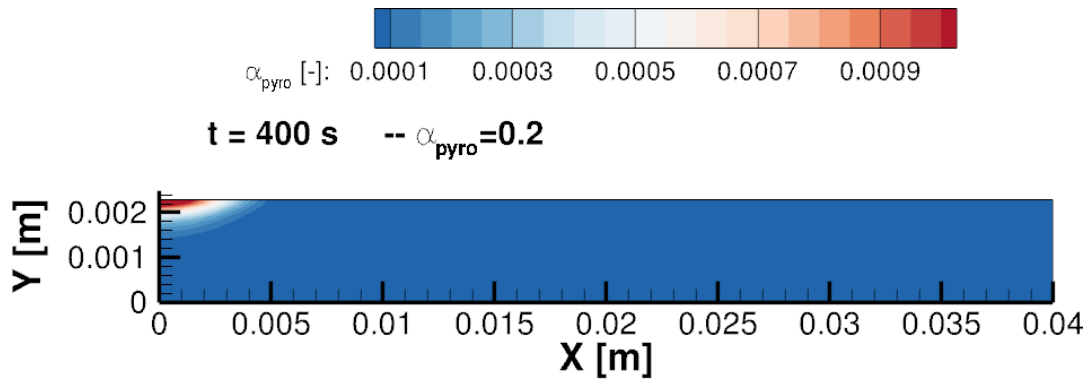


Figure 39 – Final pyrolysis evolution function field of the T700GC/M21 ISO simulation exposed to a  $53.7 \text{ kW/m}^2$  laser beam

Figure 40 shows the  $\alpha_{oxy}$  at the end of the simulation for the  $53.7 \text{ kW/m}^2$  laser flux test case. The heat flux is not high enough to activate the oxidation reactions since only zones nearby the axis have a significant pyrolysis reaction growth ( $\alpha_{pyro \text{ max}} = 0.001$ ).

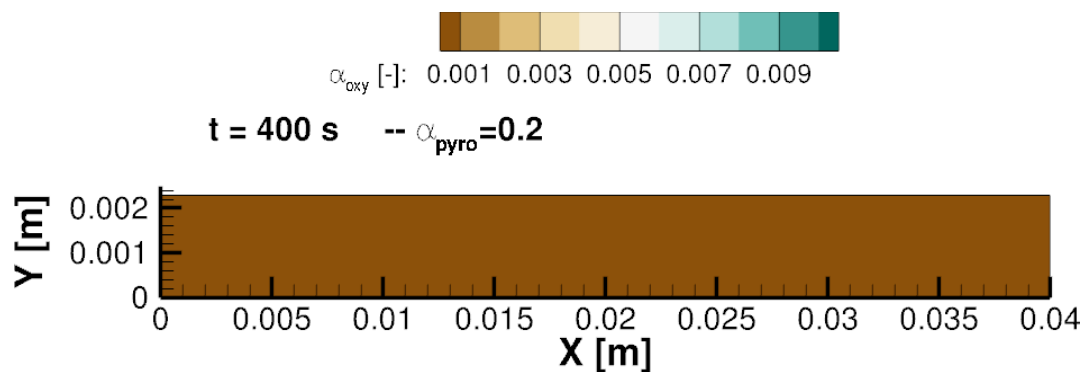
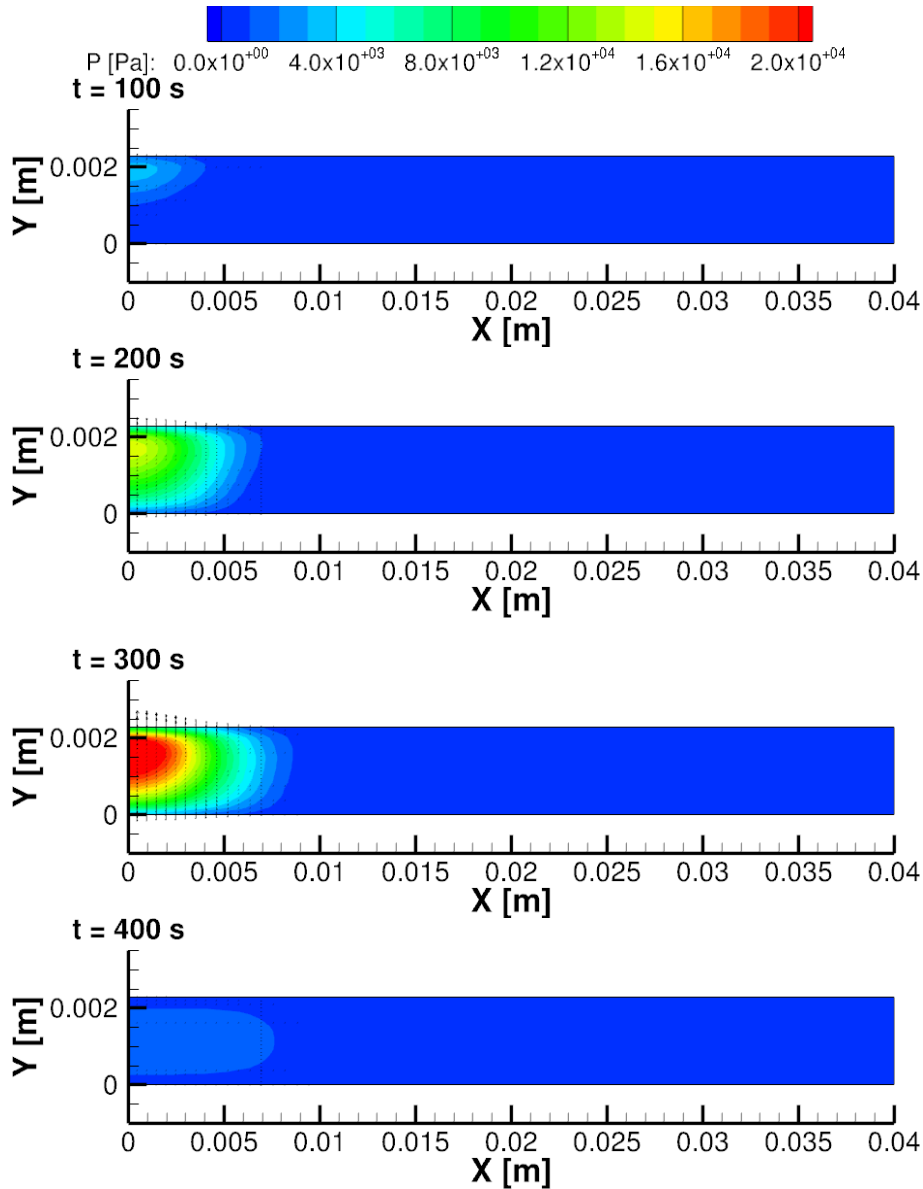


Figure 40 : – Final char oxidation evolution function field of the T700GC/M21 ISO simulation exposed to a  $53.7 \text{ kW/m}^2$  laser beam

The evolution of the decomposition reactions shows that the mass loss is insignificant whereas the experimental measurements confirm a mass loss of 0.03 %.

### 4.3.2.3. Internal pressure evolution

Figure 41 shows the internal pressure fields as well as the internal gas transport velocity vectors from the T700GC/M21 ISO simulation exposed to a  $53.7 \text{ kW/m}^2$  laser beam at different times. The internal pressure increases because of the formation decomposition gases in areas near the symmetry axis. The gas velocity vectors indicate that the gaseous products exit mainly through the centre of the front surface, where the permeability slightly increased due to the pyrolysis reaction.



**Figure 41 : Internal pressure fields at different moments from the T700GC/M21 ISO simulation exposed to a  $53.7 \text{ kW/m}^2$  laser beam**

Figure 42 shows the evolution of the internal pressure as a function of time in the mid-plane at different locations spaced every 5 mm. The pressure peak is located along the axis of symmetry and

achieves  $P = 0.21 \text{ bar}$ . As soon as the laser heating stops, the pressure falls down because the gas production is stopped and the remaining gases are very quickly released.

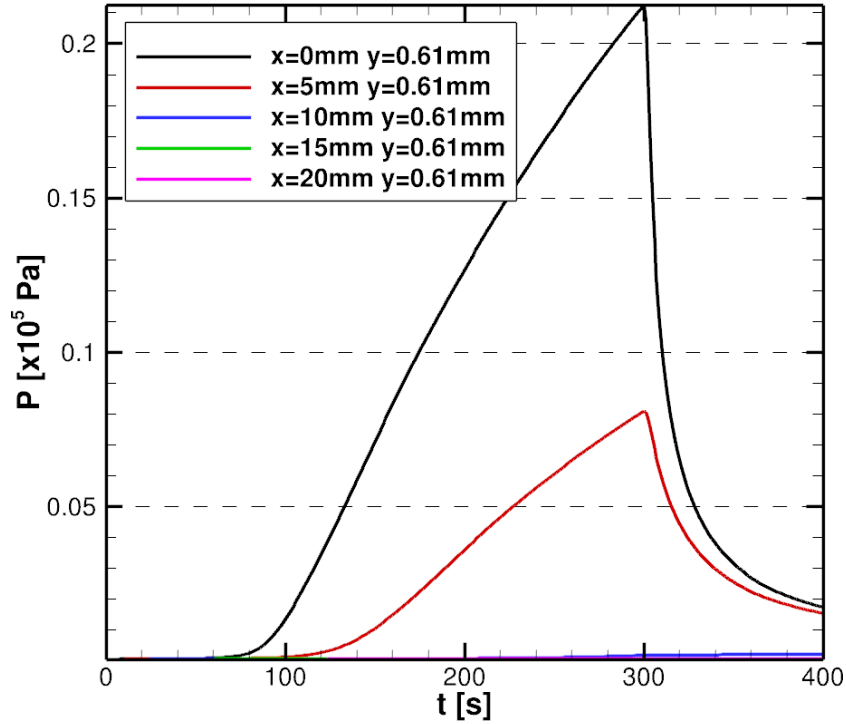
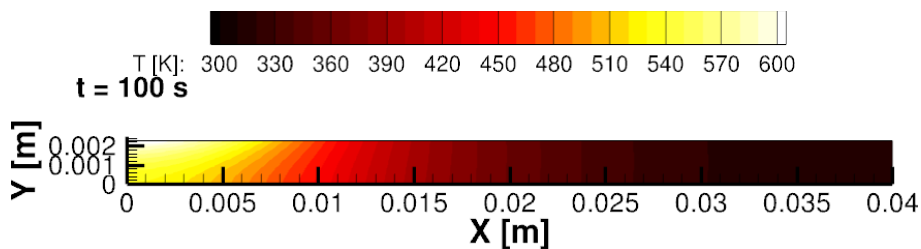


Figure 42 : Internal pressure evolution at different positions along the mid-plane from the T700GC/M21 ISO simulation exposed to a  $53.7 \text{ kW/m}^2$  laser beam

### 4.3.3. Impinging flux at $76.2 \text{ kW/m}^2$

#### 4.3.3.1. Temperature evolution

Figure 36 shows the temperature fields extracted from the simulation of the T700GC/M21 decomposition exposed to a  $76.2 \text{ kW/m}^2$  laser flux at different times during the 300 s exposure. From  $t = 300 \text{ s}$ , the material is no longer heated and the temperature quickly homogenizes, as shown by the field at  $t = 400 \text{ s}$ .



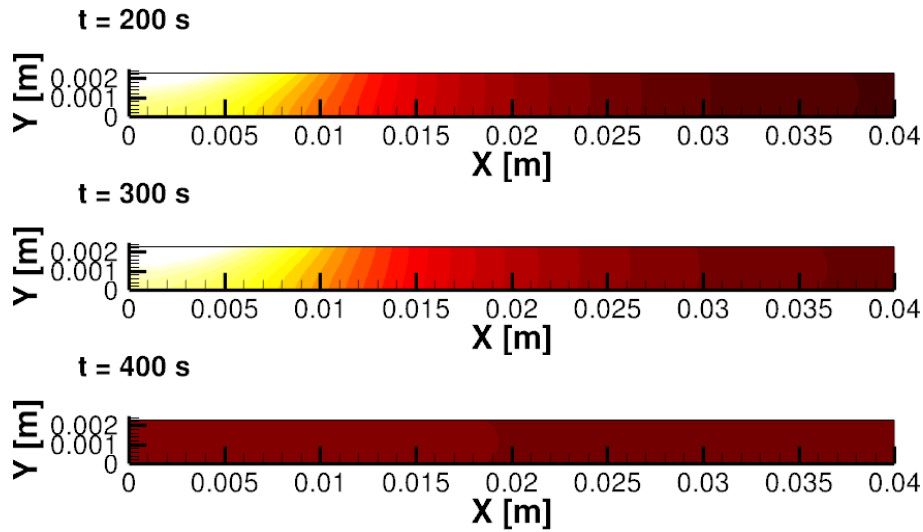


**Figure 43 - Temperature fields at different moments from the T700GC/M21 ISO simulation exposed to a  $76.2\text{ kW}/\text{m}^2$  laser beam**

On Figure 37 is plotted the evolution of the temperature along the front surface as a function of time at different positions spaced every 5 mm from the centre. The maximum temperature on the front surface is 607 K at  $t = 300\text{ s}$ . Figure 38 shows the evolution of the temperature along the back surface as a function of time and at different locations, and compared to the temperature measurements detailed in the D7.7 report. Comparisons to experimental measurements confirm a very good agreement in the first moments regardless of the location of the profile on the back surface. The mechanical damages affect the continuity of the thermal response, especially close to the axis. The cooling phase is well reproduced with a quick homogenization of the temperature and a maximum deviation between measurements and simulations of 15 K approximately.

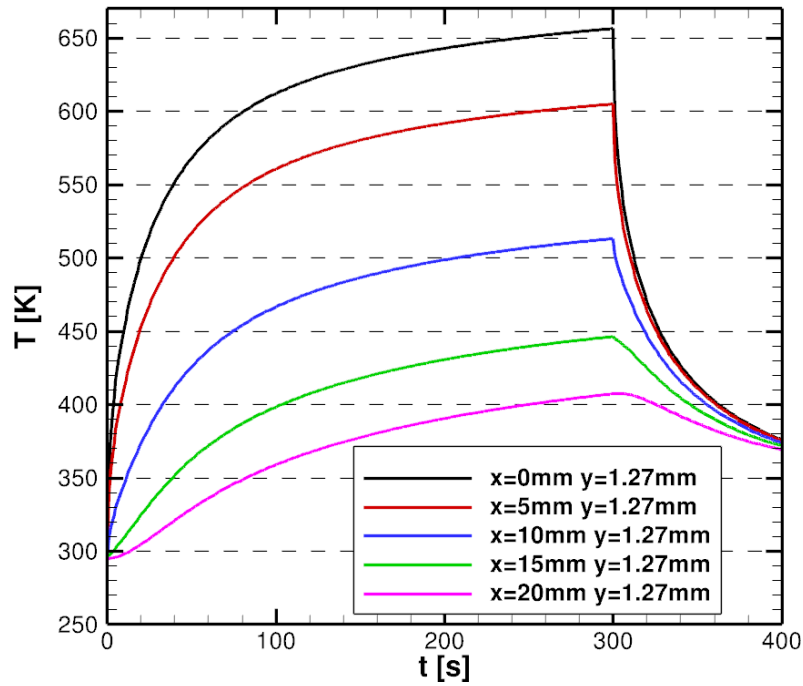


Figure 44 - Temperature evolution at different positions along the front surface from the T700GC/M21 ISO simulation exposed to a  $76.2 \text{ kW/m}^2$  laser beam

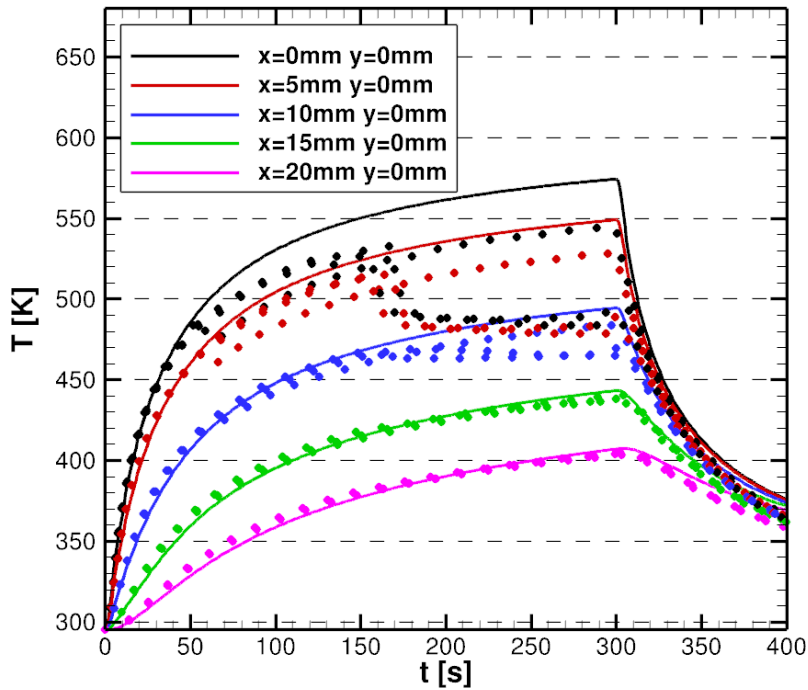


Figure 45 - Temperature evolution at different positions along the back surface from the T700GC/M21 ISO simulation exposed to a  $76.2 \text{ kW/m}^2$  laser beam and compared to experimental measures

### 4.3.3.2. Decomposition growth rate

Figure 39 shows the  $\alpha_{pyro}$  field at the end of the simulation for the  $76.2 \text{ kW/m}^2$  laser flux test case, and also an iso-contour  $\alpha_{pyro} = 0.2$ , which was identified by Mouritz et al [Ref 18] as an empirical threshold for the visible char.

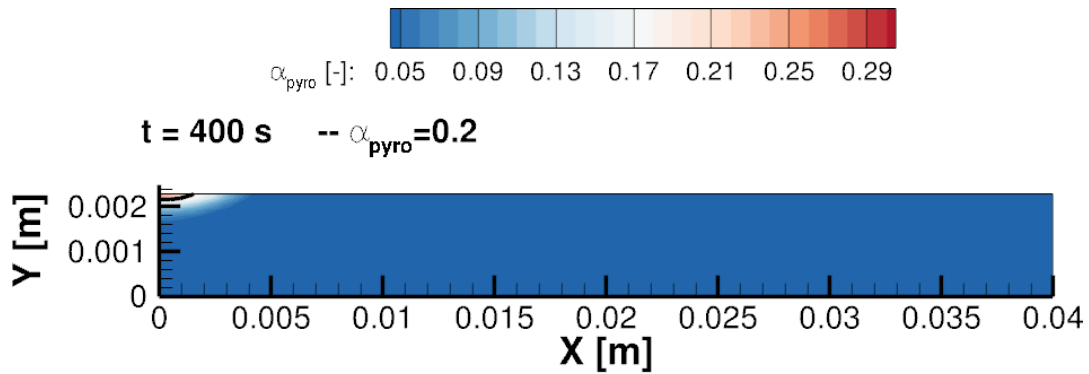


Figure 46 – Final pyrolysis evolution function field of the T700GC/M21 ISO simulation exposed to a  $76.2 \text{ kW/m}^2$  laser beam

Figure 40 exhibits the  $\alpha_{oxy}$  at the end of the simulation for the  $76.2 \text{ kW/m}^2$  laser flux test case. The heat flux is not high enough to activate the oxidation reactions since only zones very close to the axis have a significant pyrolysis reaction growth ( $\alpha_{pyro \text{ max}} = 0.29$ ).

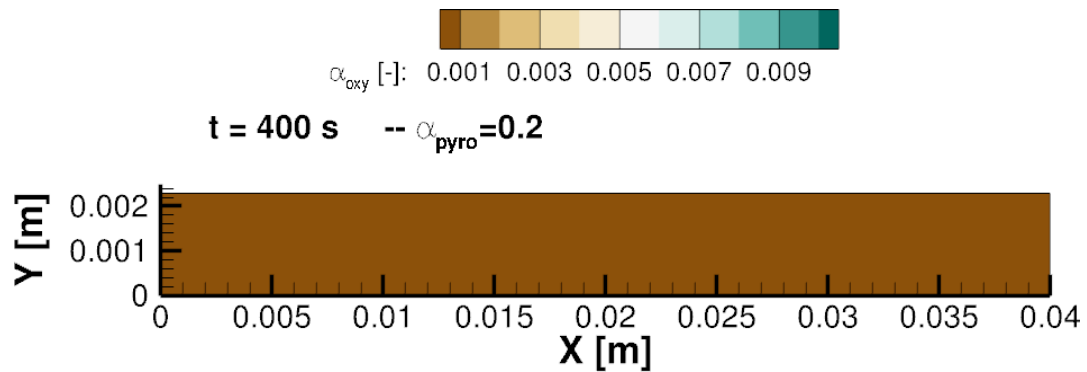
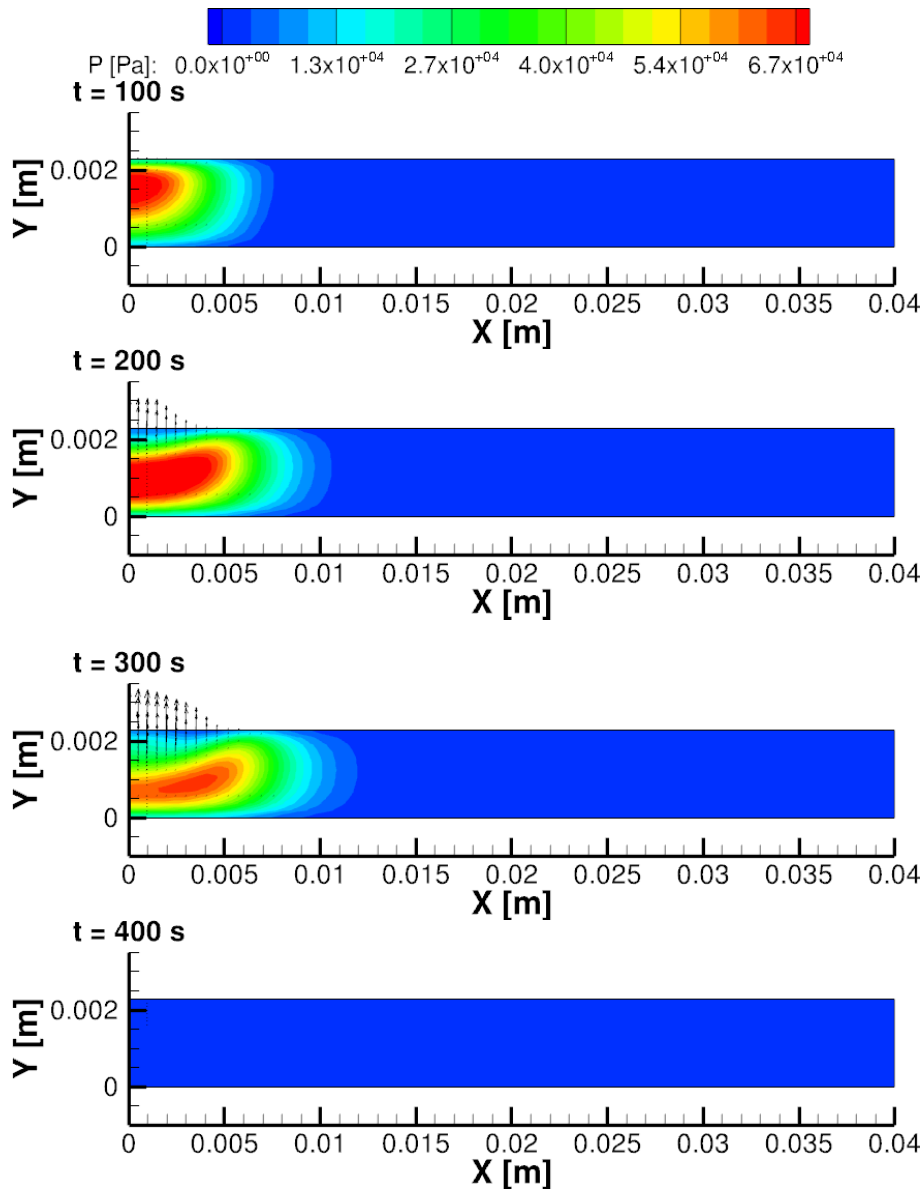


Figure 47 : – Final char oxidation evolution function field of the T700GC/M21 ISO simulation exposed to a  $76.2 \text{ kW/m}^2$  laser beam

The evolution of the decomposition reactions shows that the mass loss is insignificant whereas the experimental measurements confirm a mass loss of 0.06 %.

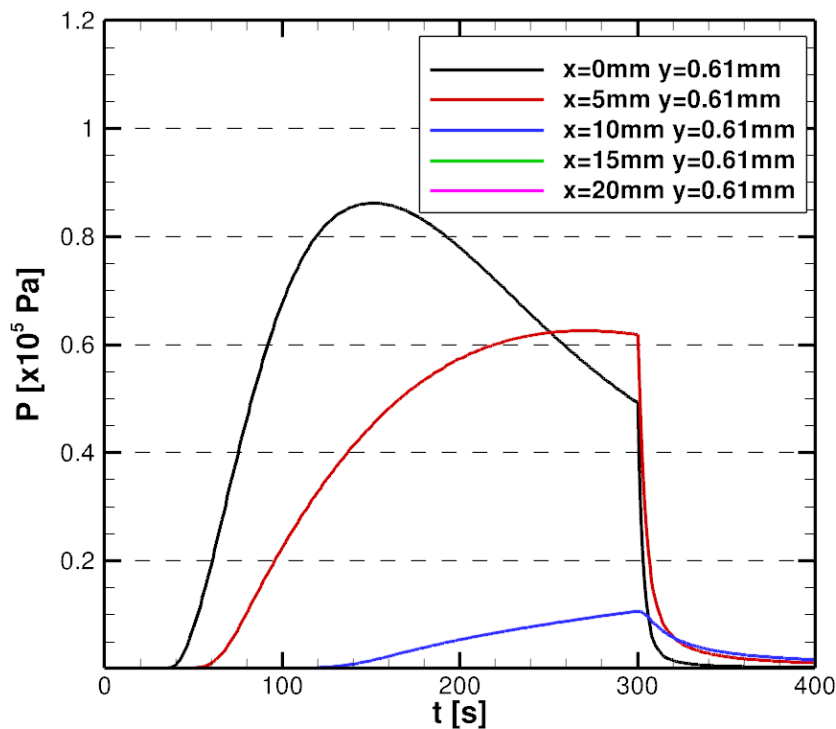
### 4.3.3.3. Internal pressure evolution

Figure 41 shows the internal pressure fields as well as the internal gas transport velocity vectors from the T700GC/M21 ISO simulation exposed to a  $76.2 \text{ kW/m}^2$  laser beam at different times. The internal pressure increases because of the formation decomposition gases in areas nearby the symmetry axis. The gas velocity vectors indicate that the gaseous products exit mainly through the centre of the front face, where the permeability increased due to the pyrolysis reaction.



**Figure 48 : Internal pressure fields at different moments from the T700GC/M21 ISO simulation exposed to a  $76.2 \text{ kW/m}^2$  laser beam**

**Figure 42** shows the evolution of the internal pressure as a function of time in the mid-plane at different positions spaced every 5 mm. The pressure peak is located along the axis of symmetry and achieves  $P = 0.87 \text{ bar}$ , and slides to the peripheral regions. As soon as the laser heating stops, the pressure falls down because the gas production is stopped and the remaining gases are very quickly released.



**Figure 49 : Internal pressure evolution at different positions along the mid-plane from the T700GC/M21 ISO simulation exposed to a  $76.2 \text{ kW/m}^2$  laser beam**

#### 4.3.4. Impinging flux at $101.2 \text{ kW/m}^2$

##### 4.3.4.1. Temperature evolution

Figure 36 shows the temperature fields extracted from the simulation of the T700GC/M21 decomposition exposed to a  $101.2 \text{ kW/m}^2$  laser flux at different times during the 300 s exposure. From  $t = 300 \text{ s}$ , the material is no longer heated and the temperature quickly homogenizes, as shown by the field at  $t = 400 \text{ s}$ .

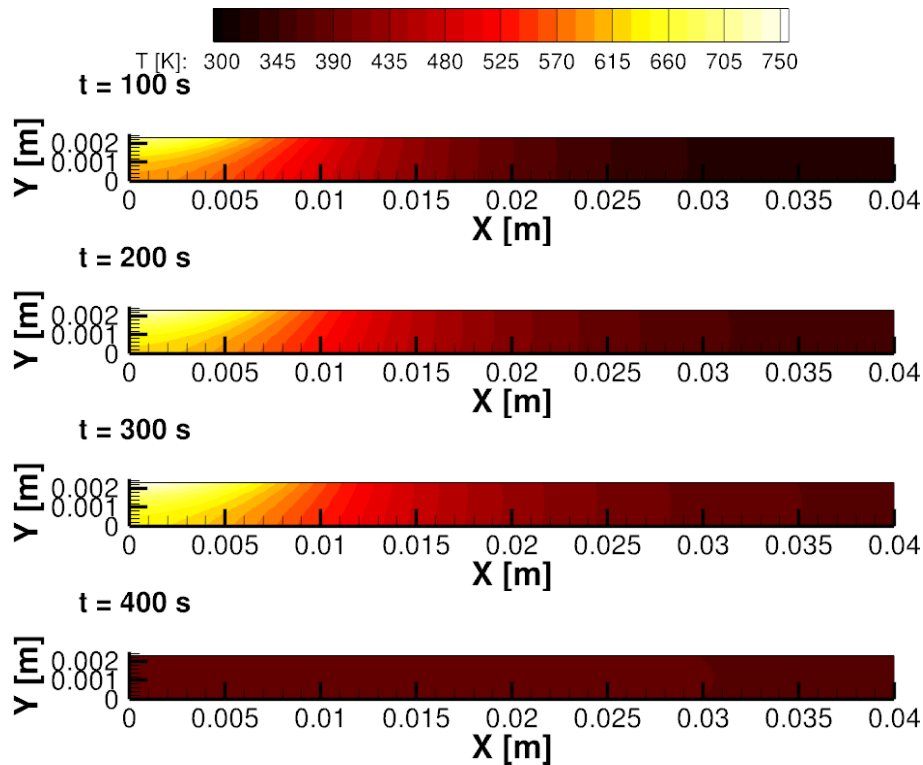


**Figure 50 - Temperature fields at different moments from the T700GC/M21 ISO simulation exposed to a 101.2 kW/m<sup>2</sup> laser beam**

Figure 37 exhibits the evolution of the temperature along the front surface as a function of time at different locations spaced every 5 mm from the centre. The maximum temperature on the front face is 754 K at  $t = 300\text{ s}$ . Figure 38 shows the evolution of the temperature along the back surface as a function of time and at different locations, and compared to the temperature measurements detailed in the D7.7 report. Comparisons to experimental measurements confirm a very good agreement in the first moments regardless of the location of the profile on the back surface. The mechanical damages affect the continuity of the thermal response, especially near the axis. The cooling phase is well reproduced with a quick homogenisation of the temperature and a maximum deviation between measurements and simulations of 16 K approximately.

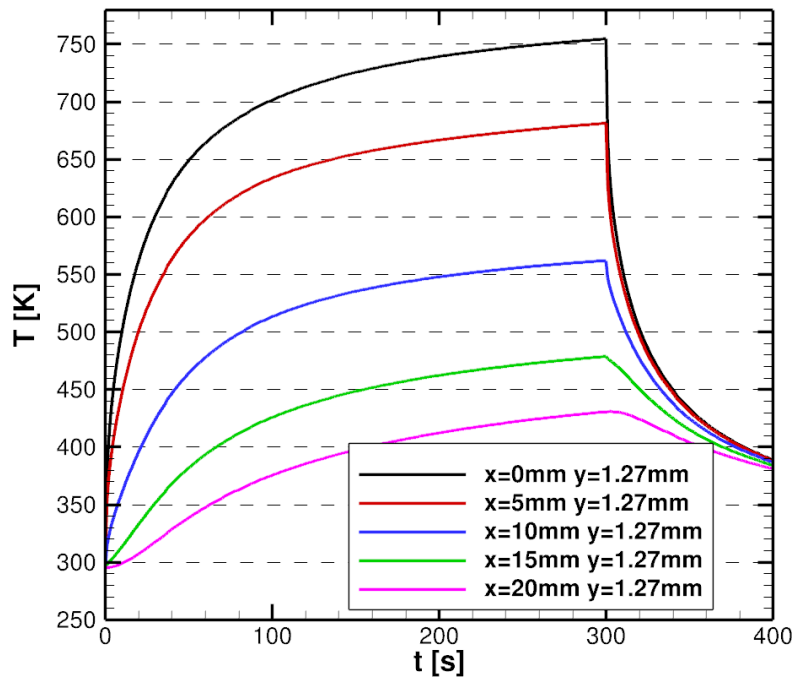


Figure 51 - Temperature evolution at different positions along the front surface from the T700GC/M21 ISO simulation exposed to a  $101.2 \text{ kW/m}^2$  laser beam

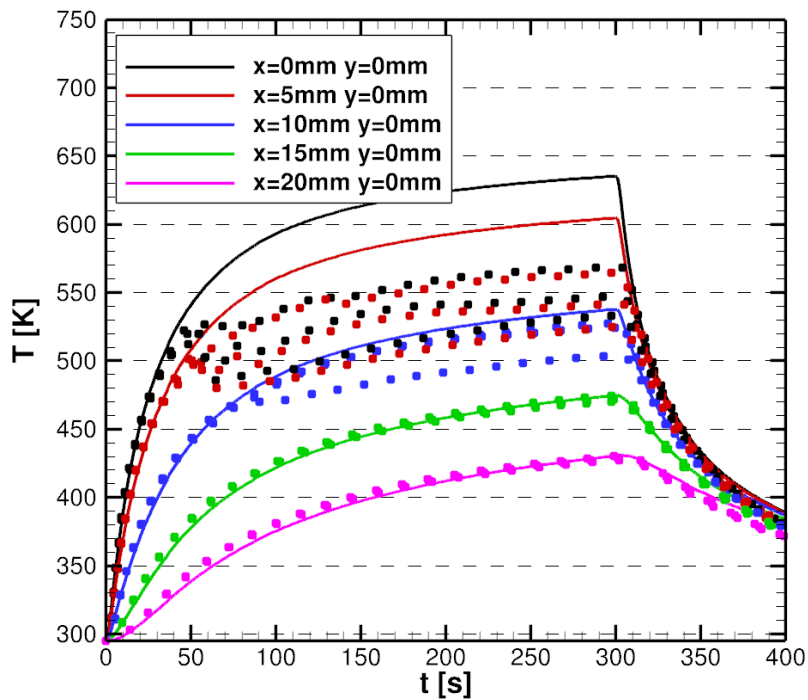


Figure 52 - Temperature evolution at different positions along the back surface from the T700GC/M21 ISO simulation exposed to a  $101.2 \text{ kW/m}^2$  laser beam and compared to experimental measures

#### 4.3.4.2. Decomposition growth rate

Figure 39 shows the  $\alpha_{pyro}$  field at the end of the simulation for the  $101.2 \text{ kW/m}^2$  laser flux test case, and also an iso-contour  $\alpha_{pyro} = 0.2$ , which was identified by Mouritz et al. [Ref 18] as an empirical threshold for the visible char.

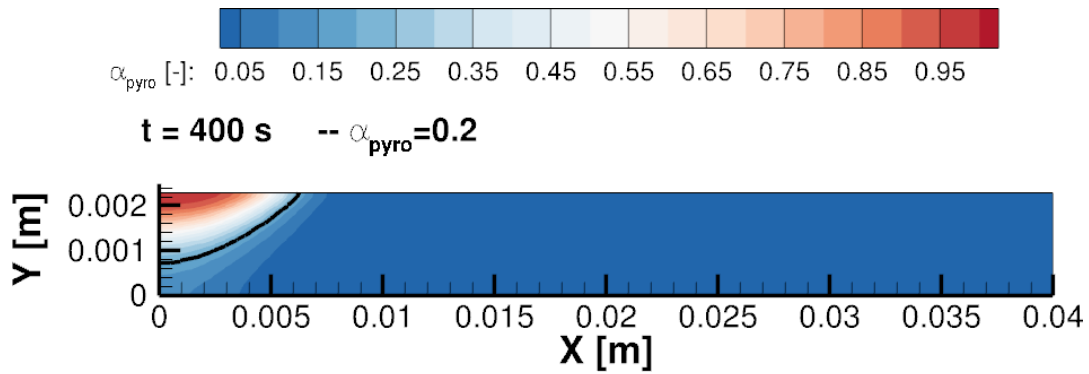


Figure 53 – Final pyrolysis evolution function field of the T700GC/M21 ISO simulation exposed to a  $101.2 \text{ kW/m}^2$  laser beam

Figure 40 plots the  $\alpha_{oxy}$  at the end of the simulation for the  $101.2 \text{ kW/m}^2$  laser flux test case. The heat flux is not high enough to activate the oxidation reactions since only zones very close to the axis have a significant level ( $\alpha_{oxy \max} = 0.01$ ).

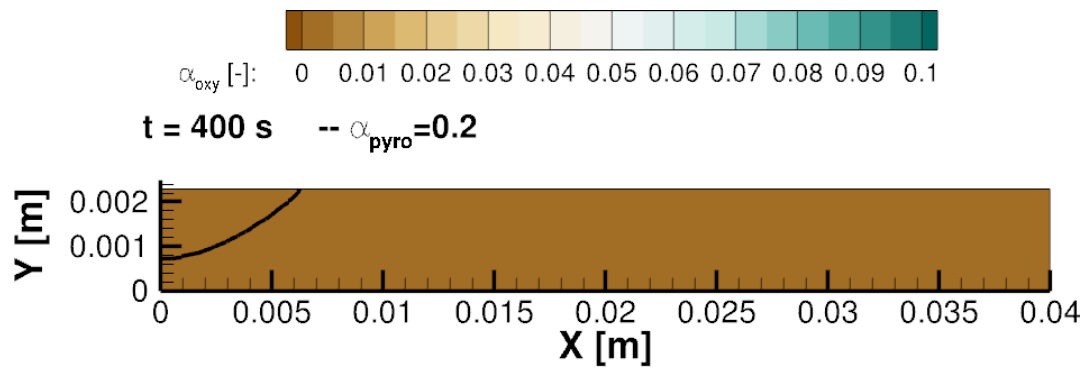
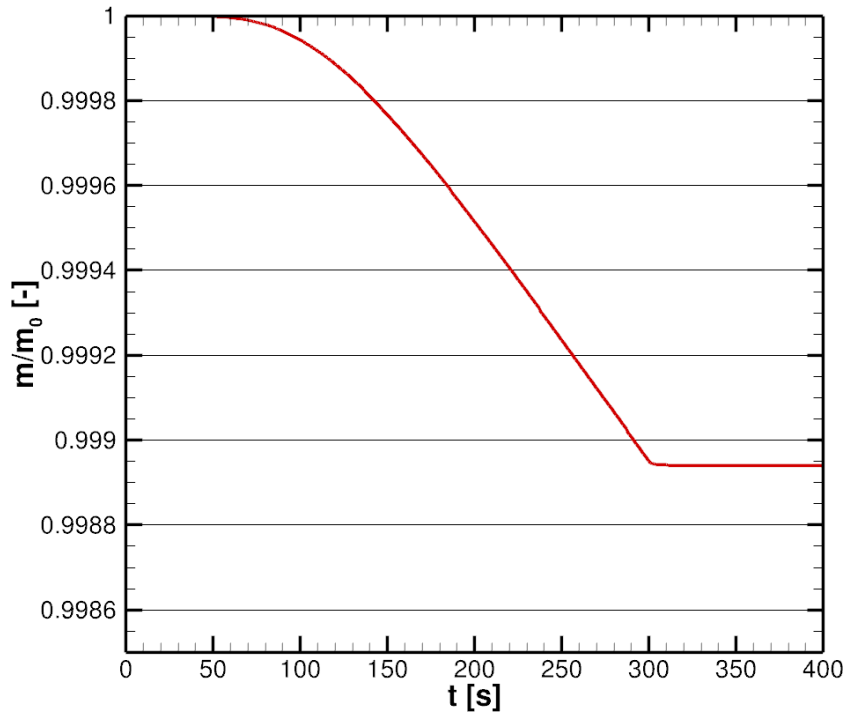


Figure 54 : – Final char oxidation evolution function field of the T700GC/M21 ISO simulation exposed to a  $101.2 \text{ kW/m}^2$  laser beam

Figure 55 shows the evolution of the relative mass loss of the coupon, weighted by a  $4/\pi$  coefficient in order to be representative of the mass loss of a square plate using a 2D axisymmetric simulation. The evolution of the mass loss is almost linear from 100 s until the laser heating stops. The total mass loss estimate is 0.105 %, which is very consistent with the experimental measurements (from 0.16 % to 0.18 %).



**Figure 55 :** Relative mass loss along time of the T700GC/M21 ISO simulation exposed to a  $53.7 \text{ kW/m}^2$  laser beam

#### 4.3.4.3. Internal pressure evolution

Figure 41 shows the internal pressure fields as well as the internal gas transport velocity vectors from the T700GC/M21 ISO simulation exposed to a  $101.2 \text{ kW/m}^2$  laser beam at different times. The internal pressure increases because of the formation decomposition gases in areas nearby the symmetry axis. The gas velocity vectors confirm that the gaseous products exit mainly through the centre of the front surface, where the permeability slightly increased due to the pyrolysis reaction.

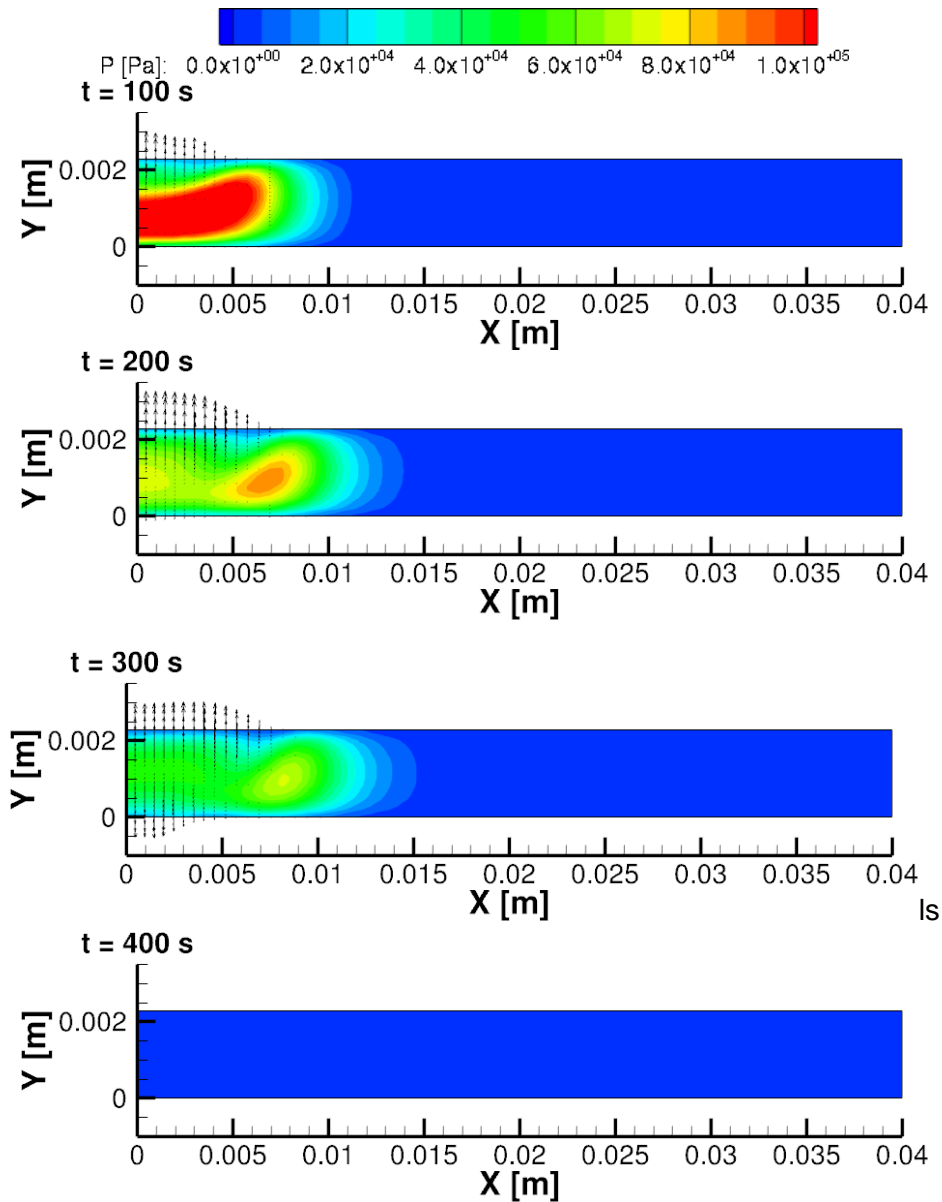


Figure 56 : Internal pressure fields at different moments from the T700GC/M21 ISO simulation exposed to a 101.2 kW/m<sup>2</sup> laser beam

Figure 42 illustrates the evolution of the internal pressure as a function of time in the mid-plane at different positions spaced every 5 mm. The pressure peak is located along the axis of symmetry and achieves  $P = 1.41 \text{ bar}$ , and then slides to the peripheral regions. As soon as the laser heating stops, the pressure falls down because the gas production is stopped and the remaining gases are very quickly released.

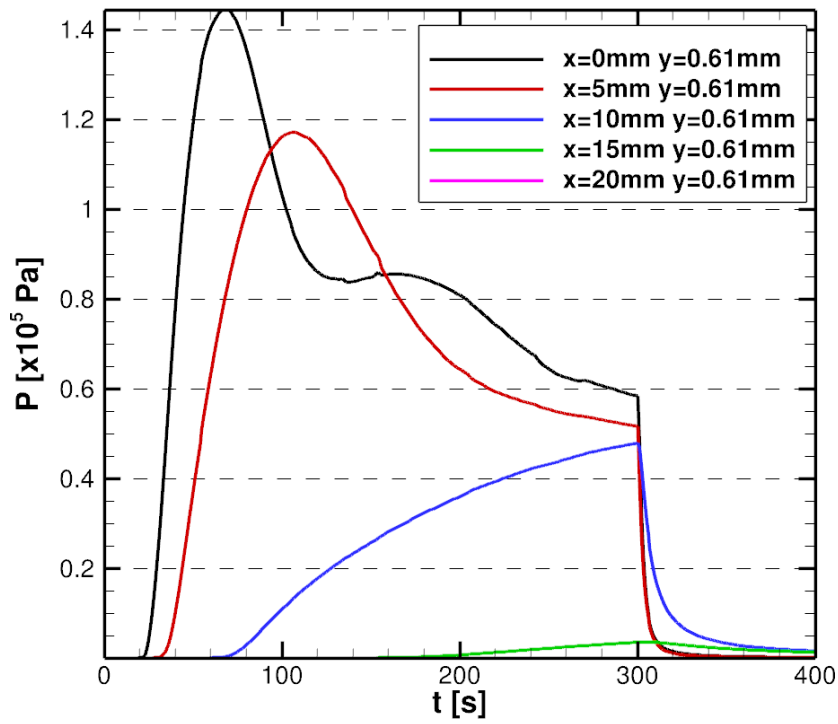


Figure 57 : Internal pressure evolution at different positions along the mid-plane from the T700GC/M21 ISO simulation exposed to a  $101.2 \text{ kW/m}^2$  laser beam

## **5 PROCEDURE FOR THE SIMULATION OF COMPOSITES MATERIALS SUBMITTED TO FIRE AND HIGH TEMPERATURE (ADS):**

As mentioned in the previous chapter, complete simulation of fire events is a quite complex scenario in which a wide variety of effects are present:

- Thermal effects: heat conduction, convection, reaction heat generation/absorption,
- Chemical reactions: pyrolysis, resin volatilization and reaction products generation
- Flame radiation, combustion, turbulence, rotation.
- Mechanical effects: mechanical softening, properties degradation, layers separation, resin volatilization.

The complete simulation of such a complex problem is quite unapproachable effort: some simplifications and delimitations are required.

At the moment, structures are certified via testing a fire campaign following section 2 procedure. The first delimitation step will consist in focusing the fire simulation to the fire testing normative. This means that the simulation does not pretend to cover certification by eliminating testing but in fact is intended to reduce the testing loops required.

The second simplification step consist to adapt the simulation to the typical configurations: normally loads in composite structures are introduced via metallic fittings bolted to the structure by fasteners or inserts. The simulation will be focused in structures with metallic fittings over composite panels. Special care should be given to the interface between them usually the failure point of the structure on a loaded testing.

A third simplification step will be performed on the flame model: thanks to the strict calibration required to the flame on ISO2685 normative, this model will focus in the ISO 2685 flame effects on this kind of structures during normalized fire tests rather than study the full mechanisms and flame behavior.

This chapter tries to address a simplified prediction procedure for fire events simulation taking into account this delimitation of the problem.

### **5.1. General procedure definition to simulate simplified thermal, mechanical and coupled problems**

The primary airframe structures are susceptible to be submitted by different actions during its duty life; the most important actions that a structure can be submitted are either mechanical load or thermal loads. As a consequence of the application of these loads over the structure provoke two different field of displacement corresponding to each one of actions applied, from the point of view of the simulation it can be difficult reproduce both fields of displacements at the same time.

Coupled thermo-mechanical models are extensively employed in the analysis of typical aeronautical structures so as to determine not only the fields displacements, also the level of stress provoked by the thermal effects over either metallic materials or composite materials due to high temperature

variations can induced stress that provokes the structural failure. As a consequence of this effect, these implications should be taken into account into the structural response either high temperatures or mechanical loadings should be considered in the process of the design of the airframe structure.

Based on the application of the finite element model technique a computational model for the simulation of the behaviour of the airframe structure can be developed. Considering the temperature application as external load, defined previously by means of a suitable procedure, it is possible to reproduce the effect of the thermal load in coupled thermo-mechanical models in separated way, by means of introducing the proper material properties, and thus obtaining the displacements field and stresses induced by only the contribution of the thermal problem.

Therefore, the case of structures with imposed temperature on the external surfaces is easily solved without the need to a priori define the temperature profile in the thickness direction. The temperature is a primary variable of the problem, and the values of temperature at the top and bottom are directly imposed: The fully coupled thermo-mechanical governing equations directly provide the displacements and the temperature through the thickness direction. In order to calculate the displacements, the partially coupled equations need an initial temperature profile in the thickness direction or calculated to define the thermal load.

Focusing in structures composed by means of composite materials, it is possible to define a general procedure to stablish in a systematic way to determine each of the process parameters involved into the simulation of these sorts of problems.

The following pictogram represents the complete process to obtain in a systematic way, the simulation of a composite material thermal behaviour by means of the application of the finite element technique. In a first approximation only a thermal loads will be considered into the simulation, stablishing in this way the whole analysis of the process separately, adding to the thermal solution as the first component and the mechanical solution as second component of the solution.

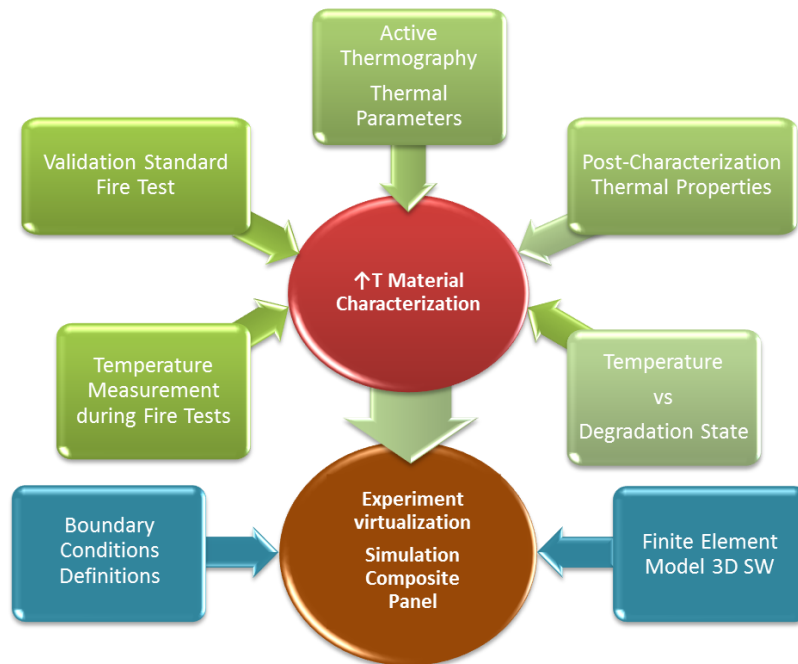


**Figure 58 Process scheme**

First of all, a non-intrusive monitoring system is defined in order to measure the temperatures fields on each side of the composite panel. With this monitoring capability, a characterization procedure based on flash method [Ref5] can be established that permits the obtainment of a preliminary validated characterization set of thermal properties, valid for ambient temperature. The monitoring system will be necessary to measure during the test performing, recording the evolution of the temperature profiles on each one of composite panel sides. Respect to the temperature distribution profiles measured during the fire test execution, the evolution of the thermal material properties are determined obtaining the limits values of each one property and in consequence and after the test performed, the different degradation states of the material are identified. In addition, by means of the non-intrusive monitoring procedure a post characterization over the charred material is carried out, determining the thermal final properties for the corresponding degradation state of the composite panel.

Once the thermal material properties have been determined with its corresponding degradation states of the material versus time and temperature, an initial finite elements model is accomplished. Choosing a suitable software commercial platform, relying on the application of the finite elements technique and with the capability of the solver package to figure out coupled thermomechanical problems, an initial model of composite panel is performed where the modelling of the boundary conditions is implemented, including the modelling of the boundary conditions of the thermal problem: the standard flame, natural and forced convection heating. Once the model has been implemented a final validation standard fire test is performed over the same composite material panel, the temperatures profiles measured in the test monitoring should be predicted by the model results simulation, and otherwise the thermal material properties implemented in the model should be adjusted. After this validation the simulation approach can be used to predict the structural behaviour of composite structures submitted to fire events.

## 5.2. Procedure described in stages to obtain a simulation of thermomechanical problem of a composite material submitted to fire conditions

In order to determine the necessary properties of the materials involved and as consequence to carry out a proper simulation of the effects either temperature or mechanical load applied over carbon fiber panels, is defined a sequence of five phases by means of which is possible to obtain all the necessary parameters, not only the material properties and its variation with the time, also other parameters that allow measure the material properties regard to the time and temperature.

### Stage 1:

In the first stage, equipment, systems and methodology to apply in following phases are established:

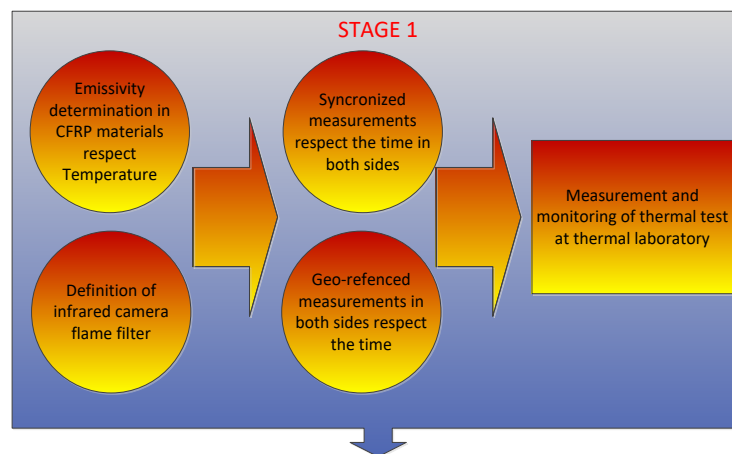


**Figure 59 First stage of the simulation procedure**

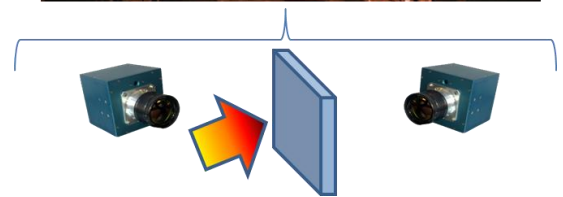
- i. Emissivity determination in CFRP materials with respect to temperature.  
One of the main points to measure with accuracy the temperature profiles over panel surfaces is the determination of emissivity parameter in each one them. The temperature measurement by means of the use the infrared cameras in the NDT-IR (Infrared Non-Destructive Testing) procedure requires the application of a suitable emissivity value, in order to post-process the energy levels obtained by the IR cameras and transform them into temperatures profiles. In consequence, it is recommended to measure this parameter previously, by means on tests, and for each one of the sides of the composite panel from ambient temperature up to high temperature values.

Therefore, it will be necessary to determine the emissivity for each material considered and for different conditions of temperature. The typical procedure for this emissivity calibration is by attaching an object with known emissivity to the measured surface in such way that both measured surface and reference are at the same temperature.

Other procedure to obtain the spectral emissivity from [ONERA Toulouse | ONERA Châtillon] of the composite material in a temperature range of 100°C to 1100°C is specified in [Ref9] Section 5.1.4 either for intact material or for charred material.

ii. Synchronization of measuring equipment .

All the measures of temperature profiles will be performed by means of an acquisition system rely on infrared cameras dual system described into [Ref6.] The temperature profiles should be synchronized and it is also necessary to establish a geometrical correspondence between each pixel and its location on the panel surface for both sides of the panel. This synchronization and geometrical reference permits the extraction of the temperature fields in each one surface and its evolution with respect to time of execution of the fire test.



iii. Geometrical referencing of recorded images to obtain complete panel temperature distribution

As has been depicted above, the temperature distribution should be obtained in a synchronized way, by a dual system of thermal infrared cameras (NDT). One of main objective is determined the evolution of the temperature distributions each one of the surfaces (cold and hot). In consequence, a suitable algorithm in order to the recording of temperature profiles be performed properly, will be developed.

iv. Definition of infrared camera flame filter.

The presence of the flame in a standard fire test implies certain problems to measure the hot side temperatures by this procedure. The flame produces a blinding effect mainly due to particles and gases that appear when exposing the panel to fire.

In order to obtain temperature fields on both sides on a specific fire test, a suitable infrared filter should be installed in the fire-side camera with the aim of obtaining the temperature distribution on the whole hot face. Otherwise, the energy emitted by the flame, particles and gases during the combustion process will cause the saturation of the infrared camera sensor. To avoid the sensor saturation a spectral filtering is incorporated into front side of the camera hardware. In addition, another infrared camera placed on the cold side of the composite panel during the fire test, due to the emission of gases and smoke from the resin of composite panel during the fire test, another spectral filter is incorporated into camera hardware in order to measure temperature through the gases emissions.

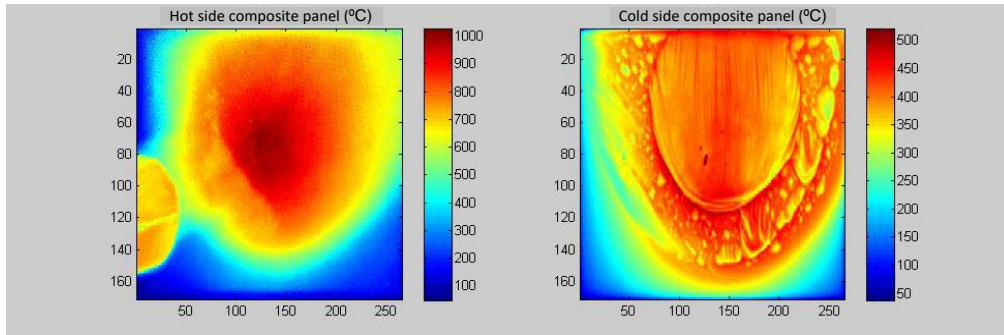


**Figure 60** Temperature distribution on both sides of a composite panel under fire

v. Measurement and monitoring of thermal test at fire test laboratory

The fire test performed should be carried out in a certified fire test laboratory with all necessary facilities in order to warrant that the test is performed according to the defined procedure described into [Ref4]. The IR cameras must be located in proper way to obtain the temperature profiles during the fire test. The fire test will be carrying out according to the corresponding standard ISO2685. The corresponding parameters measured according to the fire test standard should be recorded and stored for each one of the test performed, above all the flame calibration parameters.



**Figure 61** Fire Test lab

**Stage 2:**

In the second stage, it is described the preliminary characterization of the composite material to obtain an initial thermal model.

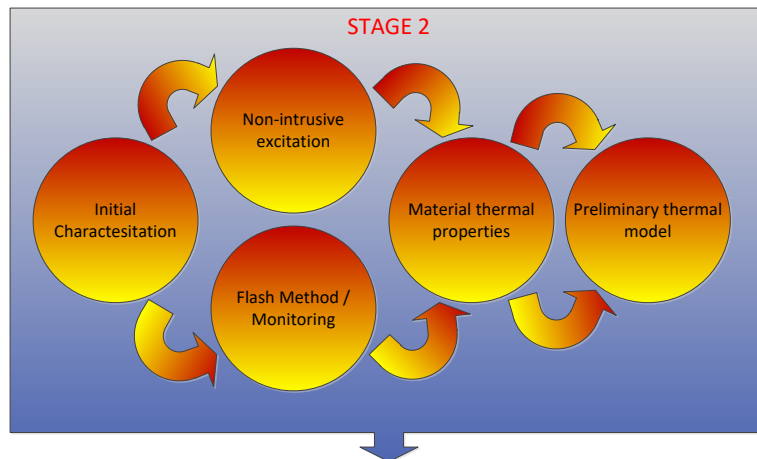


Figure 62 Second stage of the simulation procedure

i. Initial Characterisation NDT-IR

The thermal properties of the composite material will be determined by means of the application of an adaption of the “Flash Method” [Ref5] procedure or any other experimental procedure such a ‘BLADE’ from [ONERA Toulouse | ONERA Châtillon] is specified in [Ref9] Section 5.1.5 and its facility description is indicated into [Ref10] section 3.1.1. With its application is possible to obtain the main thermal properties of the material at ambient temperature conditions and for intact material in terms of diffusivity and volumetric specific heat. Conductivity is obtained as  $K = \rho \cdot C_p \cdot \alpha$ . In case of the BLADE the characterization procedure can be staged up to temperature 100°C. The results obtained of this test for the material are  $K_x, K_y, K_z$  and  $C_p$ .

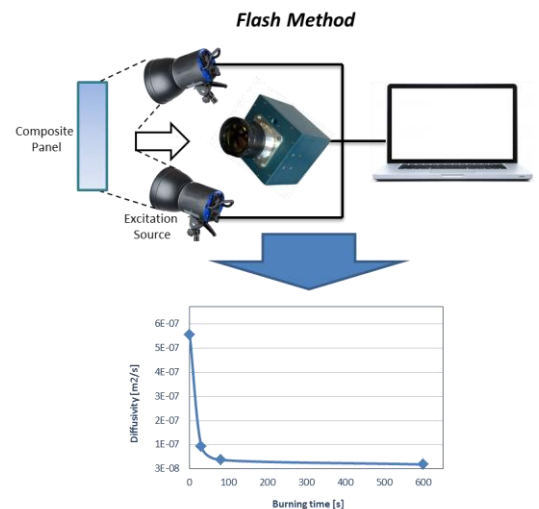


Figure 63 Adapted Flash method

ii. Non-intrusive excitation

In order to carry out the characterization process onto the specimen will be necessary to raise the surface temperature by means an IR lamp in a non-intrusive way. By means of the application of the dual system of thermographic cameras and the application of the geometrically-referred algorithm is possible to determine temperature distribution and evolution on opposite side and the initial set of the thermal material properties.

iii. Flash Method / Monitoring

The energy provided on the material surface will be performed through a specific light source during a controlled time period. Through the monitorization, recording and post-processing of

the obtained results on the cold side of the composite panel will be fundamental for the characterization process.

iv. Material thermal properties

The thermal properties of the materials will be determined by means of the application of the characterisation procedure depicted before. By means of the obtained results of these thermal material properties it is possible to implement in a model these initial properties for which represents the thermal behaviour of the material at low temperatures.

$k$ (w/m K)	Thermal conductivity
$\alpha$ (m <sup>2</sup> /s)	Thermal diffusivity
$\epsilon$	Emissivity
$\rho$ (kg/m <sup>3</sup> )	Density
$C_p$ (J/Kg K)	Specific heat at constant pressure

v. Preliminary thermal model

As an initial result a thermal material model is defined rely on the thermal properties obtained. This preliminary model of the thermal behaviour it will be representative up to low values of temperatures, 120°C approximately.

**Stage 3:**

In the third stage of the procedure, it is described the determination of degraded or charred material properties and its levels of degradation with respect to temperature reached into the composite material, to obtain a realistic material thermal parameters at high temperature validated by means of a non-standard fire test.

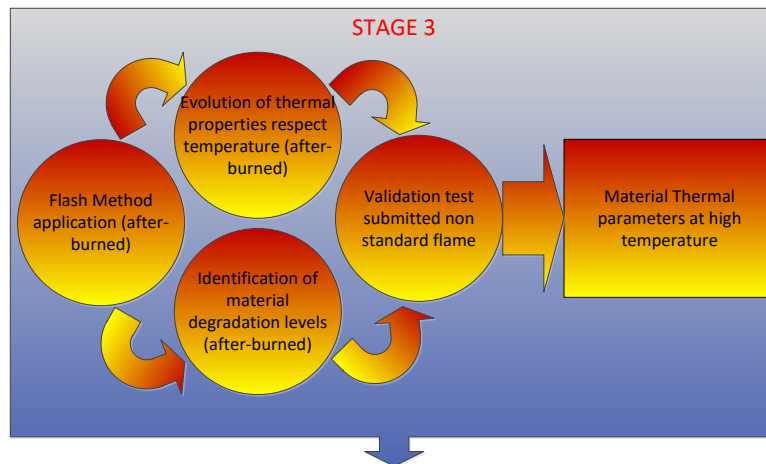


Figure 64 Third stage of the simulation procedure

i. Flash Method application (after-burned)

A characterization based on modified flash method procedure will be performed over the burned specimen to obtain a distribution of thermal properties of the burnt material after the test.



ii. Evolution of thermal properties with respect to temperature (after-burned) and degradation levels

After the fire test several degraded zones can be visually identified; during the test, each one of these zones has achieved a maximum temperature that can be determined by the thermography. By means of the determination of the thermal properties locally along these different degraded states an approximation of them at each degradation temperature can be extracted.

**Figure 65 Different degradation areas**

On the other hand, in case of the application of the procedure defined from [ONERA Toulouse | ONERA Châtillon] the characterisation procedure for composite material in a temperature range of 20°C up to 900°C is specified in [Ref9Section 5.1.1, 5.1.2, 5.13 obtaining thermal expansion, specific heat and thermal diffusivity, the thermal conductivity of the material can be determined according to the following expression:  $\alpha = \frac{k}{\rho \cdot c_p}$  from thermal diffusivity, density and specific heat.

iii. Validation test submitted non-standard flame

After the characterization process a final validation test will be performed in order to adjust the thermal properties rely on behaviour of the composite panel after the test.

iv. Material Thermal parameters at high temperature

Each one of the materials should be characterised in order to simulate its behaviour; in consequence each one of the thermal parameters of the material and its evolution regards with the time and temperature should be correlated by means of the corresponding mathematical expressions.



**Figure 66 Standard ISO 2685 flame**

**Stage4:**

In the fourth stage of the procedure, the modelling of the boundary conditions is established either the standard flame or convective heat transfer process. On the other hand, the implementation of the thermal material properties into finite element model is described.

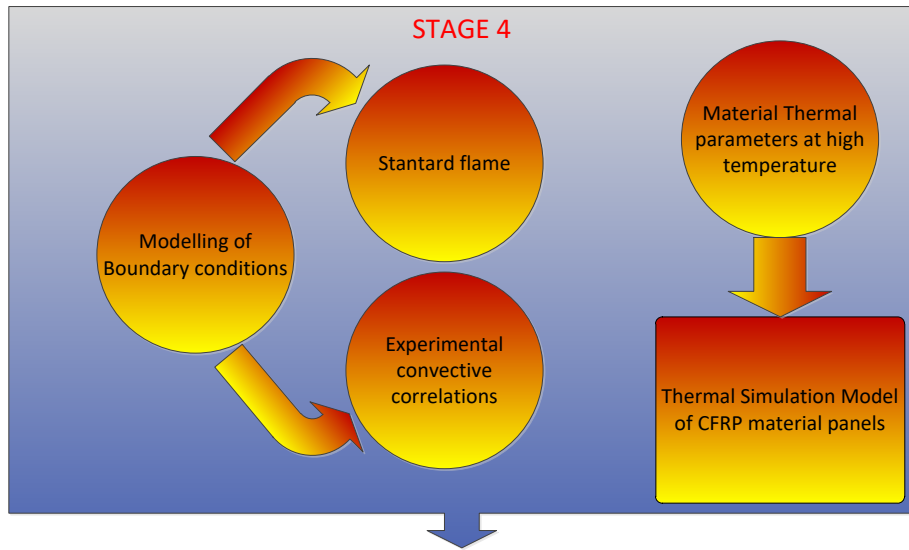
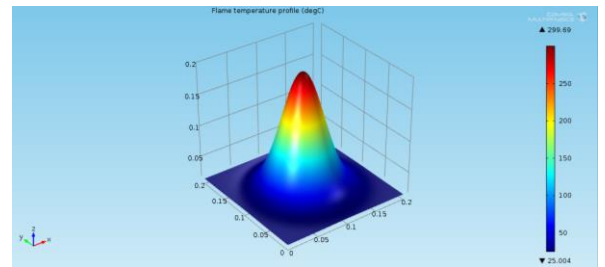


Figure 67 Fourth stage of the simulation procedure

i. Modelling of Boundary conditions

The thermal loads should be parameterized in order to simulate its effects over the composite panel, by means of its implementation into a finite element model. The boundary conditions applied into the model should take into account each one of the thermal effects present in the execution of the fire test.



F  
 Figure 68 Hot face map due to flame hypothesis

ii. Standard flame

A standard flame is applied, in an accredited laboratory fire test, by means of the control of the flame power, heating flow and flame temperature. The application of the standard flame will be parameterized by means of the results obtained, from the temperatures profiles, provided by IR cameras results measured at the composite panel hot side.



Figure 69 Flame power and temperature control at Certified Fire Laboratory test

The standard flame is defined in the standard ISO2685 as the main boundary condition applied over the specimen in a standard fire test. In order to simulate the flame behaviour properly during test performing is necessary to carry out a previous modelling of the standard flame effects over the hot side of the composite panel.

The modelling of the flame constitutes a huge effort, involving radiation, convective heat flow, flame turbulence characteristics, hardly attainable by simulation. In the proposed simplified approximation, the effect of the standard flame on a typical composite panel will be introduced as hot face boundary condition.

From previous test experience on typical composite panel–metallic fitting configurations, this temperature map in the hot face has some repeatability along the tested samples allowing the approximation of the hot face as a temperature map boundary condition.

iii. Experimental convective correlations

In order to introduce the adequate panel boundary conditions, particularly the forced convection heating, an empirical correlation should be taken into account. The introduction of the free or forced heat transfer convection is implemented by means of the boundary layer condition (by means of the Newton’s law of cooling) in consequence, the heat transfer coefficient should be introduced into the model, and thus it is necessary to define the convective parameter of Newton’s law (related with the conductivity and length) through the Nusselt non-dimensional number that relates convection transferred energy with conduction one.

The experimental correlation that is recommended to use, in order to determine the convective parameters, into heat transfer problems with composite panel submitted to fire is the Skupinski correlation [Ref13]

$$Nu_D = 4.82 + 0.0185Pe_D^{0.827} \quad q_s^* = \text{constante}$$

$$\left[ \begin{array}{l} 3.6 \times 10^3 < Re_D < 9.05 \times 10^3 \\ 10^2 < Pe_D < 10^4 \end{array} \right]$$

where Nusselt number is defined:  $Nu = \frac{h \cdot L}{K_f}$  and Péclet number is defined:  $Pe = \frac{L \cdot V}{\alpha}$

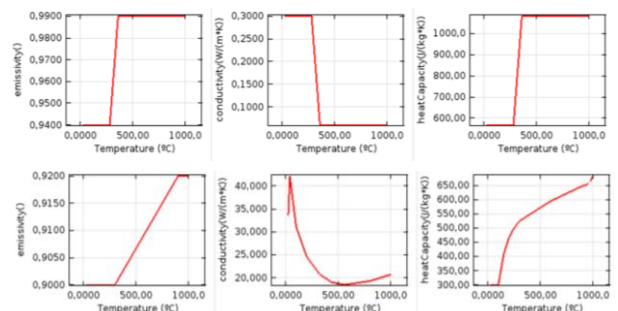
iv. Material Thermal parameters at high temperature

According to the depicted procedure before the thermal parameters of the material and its dependency on the temperatures are describe by means of a mathematical correlations for each characteristic thermal parameter involved in the heat transfer process, in consequence these expressions for each one of the thermal properties are implemented into the finite element model in order to simulate for each instant the thermal behaviour of the material with respect to the temperature.

v. Thermal Simulation Model of CFRP material panels

The calculated correlations obtained for each thermal property with respect to temperature permit the simulation of the

AIRBUS DEFENCE AND SPACE Status: Approved



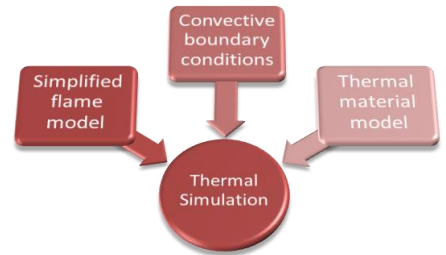
thermal material behaviour, assigning these material properties and its dependencies into a finite element model.

**FFigure 70 Thermal Properties**

The implementation of the thermal simulation should be carried out by the application, of the thermal boundary conditions:

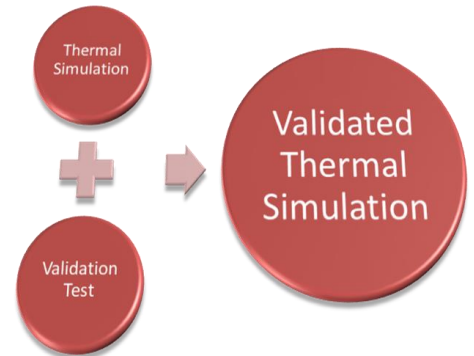
- simplified flame model and
- convective heat transfer conditions model,

Once a preliminary thermal model is implemented, an initial thermal simulation with temperature results is obtained, since should be correlated through of performing a standard fire test.



The thermal model should be correlated through the temperature profiles measured in a validation test. This validation test is a real standard fire test in which temperature profiles are measured, registered and post-processed so as to adjust the initial thermal model results obtaining a final validated thermal simulation.

The correlation of the initial thermal model used to modify some boundary condition parameters for instance; the convective parameter assigned to implement natural convection heat transfer process in order to adjust the temperature distribution onto the composite panel cold side.



**Stage5:**

In the fifth stage of the procedure, a failure criterion has to be defined by correlation of the failure instant standard fire test with numerical thermal simulation:

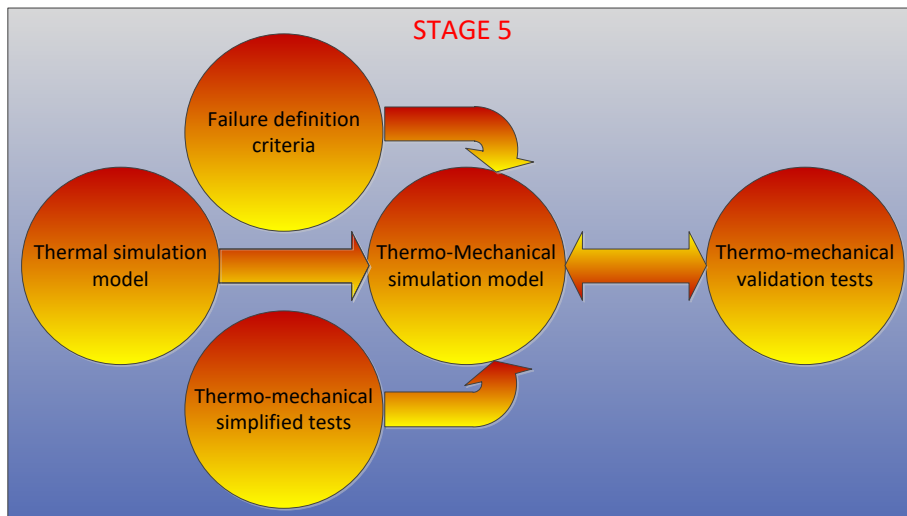


**Figure 71 Fifth stage of the simulation procedure**

i. Thermal simulation model

Based on implementation of the parameters correlations in finite element software, by means of the definitions of tables, to establish dependencies with respect to temperature of the model properties, the behaviour of the materials properties can be assigned into a model submitted to high temperatures. This behaviour material model is valid only in as first approach for a thermal model; all the boundary conditions applied are thermals.

ii. Failure definition criteria

In order to have a successful fire test on a fire proof or fire resistant structure, during the test duration:

- the assembly must withstand the load up to the end of the test
- the flame must not trespass the composite panel

If any of these events is not verified, the test is considered as failed.

In order to establish a degradation limit of material model, a failure criterion is defined based on experimental evidence of previous testing campaigns, from the evolution of the material properties with respect to time and taking into account the degradation of material related to the variation the thermal properties with regards to temperature. These failure criteria are implemented into a finite element model through the evolution of the mechanical properties with respect to temperature reached level. According to the failure observed in the standard thermal-mechanical fire test, the failure in this kind of test is provoked by the temperature level mainly; in consequence the main failure criterion should be based on temperature level reached.



**Figure 72 Typical fitting-monolithic composite Hilok joint in composite**

In a first approach, a failure criterion relying on temperature should be established related to the temperature achieved in the rivet area, where the failure of the riveting typically occurs causing the structure to collapse, detaching the hinge of the composite material panel. Establishing a criterion of failure based on the temperature reached in the riveting plane allows simplifying the results provided by the coupled model (thermal-mechanical model) and the interpretation of the results obtained in the simulation.

iii. Thermo-mechanical simplified tests

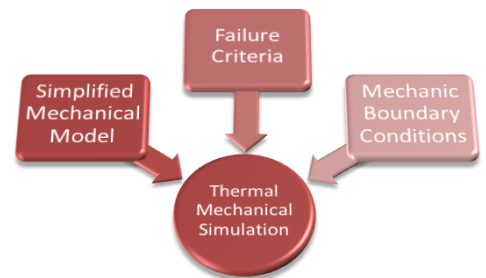
Once the thermal problem is simulated by means of finite element software with material properties and with proper boundary conditions modelled, is necessary to complete the material properties with the additional effects of the mechanical problem, just in case a mechanical load can be applied.

In order to determine the influence of mechanical load into the coupled problem a thermal-mechanical simplified tests will be defined. Therefore, a simplified test with fittings added will be defined, by means of rivets installation, over a composite panel with a simplified bearing and pull-out loads state applied. Performing a fire test applying each one of these load state, a failure criterion for the combined problem is defined and validated.

These test can be complemented by additional mechanical composite testing at temperature according to [Ref10] by means of BALI test (described in section 5.3.12), shear/compression tests (defined in section 5.3.2), in plane tensile test (section 5.3.3), in plane compression (section 5.3.4) and in plane tensile shear test. The results of these thermomechanical tests are indicated in [Ref10]

iv. Thermo-Mechanical simulation model

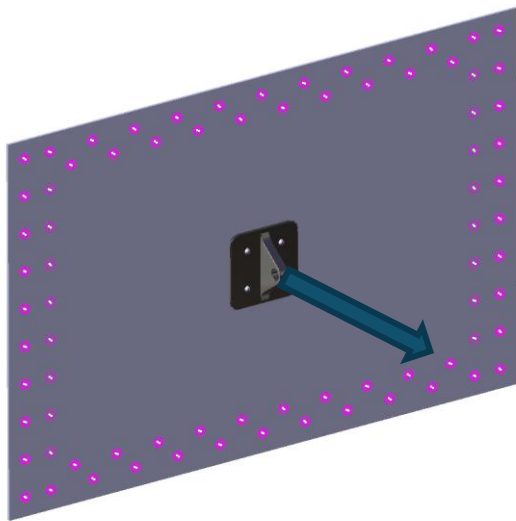
By means of the results obtained by tests of monolithic panel with a fitting joined through of rivets, the failure criteria of the combined problem is implemented into the finite element model as it has been indicated before, the main failure criterion relies on the temperature level reached by the composite material in the surroundings of the riveted joint . On the other hand, due to dilatation coefficient and the field of displacements produced into the composite material according to temperature variation during the test should be taken into account the evolution of mechanical boundary conditions. The restrictions implemented in the model due to the dilatation effects can generate a high stress levels near of areas of the fixing of the composite panel, even can provoke the break of the sample, in consequence the boundary conditions considered should take into account the field of displacements due to temperature effect.



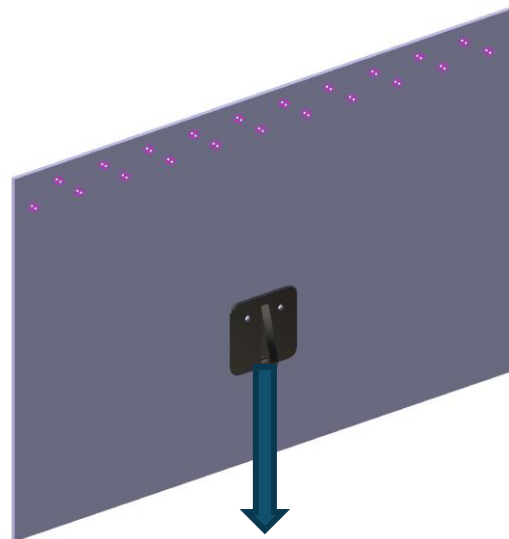
The evolution of the mechanical properties with respect to the temperature will be considered up to a certain temperature level. A limit level of temperature will be defined for the material into coupled model, where the mechanical resistance will be negligible for the combined problem and when a certain temperature level is reached into a determined model location.

v. Thermo-mechanical validation tests

For implementing a validated thermal-mechanical simulation rely on into a validated thermal model and adding the mechanical effect, it is necessary carry out a validation test in order to correlate the results obtained by thermo-mechanical model and as consequence obtaining a validated simulation.



Pull out test specimen for validation test

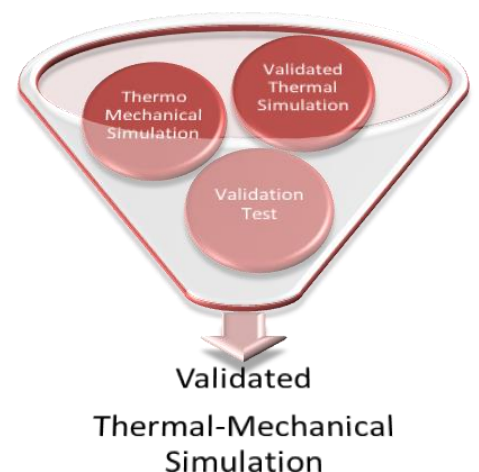


Bearing test specimen for validation test

**Figure 73 Simplified specimen configurations for fire test**

The validation test should be carried out by means of standard fire test with a defined mechanical load applied. In order to simplify the mechanical load effect a constant load application is recommended, so as to quantify its effects over the thermal-mechanical simulation.

By means of failure criteria definition implemented and with the results obtained from thermal-mechanical simulations a definition of the validation test is established, in order to check the results obtained by the simulation of the finite element model with respect to the temperatures profiles measured during the performing of the test. These results should be correlated for each of sides of the composites panel and for different sorts of load cases defined i.e. pull-out and bearing load case and as a final result a **validated thermal-mechanical simulation** should be obtained.



### 5.3. General considerations

For the simulation of non-stationary complex process in which is involved even a chemicals processes such as combustion reactions, it is necessary assume some considerations. First of all, a simplified problem should be considered with the aim to determine the influence parameter of the material behavior, also by means of this kind of problem is possible to adjust the boundary conditions modelling considered. Once the simplified problems are modelled and the simulation results are validated by test a more complicated problem can be addressed.

One of the most important advantages of this procedure proposed is the use of infrared cameras to measure the temperatures profile on materials surfaces during the tests performing. The most

important advantage of this methodology is to get the temperature distribution on the each one side of the composite panel during the test performing in non-intrusive way. The only way of achieving a proper thermal correlation between tests and simulation is to be capable of monitoring the full extent of both composite faces.

In a first approach, all the processes that occur in the composite panel during the fire test can be associated with the temperature level reached on both surfaces; not only the thermal effects considered in the thermal problem but also in certain conditions can predominate over the other effects from the mechanical problem simplifying the analysis of the coupled model and as consequence considering the temperature as the main control variable of the model behavior.

Due to the sort of geometry analyzed in first approach, simplified geometry of rectangular thin panel, a small thickness in relation with the other panel characteristic dimensions makes suitable that, the effect provoked by diffusivity matrix components in horizontal plane can be neglected taking into account the heat transfer with respect to the transversal diffusivity of the material at the central area of the panel; due to the heat thermal transfer maintains this area at the same temperature.

In this first approach a M21/T700 panel of 8 layers is modelled in order to simulate the behavior of the thermal problem. In consequence, only thermal boundary conditions are applied i.e. there is no load applied over the panel. The results obtained from the simulations based on this model, represent the thermal behavior of the composite panel submitted to fire.

After this first approach, and adjusting the model parameters in order to correlate the obtained simulation with the results of the fire test performed, the thermal behavior of the panel is characterized.

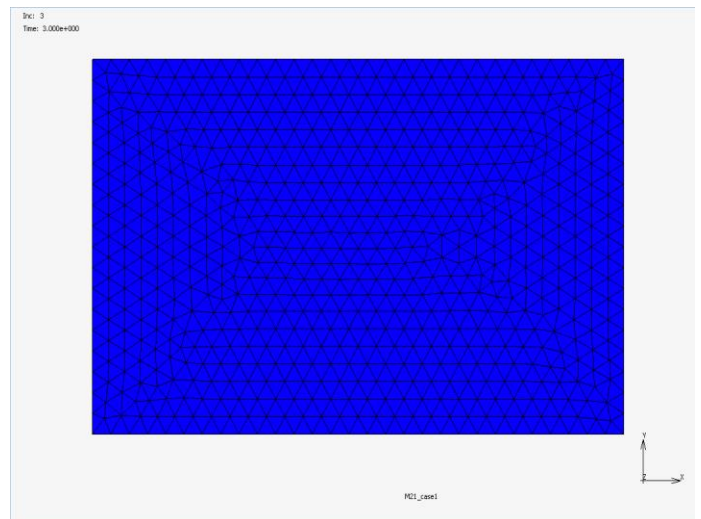


**Figure 74 Typical mesh size on a test panel**

These results are introduced in the resolution of the coupled model so as to simplifying the resolution process of the thermo-mechanical process and ease the understanding of the process that occur in this complex problem, also a failure criterion can be defined to predict the thermal behavior under determined thermal conditions.

After the modelling of this simplified component of the problem and in order to simulate the whole thermo-mechanical combined, a simplified basic load tests should be defined in order to be introduced into the coupled test.

These simplified basic loads cases should be representative enough of a load states cases in a typical situation on an airframe structure, in consequence bearing and pull-out test are be proposed.

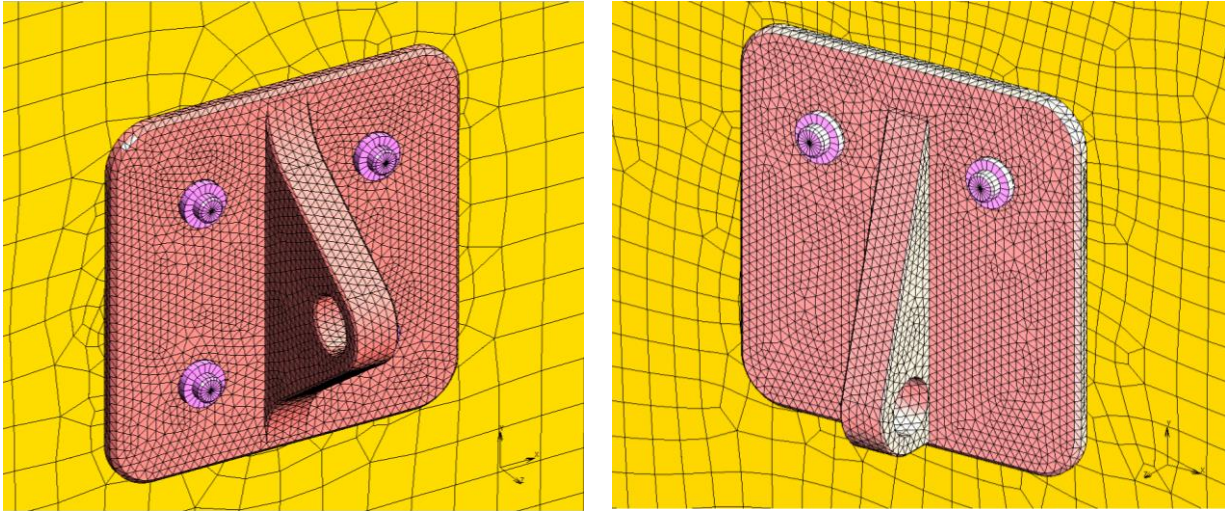


**Figure 75 Typical mesh size on a test panel: fitting detail**

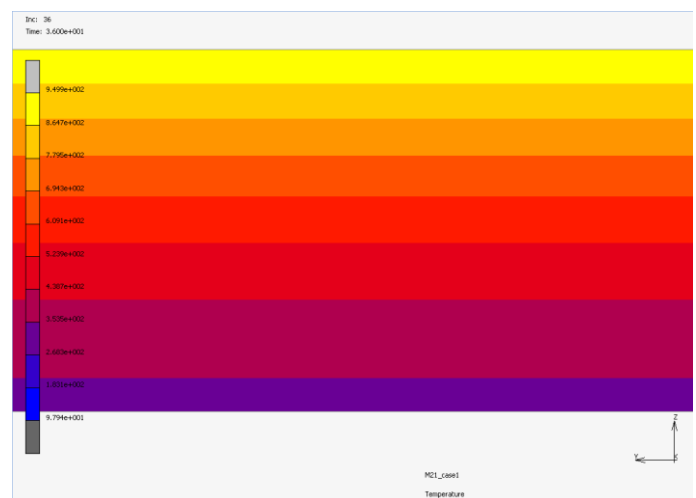
Applying by means of these fittings a pull-out load and a bearing load into a thermo-mechanical problem is possible to analyze the combined effects of each one problem over the coupled configuration.

### 5.3.1. Boundary conditions simulation

Boundary conditions should be modelled previously; some of these boundary conditions can be applied to the finite element model in a directly, otherwise as in the case of the flame excitation or forced convection heating, it is necessary to establish an empirical correlation, rely on surface temperature of the composite panel, in order to implement these boundary conditions into the finite element model.

This modelling process will be carrying out for each one of the rest of boundary conditions, above all in the simulation of the thermal model, which can be implemented directly over the finite element model and as consequence, an empirical correlations will be applied and adjusted (forced convection heat transfer). In case of the mechanical model, the boundary conditions can be applied directly; constrains and loads applied, and also taking into account the corresponding thermal dilatation coefficient for each one of the materials involved into the simulation.

The thermal boundary conditions definition should be produced very similar results that obtained during the test performing. The temperature distribution over the composite panel should be equivalent to the temperature distribution obtained from the simulation with respect to time, even the temperature distribution reached in each one sides of the composite panel after the system



AIRBUS DEFENCE AND SPACE Status: Approved

reaches thermodynamic equilibrium during the fire test simulation.

**Figure 76 Through thickness temperature distribution at 36sec from flame initiation (simulation)**

### 5.3.2. Standard flame model

As a simplified approach, but sufficiently accurate for the typical fire test, the standard flame is considered as a fixed temperature boundary condition applied on the thermal model. For the standard simulation flame is a necessary to determine an empirical correlation equivalent in order to implement the heat transfer process into finite element model. Once the calibrated flamed has been correlated by means of a mathematical expression (Gaussian distribution), this boundary condition can be implemented in most of finite element models, only in a non-simplified geometrical conditions require another technique so as to introduce this thermal excitation. In a complex geometry this approach may be inaccurate and a further hot face temperature map models should be established.

The modeling of the boundary conditions as the standard flame requires performing some fire tests, so as to characterize the flame excitation over the composite panels, by means of obtaining the temperature profiles over the hot surface of the panel during the execution of the fire test. These temperature profiles obtained with respect to the time can be adjusted by means of the suitable correlation and its expression can be implemented into the finite element model. As has been indicated before, a standard flame is possible to fit by means of a Gaussian distribution, with only two parameters to determine ( $\mu$  and  $\sigma$ ). This simplified flame modelling approach has been demonstrated sufficient to achieve good temperature correlation on the cold face on previous tests.

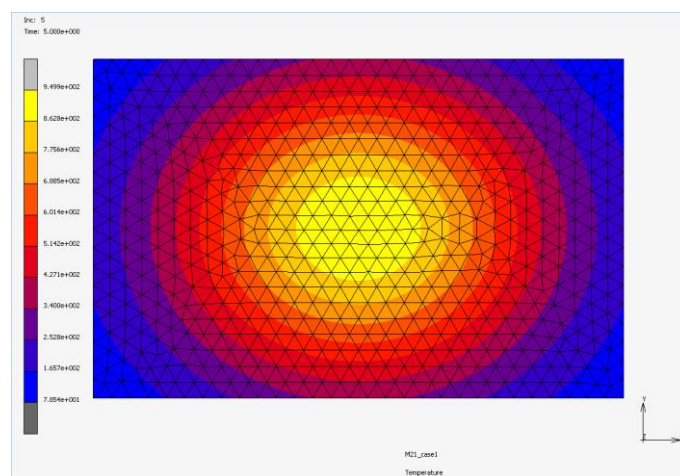


**Figure 77 Hot face simulation at 5sec flame initiation**

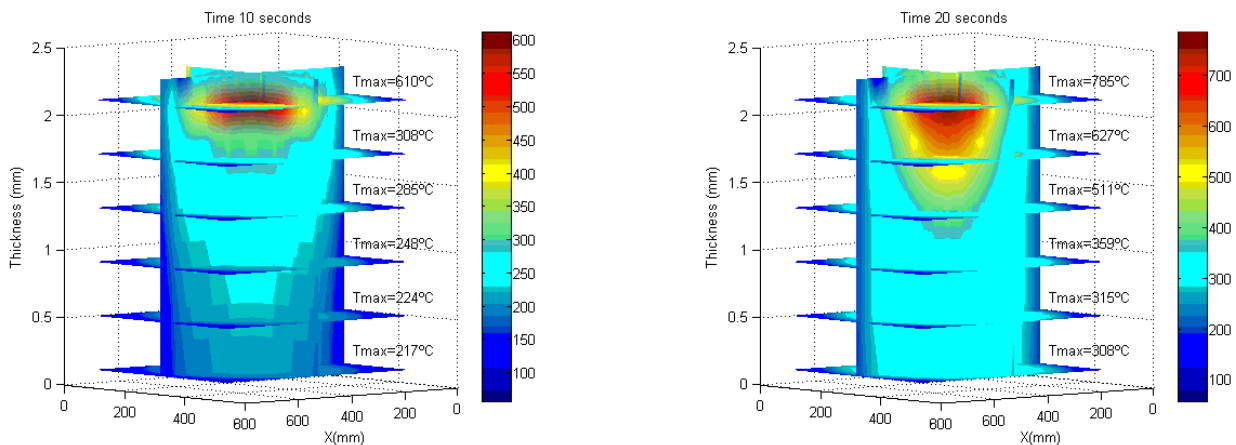
The mathematical approach considered for the standard flame modelling and its application in the thermal model is suitable always for flat panels. In case that exists a protruding object that can distorted the distribution flame over the panel surface, for instance a large fitting in order to apply a specific load, alternative modelling of the standard flame should be considered.

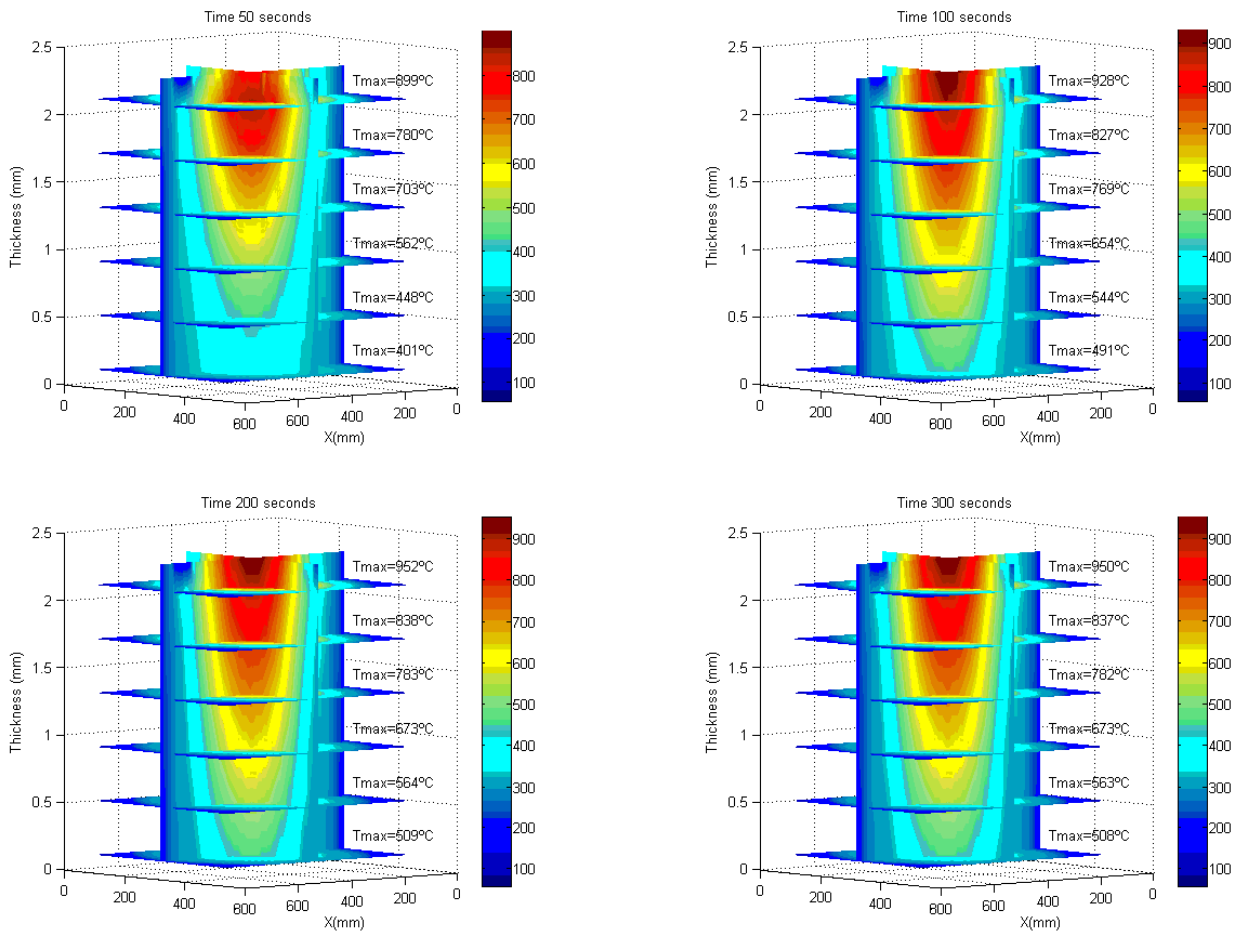
### 5.3.3. Experimental forced convection correlations.

In order to implement into a finite element model the boundary condition corresponding to process of heat transfer forced convection an experimental correlation should be applied, so as to get a representative thermal transfer on the specimen cold side. An experimental correlation is implemented into the model and adjusted by means of temperature profiles obtained as results of the fire test performed to characterize the forced convection heating, as it has been described previously. Once of this empirical correlation is adjusted for the fire test conditions, it can be implemented into finite element model in order to perform the simulation of the test taking into account the heat transfer forced convection effect.

### 5.3.4. Practical application: M21/T700G panel simulation submitted to fire.

Considering a specimen of M21/T700 panel of dimensions 690x440 mm submitted to standard fire test according to 8.1.3 without load applied and only taking into account the heat transfer process, the obtained results of the numerical simulation are depicted in the next figures, the heat transfer process goes from zero to 300 seconds, the panel has been split in 6 planes, for different timestamps:





Type	Specimen name	Orientation/Stack Sequence	Length [mm]	Width [mm]	Thickness [mm]
Laminate	Pyro 3	(45/90/-45/0) <sub>s</sub>	690.0	440.0	2.1

Specimen identification **M21/35%/268/T700GC** according to [Ref8 Hexply\_m21

**Figure 78 Cross section temperature distribution at different test time (simulation)**

#### 5.4. Thermal and Mechanical Model

The modelling approach employed permits the coupled problem to be divided in two complementary problems, thermal and mechanical problem, in order to simplify the analysis and the computation as first approximation. Several software packages based on application of the finite elements are able to solve the coupled problem adding both solutions. This methodology permits to simplify either the resolution process and the analysis of the results, i.e. each contribution to the solution can be analyzed independently. In contrast as a drawback, the final solution obtained has a problem related to the determination of the heat flow transfer and temperature level near of thermal contacts areas from the model that can have appreciable impact during the simulation and they can be relevant in some cases. The procedure to solve the whole problem by means of the addition of the both solutions reduce and simplify the analysis of the problem, the influence of the thermal and

mechanical loads can be quantified so as to determine which of both of problems have more influence in the degradation process of the composite panel during a thermo-mechanical fire test.

After obtaining the solution of each model independently, the software permits to obtain the compound solution by means on the integration of the both conditions, in each one corresponding load step, to obtain the integrated final solution which represents the real behavior of the thermo-mechanical problem.

The contribution of the mechanical problem is determined by means of the introduction of the corresponding boundary conditions applied through a mechanical load case into the model and can be analyzed separately respect to the solution of the thermal problem and the effects provoked from each one of the load cases separately.

One of the several effects that the mechanical contribution introduces in to the couple problem is the consequence of the application of the volumetric thermal expansion coefficient, that provokes a field of displacements into the mechanical problem due to the temperature effect, this additional combined field of displacements provoked by load case application establishes the component deformation, and takes into account either the effect of temperature or the load.

Above all, the thermal contact resistance exiting in a junction between two elements of a component is altered with respect to temperature evolution, modifying either the pressure distribution around the contact junction or the heat transfer process through the closest elements. Considering only for the mechanical problem contribution, the effect of the pressure variation into elements junction depends on the displacements provoked by temperature through the thermal expansion coefficient.

In the next figures, an instance of displacements field in each one of the corresponding elements of typical component in a configuration of a pull-out test model, as have been shown previously in the validation test specimens. These displacements fields can be analyzed in each one of the elements; fitting, rivets and composite panel submitted to a constant load. The mechanical contribution to the coupled problem from the starting time up to the end simulation, introduces a field of displacements in each one of the components of the assembly in consequence it should be taken into account in order to obtain a realistic simulation from the starting time, as is shown in the next images:

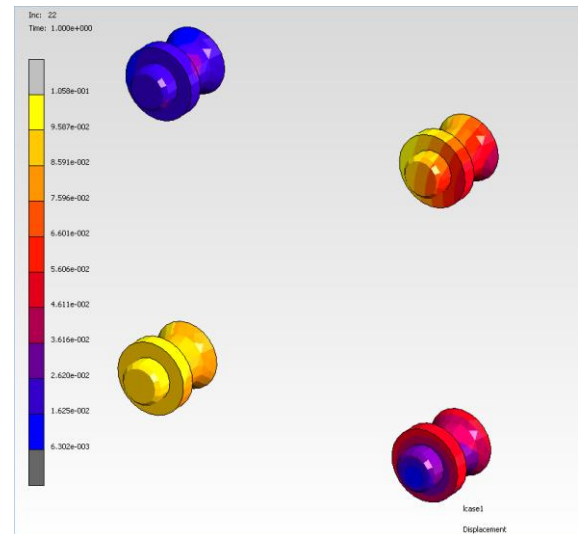
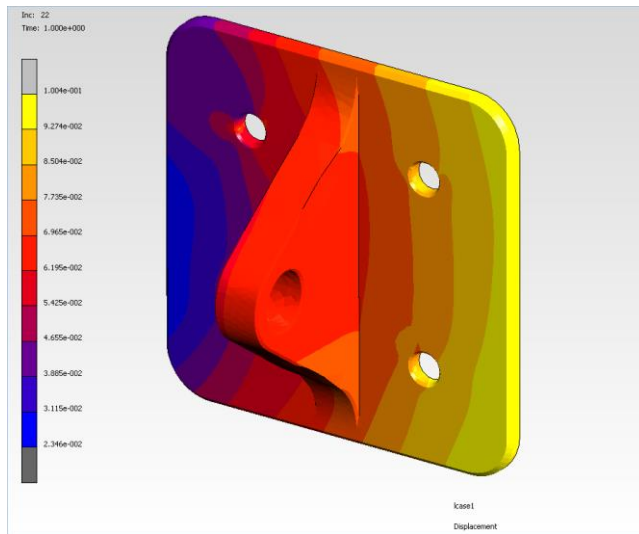


**Figure 79 Displacement at test time 1sec (Thermomechanical simulation)**

The displacements distribution is obtained from the mechanical problem contribution are also dependent on the temperature evolution, not only due to the thermal expansion coefficient but also because of the mechanical properties dependency. Throughout this fact and in order to get a complete solution of the problem based in the addition of both contributions, the solver should be synchronized in each one integration step and for both contributions with respect to time carrying out a new one resolution in each one of these steps with the new modifications of the thermal boundary conditions. Once of the thermal equilibrium is reached the resolution process is simplified and at the end of the simulation both contributions should be available for further analysis.

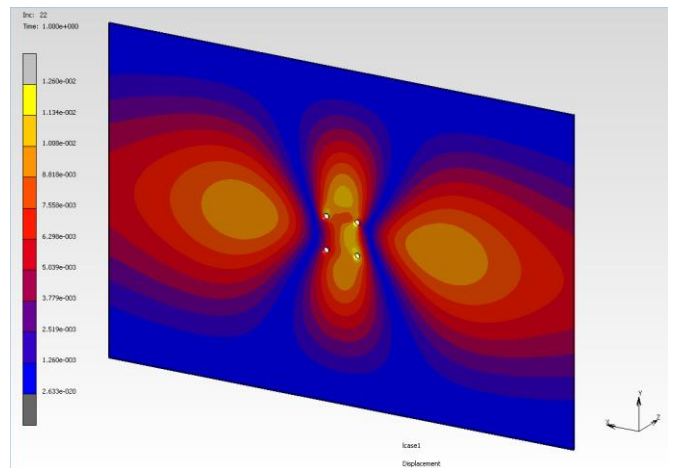


**Figure 80 Displacement at test time 1sec (Thermomechanical simulation)**

#### 5.4.1. Coupled Model

The solver capability incorporated in most software packages of finite elements permits to solve a mechanical problem in combination with a thermal one at the same time, solving for each one of the corresponding time step both, and obtaining an integrated solutions of the both problems in the same model with respect to the time. The resolution of the coupled problem by means of a coupled model has a high computing cost, in consequence and in a first approach is recommended to consider the mechanical and the thermal problem independently, if there is not any contact near of the research areas of the model the solution provided by the analysis of the both solutions integrated will be very similar.

The convergence of a coupled model solution submitted to high temperature gradients can be very difficult, so it is recommended to apply the thermal loads progressively into the model. Similar effect can be produced by the material thermal properties, any sharp fluctuations of the properties values can produce difficulties in the model convergence, and consequently some values of the thermal properties should be adapted.

A typical test configuration is commonly composed by a metallic fitting for load introduction which may be fastened to the composite panel by screws or riveting. These configurations for the coupled model also introduce non-linear effects as the appearance of contacts.

In order to obtain a suitable results from both contributions, the model should be taking into account different aspects related with the behavior of the model submitted to boundary conditions either mechanicals or thermals. This rivet modelled as instance is the sort of (\*)Hilok and according to the fire test results performed, one of the most typical failures of these test are produced at closest area of this component with respect to the composite panel, so it is a key factor to modelling this element with enough resolution for simulating the real behavior by means of a coupled model.

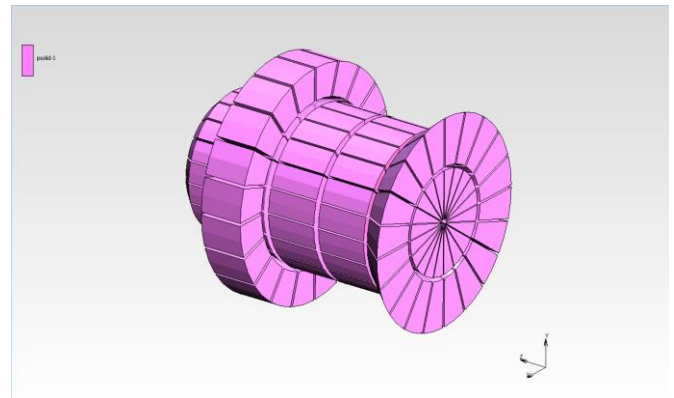


**Figure 81 Hilok mesh (Thermomechanical simulation)**

For definition of a typical failure criterion, according to the results obtained from fire test, the temperature is one of key factor that should be taking into account to establish one, in consequence the modelling of the areas closest to junction of the components where the failure starts, should be have a suitable level of detail to get the amount of enough information during the simulating process by means of the elements definition level depicted into the image for coupled models.

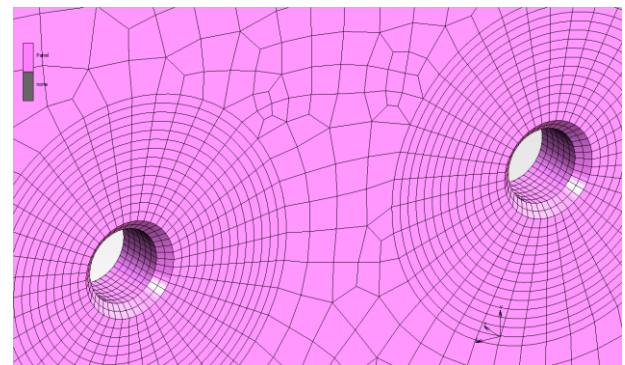


**Figure 82 Local countersunk fastener Composite mesh (Thermomechanical simulation)**

The couple model should reproduce the evolution of the contacts with respect to the temperature and also the assembly conditions of this sort of components, in other words these components introduce a pressure distribution into the elements junctions, by means of a pre-load defined in to the assembly by means of these sort of components, in particular and in this instance these components are Hilok. The junction of these elements into the model with the composite panel is a key factor regard with the behavior of the assembly in a fire test, thus the modelling should be have

a suitable grade of detail in order to obtain from the coupled model the necessary information, so as to define failure criterion contrasted with the obtained results from the fire test performed.

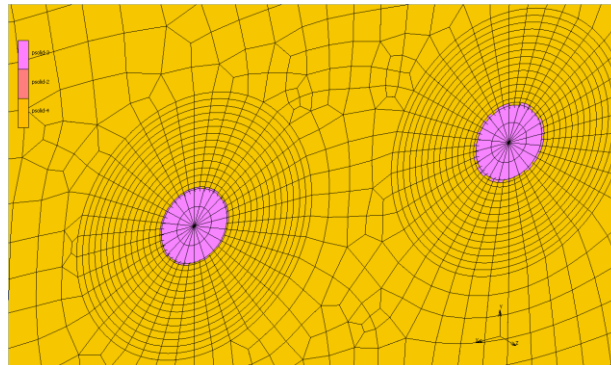


**Figure 83 Local countersunk fastener Composite mesh (Thermomechanical simulation)**

These junctions have a high dependency on the temperature; not only from the point of view of the local deformation due to thermal expansion (defined in the mechanical model) but also due to the degradation of the material properties. In consequence, an expected evolution at the joint elements takes place during the simulation; hence the resolution of the model should be adjusted. To introduce the pre-load defined in this sort of elements (\*Hilok) with respect to the composite panel instead of to introduce a compressive load into the rivet, the load is introduced to the composite panel by means of the interference defined between two elements, the rivet and the panel in contact.

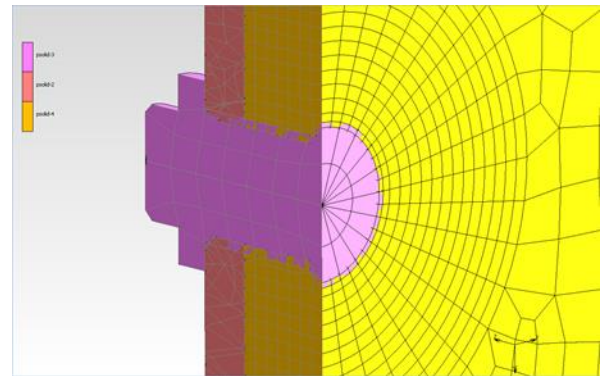


**Figure 84 Local countersunk fastener Composite mesh (Thermomechanical simulation)**

From the point of view of the coupled model and in order to ease the introduction of the initial conditions into the model, instead of introduce a load to represent the pre-load in each one of (\*)Hiloks, the pre-load is introduced controlling the interference between components. As a result, the pre-load defined is adjusted, although only as load initial condition and due to this interference is modified as consequence of the temperature effect with the application of heat transfer process. Due to the evolution of this parameter with respect to the temperature the contact resistance of the joint is modified also during the heat transfer process generated during the fire test. The estimation of the contact resistance behavior is one of key factor in the failure prediction related to couple models. In general rule, the failure is produced near of these areas, particularly into the joints between two components submitted to thermal and mechanical load, as a consequence the failure criteria definition should take into account the evolution of this parameter with the temperature reached near of these areas, in order to predict the elapsed time from the beginning up to the end of the fire test simulation. An initial failure criterion should be defined in a first approach for the first test campaign, after that with the time and depending on the accuracy required for the results, the failure

criterion should be enhanced by means of performing a test campaigns and improving the modelling information around these areas.

(\*)HI-LOK™, Component of consistently controlled preload, minimum size and weight.

### 5.4.2. Coupled Model Inputs

According to the characterization of the material M21/T700G parameters obtained by means of the application of the methodology proposed, some of these material parameters introduced into the properties into the coupled model are shown in the next figures:



**Figure 85 M21/T700G thermal properties**

### 5.4.3. Coupled Model Results

According to the results obtained the evolution of the most critical areas with the temperature can be identified and analyzed. By means of the model post-processing set of relevant variables are obtained in order to characterize the process. The main variables obtained from the resolution of the coupled model are:

- The field of displacements,
- Temperature distribution
- Stress distribution.

As an example, the displacements of a composite panel for submitted to a standard flame and a constant load, considering 20 seconds after the load application as a representative intermediate time related to with the typical failure period, is shown in the next figures:

According to the experimental test results obtained, the critical area is the one surrounding the bolts in consequence are required major information near of this panel zones. Through the output variables provided by the model these regions can be identified, either maximum displacements or maximum stress level should be taking into account considering the evolution if its effects regard with the temperature distribution. The combination results obtained by model permit to characterize the behavior of the critical elements identified inside this areas. The information from the model obtained for these elements sets can be configured in a straightforward way with the aim of to be post-processed in a suitable way.

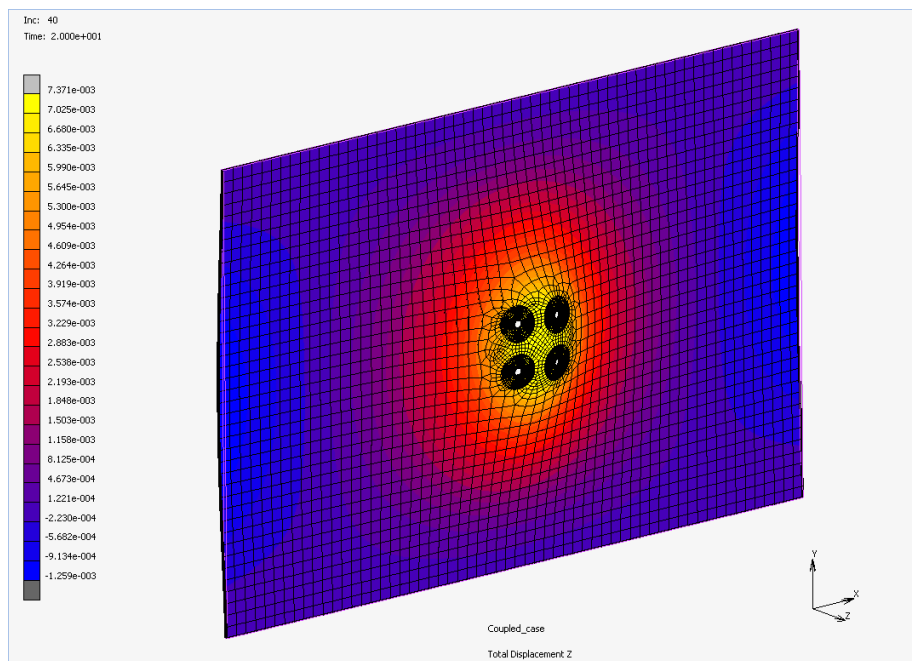


**Figure 86 M21/T700G panel displacements (20 sec from flame init) (Thermomechanical simulation)**

The temperature distribution for this zone has a direct impact into the behavior response of the model, in the next figures are considered this temperature distribution also for 20 seconds after the standard flame application:

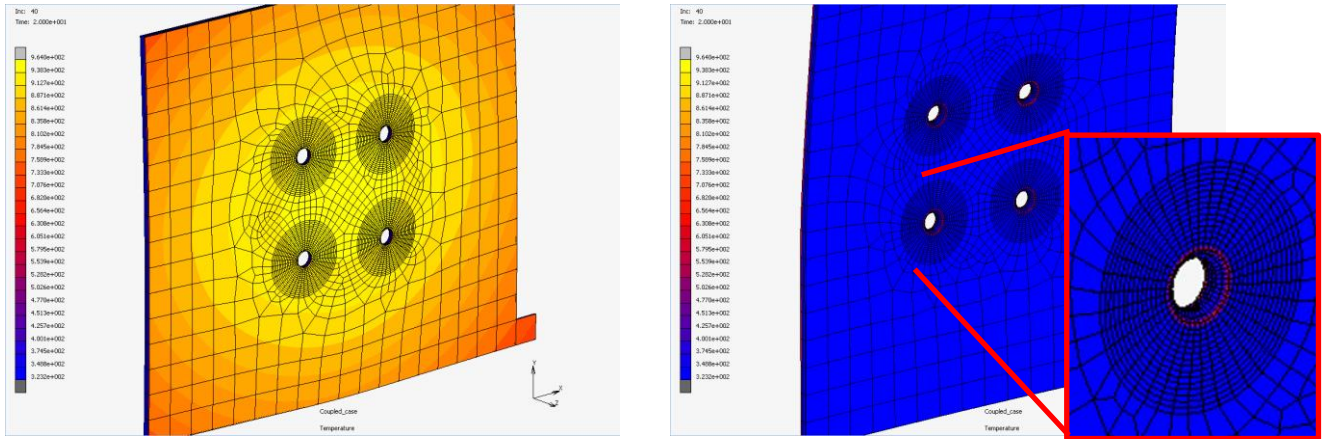


**Figure 87 M21/T700G panel thermal map (20 sec from flame init) (Thermomechanical simulation)**  
**Local temperature peak at cold face.**

In each one of sides of the composite panel and for this instant considered there is a relevant temperature difference between both sides. In the cold side, a local increment of temperature due to the effect of thermal conductivity of the bolts can be identified close to them; also the concentration of stress in the same region will provoke the failure with the detached of the fitting.

The fields of displacement as a consequence of the load application and also for the same previous instant are shown into the following images:

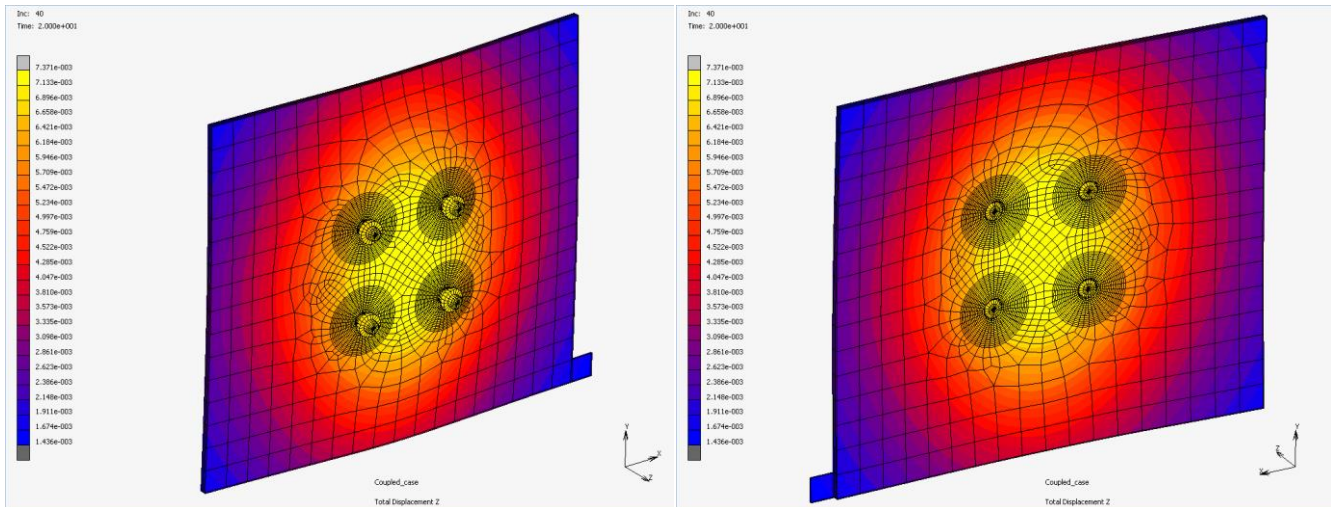


**Figure 88 M21/T700G panel displacement map (20 sec from flame init) (Thermomechanical simulation)**

The fields of displacement as a consequence of the application of a specific load remain constant regards with the time, considering the results provided by the coupled model after the simulation of the transient problem. Taking into account the results obtained by the experimental test performed, in fact it is not true, since the failure of the assembly is produced with the time of application of the standard flame and with the load application and with the corresponding detaching of the fitting. Due to that the panel degradation process is focused close to the composite panel bolts, the analysis of the failure criteria are based on these regions.

The equivalent Von Mises stresses introduced by the application of the specific load are concentrated in the same areas indicated previously, as it is depicted into the next images:

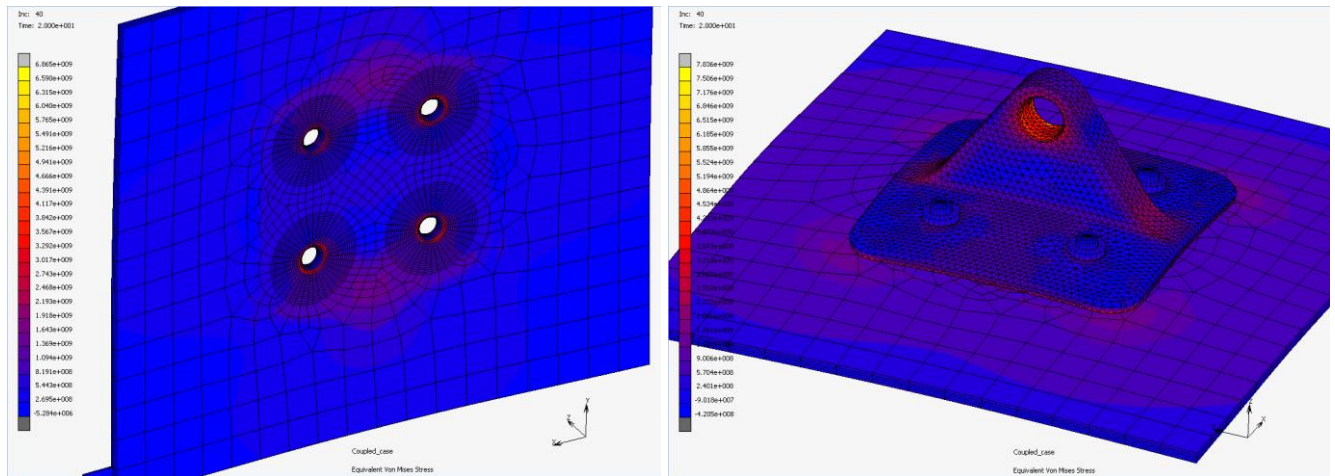


**Figure 89 M21/T700G panel von misses stress map (20 sec from flame init) (Thermomechanical simulation)  
Local temperature peak at cold face.**

The stresses concentration and the temperature near of these regions are analyzed regards with time to define simplified failure criterion in order to represent the model behavior respect to the experimental test results obtained into a different test campaigns.

#### 5.4.4. Failure Criterion Definition

The results obtained with the solution of the coupled model can't represent in a straight forward way the failure that appeared in the experimental test carried out corresponding with the assembly modelling.

The model areas involved in the failure according the experimental and coupled simulation results are related to the maximum temperature level reached near of the critical areas located into the limit of the composite panel with the bolts installed. These areas in contact with the external extreme of the bolts are shown in the next images:

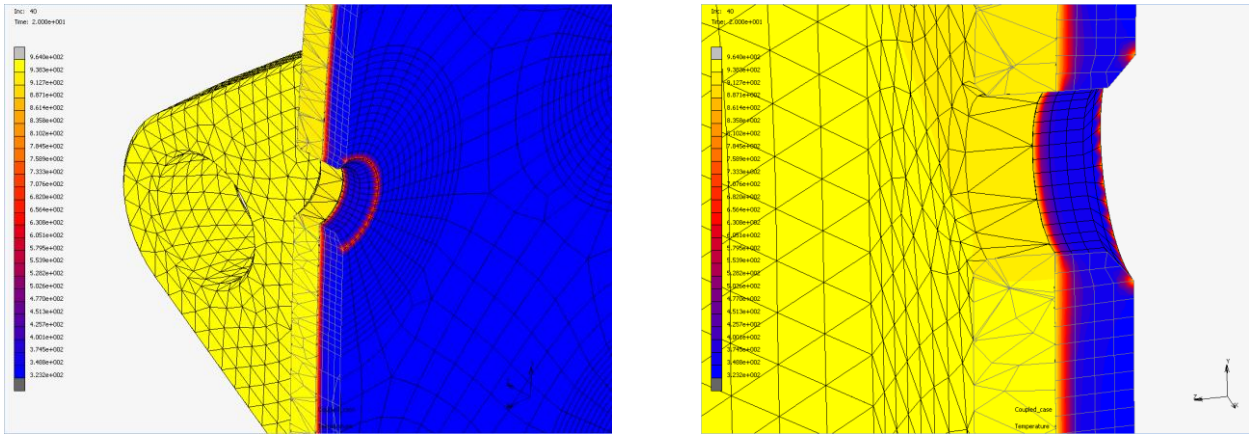


Figure 90 M21/T700G panel: temperature distribution detail (20 sec from flame init) (Thermomechanical simulation)

In consequence, these regions should be analyze with respect with time, its evolution of the maximum temperature distribution closed to these indentified elements where the model criterion failure definition should be apply on.

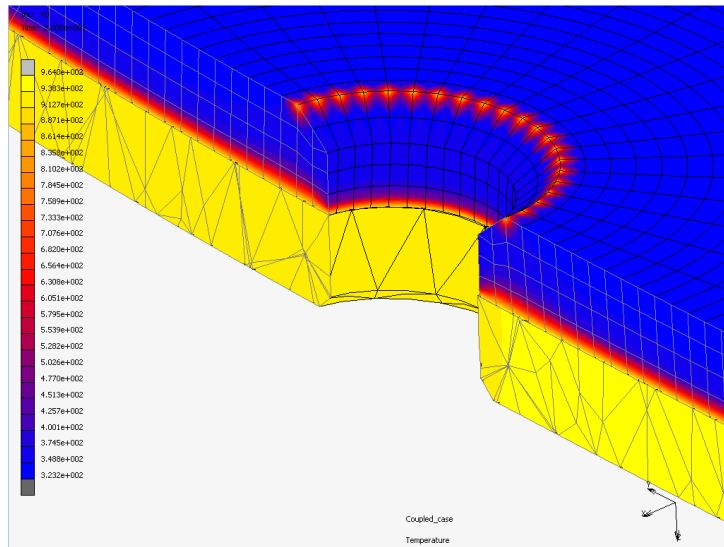
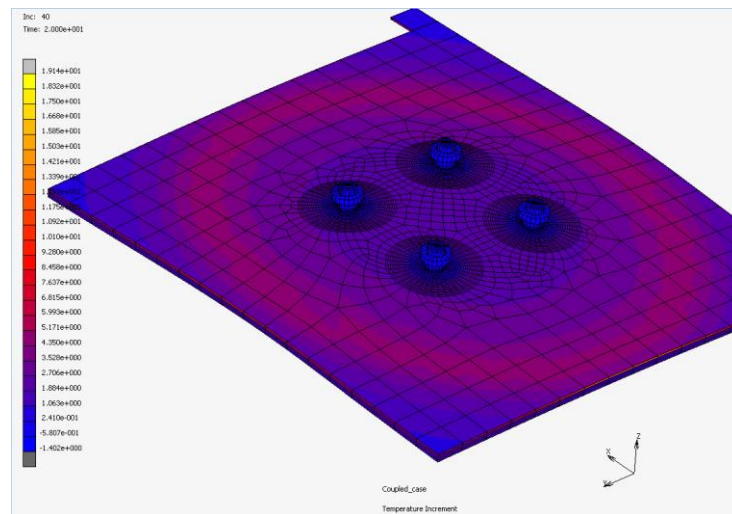


Figure 91 M21/T700G panel: temperature distribution detail (20 sec from flame init) (Thermomechanical simulation)

In the next image is depicted the field of the temperatures increments of the composite panel after 20 seconds of the application of the standard flame. Where, according to the experimental test performed, the failure doesn't take place yet and can be analyze the evolution of the temperature differences boundary areas.



### Failure criterion:

Thermal properties characterization establishes a clear thermal property change in the range of (270-400°C as per Ref 12). A direct relation between thermal and mechanical properties is supposed (and confirmed by fire tests experimental results) implying a complete loss of resin resistance at this temperature range.

The following failure criteria could be established: failure occurs when the temperature at the maximum temperature spot of cold face (commonly the resistant surroundings of the bolt joint) reaches this temperature range (conservatively 270°, to be determined with further fire testing). This failure is supposed to occur independently of the load of the bolt, as the stiffness of the resin is supposed to be null beyond this range.

### 5.5. Future tasks

According to the systematic application of the coupled models to solve particular problems, not only oriented to the assemblies submitted to fire but also focused on solving another kind of problems submitted to a high temperatures gradients therefore, makes necessary to improve the material properties and boundary condition modelling which the model is based on. Therefore, in order to use an enhanced thermo-mechanical model for the prediction of a determine composite material behavior submitted to a medium temperature levels, is necessary to redefine the material properties introduced into the model by means of the performing of new thermal tests according to the defined environment that should be figured out, so as to complete the data base of the finite element model that has been implemented.

To complete the all range of temperatures prediction, thermo-mechanical problems can be addressed in the range of the low and medium temperature to do so; new information based on experimental test should be obtained in order to improve the model behavior in these new boundary conditions and into a new environments. The material degradation kinetic with respect to the

temperature level reached should be incorporated with the material properties definition into the coupled model, in order to reproduce the material behavior submitted to these new conditions by means of the simulation.

Improving the definition of failure criteria by means of carrying out different thermo-mechanical tests, is a key factor in order to simulate the failure mechanism into the thermal-mechanical problem, in consequence improving the test data obtained near the fitting riveted plane (the failure of the assembly will be located in the rivets joint with the composite material) therefore, the failure criteria should be based on the behavior of the near zones. Experience shows that all failures are located in the joint CFRP-fittings in consequence, to have a better and more accurate failure criterion so as to implement in a thermal-mechanical model is advisable.

As it has been indicated before, the heat convection coefficient is implemented into the model through an empirical correlation adjusted by means of experimental tests; this modelling process is not a trivial issue. Considering new solver capabilities and software packages which are able to perform multiphysics analysis, is possible the resolution of the Navier-Stokes equations into the fluid field defined coupled with thermo-mechanical problem, by means of the application of finite elements techniques and permitting the direct determination of a heat convection factor distribution on each one of the panel surface submitted to heat thermal transfer. Finally and as a result, the characterization process of the heat convection factor is not necessary in order to implement the thermal boundary conditions of the coupled thermal model.

## 6 CONCLUSIONS AND RECOMMENDATIONS

### 6.1. Conclusions

Structural thermal requirements for primary and secondary structures have been stated based on current EASA CS-25 regulation. A study of the current bibliographic state of the art of thermal and thermomechanical simulations has been included in section 3. An approach for the simulation of thermal and chemical behavior of specific tests has been proposed in section 4.

A simplified methodology for fire testing prediction has been proposed throughout section 5. This methodology is applicable to the prediction of standard fire test on composite loaded panels. This methodology relies on:

- Simplified thermal boundary conditions:
  - Flame model, based on the repetitivity of thermal hot face map on a standard fire test.
  - Convection model based on constant heat transfer coefficient dependent on the cold face flow speed.
- A thermal characterization on an intact panel and a degraded panel.
- Simplified assumption of a direct relation between thermal and mechanical degradation
- Simplified failure criteria based in cold face temperature map evolution through test.
- Confirmation, by dedicated and especially monitored test, of the adequacy of these assumptions for a typical composite configuration in a typical load range.
- Thermal (only) transient problem resolution to establish the cold face temperature map evolution
- Determination of the failure instant based in the failure criteria defined.
- Thermomechanical problem resolution, with the same assumptions, to evaluate impact of secondary effects that may impact on the problem (large deformations with impact on thermal contact between elements)

Due to the relevant thermal parameters in the heat transfer process from the panels of which will be tested and not be determined experimentally, through the direct application of the procedure developed by Airbus D&S, (these properties are the emissivity, Cp, thermal conductivity and thermal diffusivity,) can be determined these main thermal properties of the materials in a non-intrusive way, by means of the application of infrared technology.

The objective of thermo-mechanical modelling is to understand the response and performance of a physical system including the effects of heat transfer processes convection and radiation combined with the effects of the loads applied. Many times this requires multiphysics simulations where temperature has a key effect on the behavior and performance of components, structures or processes including effects on material properties and boundary conditions, loading etc.

In order to be able to approach a complex thermal-mechanical problem it is necessary to assume some considerations by means of the simultaneous determination, through experimental procedures of values of temperature and deformation, series of analytical numerical correlations to their later

implementation in a numerical model should be able to be established for their simulation. In consequence, a test campaign is defined to correlate the results of the simulations performed and with the accomplishment of the defined tests, a great amount of numerical results corresponding to the panels tested will be obtained; this test matrix has to be adequately defined in order to obtain usable results for the model definition parameters.

The use of thermo-mechanical modelling in order to obtain a couple simulation of the real problem is a key factor to predict the behavior of the composite material submitted to fire under real conditions. The analysis simulation results can provide an estimation of the degradation state of the composite materials submitted to fire and other boundary conditions.

The analysis of simulation of the coupled problems can support to the designer to the designer to take decisions related to with aircraft fire wall with loads applied and to define geometries and configurations suitable from the point of view of its behavior under generalized fire.

## 6.2. Recommendations

The following recommendations can be made:

- i. Implement the **model** into suitable simulation **platform software** to carry out the Coupled-Simulation.
- ii. Generate a Thermo-Mechanical model by means of finite element method representative of the behavior of materials submitted to applied loads, temperature and degradation.
- iii. Work out and analyze problems with interaction thermal and mechanical, initial thermally uncoupled followed by coupled.
- iv. Establish a systematic procedure to perform correlations of the model through results obtained in laboratory tests.

The experience related to monolithic composite fire testing when loaded through common fitting assemblies determines that the main failure occurs on the joint between load introduction device (fitting) and the composite. This joint is typically a fastened connection (bonding joint is not a non-destructively inspectable procedure and not actually accepted by EASA); the presented work has simplified the possible loading states on a fastened joint to an in plane load state and a through the plane pull out. The characterization, test and correlation with simulation of these basic configurations may be a enough information to propose a simplified simulation of a complex fitting-composite configuration. A more detailed campaign could explore alternate configurations:

## 7 REFERENCES

- [Ref1] ISO 2685:1998(E): "Aircraft- Environmental test procedure for airborne equipment – Resistance to fire in designated fire zones".
- [Ref2] FAA'S ADVISORY CIRCULAR N° 20-135: "Power plant Installation and Propulsion System Component Fire Protection Test Methods, Standards and Criteria"
- [Ref3] SPO705382\_ Issue1.4: Airbus Fire Test Generic Specification
- [Ref4] NT-0-SGL-05001\_IssueC: Fire Test Laboratory Procedure
- [Ref5] ASTM E1461 – 13 "Standard Test Method for Thermal Diffusivity by the Flash Method"
- [Ref6] UC3M D16.2 "Characterization of thermo-mechanical behaviour of composite materials in fire and empirical determination of their properties"
- [Ref7] Federal Aviation Administration, "Aircraft Materials Fire Test Handbook," 2000.
- [Ref8] "Hexcel® HexPly® M21/35%/268/T700GC Data Sheet," 2007.
- [Ref9] M. Oliveira et al., Future Sky Safety, Plan of Experiments - Primary Structures Materials – Final Requirements, Selection and Specification of Materials and Tests, D7.1, September 2015.
- [Ref10] E. Deletombe et al., Future Sky Safety, Project Plan P7 - Mitigating the risk of fire, smoke and fumes (V3.0), D8.1 - Appendix P7, September 2015.
- [Ref11] J.Berthe et al., Future Sky Safety, Primary structure materials – Test results (first batch) (V2.0).
- [Ref12] J.Berthe et al., Future Sky Safety, Primary structure materials – D7.7 Test results (second batch)
- [Ref13] Betancourt Grajales R., 2003 ISBN: 9589322832 "Transferencia molecular de calor, masa y/o cantidad de movimiento", P366
- [Ref 14] A. Mouritz, A Gibson, "Fire Properties Of Polymer Composite Materials" - (Springer, 2006)
- [Ref 15] Gillian Leplat, Cécric Huchette, and Valentin Biasi. «Thermal and damage analysis of laser-induced decomposition within carbon/epoxy composite laminates. Journal of Fire Sciences.» *Journal of Fire Sciences* (2016): 34(5):361–384.
- [Ref 16] Valentin Biasi. « Modélisation de la dégradation d'un matériau composite soumis au feu » thèse de l'université de Toulouse, (2014)
- [Ref 17] Lautenberger, Chris and Carlos Fernandez-Pello. « Generalized Pyrolysis Model for Combustible Solids. » *Fire Safety Journal*: 44(6):819–39 (2009)

- [Ref 18] Mouritz, A. P. et al. « Review of Fire Structural Modelling of Polymer Composites. » *Composites Part A: Applied Science and Manufacturing* : 40(12):1800–1814.
- [Ref 19] David Le´vèque et al. «Analysis of how thermal aging affects the long-term mechanical behavior and strength of polymer–matrix composites» *Composites Science and Technology*: 65 (2005) 395–401.
- [Ref 20] Juhyeong Lee, Thomas E. Lacy, Charles U. Pittman, Jr., Michael S. Mazzola. « Temperature Dependent Thermal Decomposition of Carbon/Epoxy Laminates Subjected to Simulated Lightning Currents» *Polymer Composite*.
- [Ref 21] A. Mlyniec, J. Korta, R. Kudelski, T. Uhl «The influence of the laminate thickness, stacking sequence and thermal aging on the static and dynamic behavior of carbon/epoxy composites» *Composites Science and Technology*: 118 (2014) 208–216
- [Ref 22] Pauline Tranchard, Fabienne Samyn, Sophie Duquesne, Bruno Estèbe and Serge Bourbigot «Modelling Behaviour of a Carbon Epoxy Composite Exposed to Fire: Part I Characterisation of Thermophysical Properties Materials 2017» 10, 494; doi:10.3390/ma10050494
- [Ref 23] Pauline Tranchard, Fabienne Samyn, Sophie Duquesne<sup>1</sup>, Matthieu Thomas, Bruno Estèbe, Jean-Luc Montés and Serge Bourbigot, «Fire behaviour of carbon fibre epoxy composite for aircraft: Novel test bench and experimental study» DOI: 10.1177/0734904115584093
- [Ref 24] Pauline Tranchard, Fabienne Samyn, Sophie Duquesne, Bruno Estèbe and Serge Bourbigot, «Modelling Behaviour of a Carbon Epoxy Composite Exposed to Fire: Part II— Comparison with Experimental Results» doi:10.3390/ma10050470
- [Ref 25] Gregory E. Gorbett, Msc, CFEI, CFPS, IAAI-CFI, «MIFireE Computer Fire Models for Fire Investigation and Reconstruction» *International Symposium on fire Investigation and Technology. ISFI 2008*.
- [Ref 26] Wladyslaw Mitianiec «Factors Determining Ignition and Efficient Combustion in Modern Engines Operating on Gaseous Fuels» *Internal Combustion Engines*: <http://dx.doi.org/10.5772/48306>
- [Ref 27] F.Jia, M.K.Patel and E.R.Galea, «Simulating the Swissair Flight 111 In-Flight Fire Using the CFD Fire Simulation Software SMARTFIRE» *Fire Safety Engineering Group University of Greenwich, London SE10 9LS. U.K.* <http://fseq.gre.ac.uk>
- [Ref 28] Richard D. Peacock, Kevin B. McGrattan, Glenn P. Forney, Paul A. Reneke, «CFAST– Consolidated Fire and Smoke Transport» *NIST Technical Note 1889v1*: <http://dx.doi.org/10.6028/NIST.TN.1889v1>
- [Ref 29] Jason E. Floyd «Comparison of CFAST and FDS for Fire Simulation with the HDR T51 and T52 Tests» *NISTIR 6866*

**Project:** Mitigating risks of fire, smoke and fumes  
**Reference ID:** FSS\_P7\_ADS\_D7.9  
**Classification:** Public



[Ref 30] Kevin McGrattan, Simo Hostikka, Randall McDermott, Jason Floyd, Marcos Vanella, Craig Weinschenk, Kristopher Overholt, «Fire Dynamics Simulator Technical Reference Guide» *NIST Special Publication 1018-1 Sixth Edition* <http://dx.doi.org/10.6028/NIST.SP.1018>

[Ref 31] Aircraft Technical Books, LLC «Fire Investigation», [www.ACTechbooks.com](http://www.ACTechbooks.com) 970-726-5111

[Ref 32] U.S. Department of Transportation Federal Aviation Administration, «Fire-Safe Polymers and Polymer Composites» *DOT/FAA/AR-04/11*

[Ref 33] Aviation Rulemaking Advisory Committee Transportation Federal Aviation Administration, «Harmonize Guidance Material and 14 CFR 25.603»

## 8 ANNEXES

### 8.1.1. Annex I: Standard FAR/CS25 requirements

#### **CS 25.867 Fire protection: other components**

- (a) Surfaces to the rear of the nacelles, within one nacelle diameter of the nacelle centreline, must be constructed of materials at least equivalent in resistance to fire as aluminium alloy in dimensions appropriate for the purpose for which they are used.
- (b) Sub-paragraph (a) of this paragraph does not apply to tail surfaces to the rear of the nacelles that could not be readily affected by heat, flames, or sparks coming from a designated fire zone or engine compartment of any nacelle.

#### **POWERPLANT FIRE PROTECTION**

##### **CS 25.1181 Designated fire zones: regions included**

(See AMC 25.1181.)

- (a) Designated fire zones are –
- (1) The engine power section;
  - (2) The engine accessory section;
  - (3) Any complete powerplant compartment in which no isolation is provided between the engine power section and the engine accessory section;
  - (4) *Reserved*.
  - (5) Any fuel-burning heater and other combustion equipment installation described in CS 25.859;
  - (6) The compressor and accessory sections of turbine engines; and
  - (7) Combustor, turbine, and tailpipe sections of turbine engine installations that contain lines or components carrying flammable fluids or gases.
- (b) Each designated fire zone must meet the requirements of CS 25.863, 25.867, 25.869, and 25.1185 to 25.1203

##### **CS 25.1182 Nacelle areas behind firewalls, and engine pod attaching structures containing flammable fluid lines**

- (a) Each nacelle area immediately behind the firewall, and each portion of any engine pod attaching structure containing flammable fluid lines, must meet each requirement of CS 25.1103 (b), 25.1165 (e), 25.1183, 25.1185 (c), 25.1187, 25.1189 and 25.1195 to 25.1203, including those concerning designated fire zones. However, engine pod attaching structures need not contain fire detection or

retractable landing gear, compliance with that sub-paragraph need only be shown with the landing gear retracted

##### **CS 25.1191 Firewalls**

- (a) Each engine, fuel-burning heater, other combustion equipment intended for operation in flight, and the combustion, turbine, and tailpipe sections of turbine engines, must be isolated from the rest of the aeroplane by firewalls, shrouds, or equivalent means.
- (b) Each firewall and shroud must be –
- (1) Fireproof;
  - (2) Constructed so that no hazardous quantity of air, fluid, or flame can pass from the compartment to other parts of the aeroplane;
  - (3) Constructed so that each opening is sealed with close fitting fireproof grommets, bushings, or firewall fittings; and
  - (4) Protected against corrosion.

##### **CS 25.1193 Cowling and nacelle skin**

(See AMC 25.1193)

- (a) Each cowling must be constructed and supported so that it can resist any vibration, inertia, and air load to which it may be subjected in operation.
- (b) Cowling must meet the drainage and ventilation requirements of CS 25.1187.
- (c) On aeroplanes with a diaphragm isolating the engine power section from the engine accessory section, each part of the accessory section cowling subject to flame in case of fire in the engine power section of the powerplant must–
- (1) Be fireproof; and
  - (2) Meet the requirements of CS 25.1191.
- (d) Each part of the cowling subject to high temperatures due to its nearness to exhaust system parts or exhaust gas impingement must be fireproof.
- (e) Each aeroplane must –
- (1) Be designed and constructed so that no fire originating in any fire zone can enter, either through openings or by burning through external skin, any other zone or region where it would create additional hazards;
  - (2) Meet subparagraph (e)(1) of this paragraph with the landing gear retracted (if

extinguishing means.

applicable); and following:

- (b) For each area covered by subparagraph (a) of this paragraph that contains a (3) Have cowlings and nacelles skins, in areas subject to flame if a fire starts in an engine fire zone, complying with the
    - i) For in-flight operations, cowlings and nacelles skins must be fireproof in the complete concerned. areas, and
    - (ii) For ground operations, cowlings and nacelles skins must be:
      - (a) Fireproof in the portions of the concerned areas where a skin burn through would affect critical areas of the aeroplane, and
      - (b) Fire-resistant or compliant with subparagraph (e)(1) of this paragraph in the remaining portions of the concerned areas.
- (See AMC 25.1193(e))  
[Amdt No: 25/13]  
[Amdt No: 25/18]

#### **AMC 25.1181 & AMC 25.1193**



AMC25.1181-1193-C  
S25Am18.pdf

## 8.1.2. Annex II: Standard AC20-135 (FAA) requirements



# Advisory Circular

Subject: POWERPLANT INSTALLATION AND PROPULSION SYSTEM COMPONENT FIRE PROTECTION TEST METHODS, STANDARDS, AND CRITERIA. Date: 2/6/90 AC No: 20-135  
Initiated by: ANM-110 Change:

1. **PURPOSE.** This advisory circular (AC) provides guidance for use in demonstrating compliance with the powerplant fire protection requirements of the Federal Aviation Regulations (FAR). Included in this document are methods for fire testing of materials and components used in the propulsion engines and APU installations, and in areas adjacent to designated fire zones, as well as the rationale for these methods. Since the method of compliance presented in this AC is not mandatory, the terms "shall" and "must," as used in this AC, apply only to an applicant who chooses to follow this particular method without deviation.

2. **RELATED FAR SECTIONS.** The applicable FAR sections are listed in appendix 1 of this AC.

3. **BACKGROUND.** Although § 1.1 of the FAR provides general definitions for the terms "fireproof" and "fire resistant," these definitions do not specify heat intensity, temperature levels, duration (exposure time), or an appropriate wall thickness or other dimensional characteristics for the purpose intended. With the advent of surface coatings (i.e., ablative/intumescent), composites, and metal honeycomb for acoustically treated ducting, cowling, and other components which may form a part of the nacelle firewall, applicant confusion sometimes exists as to how compliance can be shown, particularly with respect to the definition of "fireproof" and "fire resistant" as defined in § 1.1.

4. **DEFINITIONS.** For the purposes of this AC, the following definitions apply:

a. **Fireproof:** The capability of a material or component to withstand, as well as or better than steel, a 2000°F flame (±150°F) for 15 minutes minimum, while still fulfilling its design purpose. The term "fireproof," when applied to materials and parts used to confine fires within designated fire zones, means that the material or part will perform this function under conditions likely to occur in such zones and will withstand a 2000°F flame (±150°F) for 15 minutes minimum.

b. **Fire Resistant:** When applied to powerplant installations such as fluid-carrying lines, flammable fluid system components, wiring, air ducts, fittings and powerplant controls, "fire resistant" means the capability of a material or component to perform its intended functions under the heat and other conditions likely to occur at the particular location and to withstand a

2/6/90

AC 20-135

minutes when exposed to a 2000°F flame temperature. "Fireproof" means the material or component will maintain its integrity and function for a minimum of 15 minutes when exposed to a 2000°F flame temperature.

6. **FIRE TEST EQUIPMENT STANDARDS AND TEST CRITERIA.** Fire tests should meet and produce the following conditions and environment:

a. **Test Equipment Criteria.**

- (1) Specified flame impingement temperature, heat flux density, and flame distribution.
- (2) Critical actual operating loads and environmental conditions (air and fluid flow rates, pressures, structural loads, and the like).
- (3) Specified fire and heat flux exposure duration.

b. **Burner Equipment:** Heat flux density and temperature capability.

(1) The basic torch or burner requirements are that the flame should produce a 2000°F temperature within 1/4 inch of the specimen and engulf or provide representative impingement coverage, dependent on specimen size. In addition, the burner or torch should provide a heat flux density of at least 9.3 BTU/ft<sup>2</sup>-sec or 4500 BTU/hr using the BTU heat transfer device, unless it can be shown that the heat flux density for the configuration under test will not inherently affect the results of the test (ref. paragraph d(4) below).

(2) **Procedure:** The burner shall be lit, allowing a 5-minute warm up. Conduct the calibration for heat flux density and obtain a flame temperature of 2000°F. Immediately after successfully completing the calibration, rotate or move the burner to the test specimen, maintaining the same distance of the specimen from the burner as the thermocouples/heat flux density device were from the burner during burner calibration. Do not shut off the burner between the calibration and the actual test. Ensure the thermocouple(s) is positioned in the flame, 1/4 inch in front of the test specimen.

c. **Acceptable Burner/Torch Configuration.** Depending on the specific application, the following burners have been used:

(1) The type specified in Powerplant Engineering Report No. 3A (see appendix 2, Nos. 1, 5, and 6). This burner has been used to test flammable fluid-carrying components, cowling, composite materials, firewall materials, fuel and hydraulic hoses, and other similar applications.

(2) SAE 401 Burner (standard). This burner has been used for testing fire detectors, associated electrical wiring, and similar applications and is specified in various Technical Standard Orders (TSO)

Par 5

3

AC 20-135

2/6/90

2000°F flame (±150°F) for 5 minutes minimum. (Example: A fire resistant hose which will withstand a 2000°F flame for 5 minutes.)

c. **Engine Case Burnthrough:** A fire condition within the engine which burns through the engine case, allowing a high pressure and high temperature gas stream to escape from the engine.

d. **Heat Flux Density:** The rate of thermal energy in BTU/ft<sup>2</sup>-sec of the flame. One of the following devices shall be used to measure heat flux density of the test flame:

(1) **Calorimeter:** The calorimeter to be used in testing must be a 0-15.0 BTU/ft<sup>2</sup>-sec (0-17.0 W/cm<sup>2</sup>) Calorimeter, accurate to ± 3 percent.

(2) **BTU Heat Transfer Device:** See FAA Powerplant Engineering Report No. 3A (appendix 2 of this AC) for fabrication details of a copper tube device used to measure heat flux density.

NOTE: In accordance with Powerplant Report 3A, the copper tube shall be set up without any type of backing plate behind the copper tube.

e. **Thermocouples:** The thermocouples to be used should be bare junction 1/16 to 1/8-inch metal sheathed, ceramic packed, chromel-alumel, thermocouples with nominal 22 to 30 AWG (American Wire Gauge) size conductors or equivalent. An air aspirated, shielded, thermocouple should not be used.

### 5. FIRE PROTECTION PRINCIPLES AND OBJECTIVES.

a. The primary objectives of fireproof and fire resistant materials and components are to contain and isolate a fire and prevent other sources of fuel or air from feeding the existing fire, and to ensure that components of the engine control system will function effectively to permit a safe shutdown of the engine or APU and safe feathering of the propeller.

b. To demonstrate satisfactory containment capability, the materials or components must have adequate strength for the foreseen flight and operating loads under the conditions of a fire to allow proper fire detection, firefighter recognition, and subsequent corrective action. In addition gaseous emissions from fire protection materials shall be precluded from entering the cabin air conditioning system.

c. Fire testing should simulate the likely fire environment to prove the materials and components will provide the necessary fire containment to meet the above objectives when exposed to a fire situation in service.

d. The descriptors "fireproof" and "fire resistant" differ only in the time duration that the material or component should maintain its integrity or perform its function. "Fire resistant" means the material or component will function and maintain its integrity for a minimum of 5

2

Par 4

AC 20-135

2/6/90

and military standards. NOTE: This burner should not be used for powerplant installation fire testing in accordance with this AC.

(3) SAE 401 Burner adjusted to increase the output to at least 9.3 BTU/ft<sup>2</sup>-sec heat flux density. This adjusted burner has been used to test firewall materials, composite materials, cowling, electrical wiring, fuel flowmeters, firewall fittings, and other components.

(4) Propane and oxy-acetylene torch-standard and diverging nozzles. The propane or oxy-acetylene burner has been used for wiring, flow meters, firewall penetrations, and other "small" component type applications.

(5) Miscellaneous burners have been found acceptable by the FAA for the intended applications. Component and material fire testing has been accomplished using the manufacturer's choice of burner, provided acceptability by the FAA has been determined with respect to flame size/impingement area and heat flux density, and the temperature at the test article was 2000°F. The adequacy of the burner depends on the size of the component, installation considerations, and on the flame completely engulfing the exposed portion or "face" of the component, or covering a representative portion of sheet material.

d. **Acceptable Test Criteria and Philosophy.**

(1) The test for demonstrating compliance with the criteria for "fireproof" and "fire resistant" materials, components, and fittings is to expose the specimen to the required flame temperature and heat flux density for the required time (15 minutes for "fireproof" and 5 minutes for "fire resistant"). The specimen shall withstand flame penetration and not exhibit backside ignition for the required test time. Sheet materials and panels shall be tested by exposing a sample size approximately 10 inches on a side (10"x10", or a size appropriate for the intended application) to a flame from an acceptable burner at the test operating conditions outlined in paragraph 7. The flame size and temperatures shall be sufficient to maintain the required test temperature and heat flux density over an area of approximately 5"x5" for sheet materials and panels.

(2) Fittings used in firewalls and in fire zones shall be completely enveloped in the flame on the side that would normally be exposed to fire in the fire zone. The fittings shall be mounted in a manner simulating the actual installation, and fluid lines or tubing may be connected to both ends of the fitting to simulate the installation that would be present during a typical fire event. However, for the testing of fluid-fittings, there should be no fluid in the line on the engine side of the fitting in the fire zone, since the fire may have been caused by a failure of the line to the fitting under evaluation. Likewise, if failure of the line on the engine side of the firewall could drain the fluid from that portion of the line upstream of the firewall, up to the fluid shutoff valve, then the lines connected to both sides of the fitting should not

4

Par 6

Approved

2/6/90

AC 20-135

contain fluid for this testing. If the fitting is part of the shutoff valve, then the line behind or upstream of the valve should contain fluid. For operational components, such as check valves, lines, etc., the flame should completely envelop the unit.

(3) Technical Standard Order, TSO-C53a, Fuel and Engine Oil System Hose Assemblies, and TSO-C75, Hydraulic Hose Assemblies, specify hose assembly fire resistance requirements. These hose assemblies should be exposed to a 2000°F flame for 5 minutes while maintaining the fuel or oil at critical (minimum or maximum) operating flow rates and pressures without evidence of any leakage. The 5-minute exposure provides a reasonable time for the flightcrew to recognize a fire condition, shut down the appropriate engine, and close the appropriate shutoff valve(s), thus shutting off a liquid flow to the engine compartment. It is important to evaluate the particular installation and obtain the minimum flow rate over the entire operating envelope. Although the TSO specifies a flow rate in gallons per minute of 3 to 5 times the (ID)<sup>2</sup>, ID measured in inches, experience has shown, for example, that a hydraulic system drain or return line not under system demand can have no flow or a flow quite a bit less than that specified by 3 times (ID)<sup>2</sup>. The lower flow rate should then be used for the fire resistant or fireproof testing. The fire test procedure for hoses is outlined in FAA Powerplant Engineering Report No. 3A, (see appendix 2, Nos. 1, 5, and 6).

(4) The operational criteria required for various components depends on the kind of component to be tested. For example, if the unit is an oil line routed through a fire zone with the shutoff valve located outside and downstream of the fire zone, the line should withstand the test flame, without leakage or failure, for 15 minutes. If the unit under test is a shutoff valve located in the engine compartment fire zone, the valve should be exposed to the burner or flame for 5 minutes. The valve should not leak and should be able to be closed by normal application means at the end of the 5-minute exposure. After the valve has been closed, it is to be exposed to the flame for an additional 10 minutes, and the valve should not leak. Operational components should be subjected to the fire tests in every installation, unless similarity to previously approved configurations can be shown, or they are made of steel or copper based alloys, or they are of such construction that their capability to operate satisfactorily under fire conditions is obvious.

(5) Electrical and mechanical controls (cables, electrical wires, drive links, etc.) for components such as shutoff valves located in the engine compartment or other designated fire zones are required to be "fire resistant." These shall be tested at a 2000°F temperature for 5 minutes. At the end of 5 minutes, the control shall perform its intended function without failure or malfunction. The flame should completely envelop the control and the end fittings and connections from one direction, all as a unit. Where control rods or cables are to be tested, a typical section is all that is

Par 6

5

AC 20-135

2/6/90

required to be evaluated. About 8 inches of the typical section will suffice in most tests, including the end connections and fittings. For testing cable controls, the normal rigging load should be simulated. Control rods which act in compression to operate their component should have the flame applied over the center portion of the rod length where the column compression action will most likely cause failure of the material. Flammable fluid shutoff valve controls should be tested for fire resistance in each installation, except where the cables or rods are purely tension controls and constructed of steel or other materials shown to be "fire resistant" or are designed such that their operation in fire conditions is obvious.

(6) The following minimum thickness materials are considered acceptable for use in firewalls or shrouds for non structural/non load-carrying applications, without being subjected to additional fire tests:

- (i) Stainless steel sheet, .015 inch thick.
- (ii) Mild steel sheet protected against corrosion, .018 inch thick.
- (iii) Titanium sheet, .016 inch thick.
- (iv) Murel metal sheet, .018 inch thick.
- (v) Steel or copper base alloy firewall fittings/fasteners.

**NOTE:** Distortion of thin sheet materials and the subsequent gapping at lap joints or between rivets is difficult to predict; therefore, testing of the simulated installation is necessary to prove the integrity of the design. However, rivet pitches of 2 inches or less on non load-carrying titanium firewalls of .020 inch or steel firewalls of .018 inch are acceptable without further testing.

(7) In every application the applicant should coordinate and obtain approval for the fire test verification plan and other certification testing for the fireproof and fire resistant aspects of the proposed installation with the FAA office responsible for the project.

(8) At the conclusion of the testing, a report, including photographs, which describes the fire test results and addresses the pertinent items identified in this advisory circular should be submitted for FAA approval.

#### 7. FIRE PROTECTION INSTALLATION AND DESIGN FEATURES.

a. **Structural Operating Environment.** The structural static and dynamic loading to be simulated during the testing is a function of the component or material and the intended use and location, and should be

6

Par 6

2/6/90

AC 20-135

addressed in the test plan. Firewall or component structural loading conditions must be identified and incorporated in the fire test setup. Flexible hoses are fire tested at anticipated fuel or oil internal pressures, flow rates, and vibratory conditions. The test is intended to simulate aircraft powerplant fire conditions, with the fuel, oil flow, and pressures at critical operating conditions.

b. **Design and Application Factors.** There are a number of other important factors which can influence the test conditions required to substantiate firewalls and fire resistant surfaces. These considerations are classified into two categories. One is the "intended use" of the firewall or fire resistant surface. For example, is its intended use a cowl door or the inner wall of an engine fan exhaust duct or an inlet duct, or an isolating diaphragm with its primary purpose being a firewall? The second category relates to the firewall or fire resistant surface construction. Is it a complex composite structure bonded with resin and coated with a fire retardant, or is it an acoustic panel, or simply a stainless steel, titanium, or other basic metallic configuration? Typically, panels representative of the proposed structure (approximately 1-1/2 by 2 feet) have been acceptable for demonstrating fire protection capability.

#### (1) "Intended Use" Test Criteria.

(i) If the firewall is a diaphragm or simple separation type non load-carrying bulkhead in a nacelle area with low ventilation and circulation air flow and a small pressure load, a simple fire test at ambient environmental laboratory conditions is acceptable to demonstrate fireproof properties.

(ii) If the firewall is the nacelle cowl with approximately 1/2 psi or less nacelle pressurization, scrubbing airflow may be utilized without consideration for having to run the test with nacelle pressurization.

(iii) If the firewall is an engine fan air exit duct or inlet adapter, "cool side" (backside) pressure and airflow conditions should be properly simulated during the testing. The test should be performed with the airflow and pressure the duct will normally be exposed to during critical power operating conditions for the initial 5 minutes and at windmilling conditions for the additional 10 minutes of the fire test, if this is the most severe heat condition. Fan exhaust ducts normally have their critical differential pressures existing across the duct at sea level, takeoff conditions. Inlet adapter type ducting will usually be at the maximum pressure when the engine is shut down in flight and allowed to windmill. These operating conditions should be determined by the applicant for use in the fire test. Typically, unprotected acoustic honeycomb specimens which fail this test will rupture due to loss of

Par 7

7

AC 20-135

2/6/90

strength under pressure during the first few minutes of testing, allowing air flow into the fire zone.

(iv) The test criteria in paragraph 7b(1)(iii) above, addressing the addition of airflow to a firezone during a fire condition, also applies to cooling air ducts, bleed air ducts, etc., located or routed within the fire zone.

(v) Aircraft engines with turbochargers operate at elevated temperatures and pressures within the engine compartment. Components adjacent to the turbocharger and exhaust systems should be evaluated for operation at these elevated temperatures and pressures. Also, any flammable fluid-carrying component or other system should be evaluated for a possible exhaust system component failure with resultant exhaust gas leakage. When those turbochargers are used for cabin pressurization, all air inlet ducts within the engine compartment should be evaluated for component burnthrough or release of noxious fumes within the cabin ventilation system.

(2) **Firewall Construction Test Considerations.** Bonded construction firewalls (composites or bonded metal matrix), in addition to being pressurized during testing, may need to be vibrated. This should be accomplished for all specimens with a sprayed, painted-on, or bonded-on protective coating intended to insulate the base material from the fire conditions. Past tests have shown some ablative and intumescent coatings become extremely brittle when exposed to flames. Vibration can cause the coating to flake off, exposing the base material. Current experience has not supported the use of an intumescent coating as an acceptable fire protection coating, because the coatings have lacked durability and exhibited poor adhesion characteristics in service. For composites or other "new" materials, more than one test panel may be required to show repeatability of the configuration.

c. **Outgassing.** A characteristic of bonded construction firewall materials and seal materials is the outgassing of the volatile constituents of the bonding resins or seal materials. This can occur from either the hot or cool side surface of the specimens during the test. These gasses are, in most instances, highly flammable. Ignition occurring on the cool side is unacceptable in passing the fire test. Where the cool side surface is exposed, visual observations will suffice to note if ignition has occurred. However, if the specimen is subjected to pressure loading during the test, or the cool side is hidden from view, then other methods to detect the ignition should be defined. It should be noted that some acoustically treated ducts are of metal construction, and the face sheets are bonded to the honeycomb core with resins which can exhibit outgassing. For these types of construction, no "cool side" ignition is allowed and verification is required.

**CAUTION:** Specimen size should be large enough to prevent flame wraparound of the specimen edge to provide a more accurate simulation of the actual installation.

8

Par 7

2/6/90

AC 20-135

(1) Upon initial application of the test torch flame, minor flareup at the flame impingement area may occur; however, continuous burning or a significant increase of the flame pattern over the entire specimen is unacceptable. Ignition of the backside as well as penetration are the other anomalies which are cause to reject the component. Excessive outgassing, especially from composite construction, should be investigated to ensure the smoke will not ignite. Additional testing of samples should be requested to ensure that:

- (i) Any surface flareup is self extinguishing and does not burn after removal of the test flame and,
- (ii) Self re-ignition of the material does not occur when the flame is removed.

(2) If the gases emitted during the fire tests can enter the personnel compartment, the gases must be evaluated for their toxicity, volatility, and possible impairment of the crew or passengers.

**d. Unique Design Testing Considerations.**

(1) The applicant should evaluate firewall designs, putting special emphasis on fuel and oil lines, cowling and/or bleed duct, and other firewall penetration points to determine the need for a specific fire test setup and incorporation of the penetrations in the firewall test specimen. As noted in paragraph 6d(2), flammable fluid-carrying lines and fittings need careful consideration. The use of previously approved corrosion-resistant steel or equivalent material is considered satisfactory without further tests. Use of aluminum alloy for any size line/fitting on either side of a firewall should be avoided. An evaluation of the specific installation configuration and actual minimum flow rates should be accomplished to determine fire resistant or fireproof capability. Previous tests (appendix 2, No. 3) have shown aluminum couplings (3/4 inch or larger) have leaked after exposure to the test flame for 5 minutes with nominal 30 psi pressure and a fluid flow rate in gallons per minute equal to 5 times the (ID)<sup>2</sup>, ID measured in inches. All sizes of aluminum fittings up to 2 inches failed the "no flow" conditions. Five minutes is acceptable for fire resistant tubing; however, all firewall fittings/penetrations are required to maintain the integrity of the firewall without flame penetration or leakage for 15 minutes. Other designs which require special considerations are butt-joint seals between firewall diaphragms, cowl doors and where a cowl door is part of the firewall, seals between the doors, and drain/vent masts interfacing with the doors. Special fire tests of these "kiss" seals will be necessary to ensure the capability of the overall firewall.

Par 7

9

AC 20-135

2/6/90

**NOTE:** When dedicated protection devices or specific procedures or techniques are required to provide fire protection for an installation, development of periodic maintenance or requirements for inspection of these devices or techniques is required so that continued airworthiness is assured.

(2) For engine cowling and nacelles of small airplanes and helicopters, the fire resistant requirements of § 23.1193(c) and § 27.1193(d) have been interpreted to allow use of any material shown to be equivalent to aluminum alloy. Cowlings are subject to airflow over one or both sides, which greatly improves the fire resistant capability of the aluminum and has been found to be acceptable. For example, a .04-inch aluminum panel with an 80 Kt minimum scrubbing airflow over the backside has been shown to maintain its integrity when subjected to a 2000°F flame for 15 minutes.

**a. Special Test Consideration.** In tests, particularly where testing is conducted using a burner other than one specified in Powerplant Engineering Report No. 3A, anomalies may be encountered due to torch blast effects and local hot spots created due to nonuniform heating of the specimens. These anomalies may be overcome with carefully designed burner tube extensions which spread the flame over a larger surface, as described in the report. An example of a fire test setup is shown in Figure 1.

10

Par 7

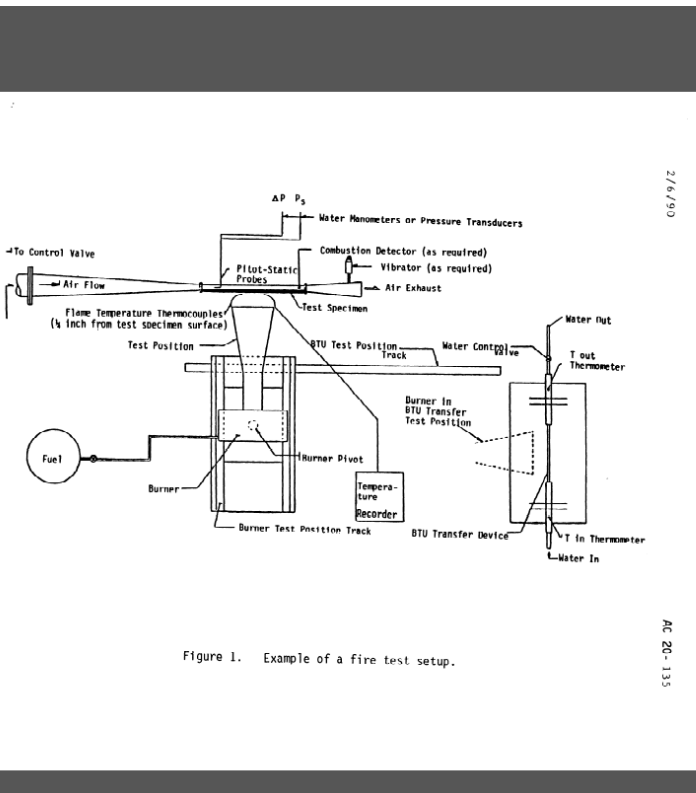


Figure 1. Example of a fire test setup.

2/6/90

AC 20-135

AC 20-135

2/6/90

This setup is intended to illustrate the necessary equipment for fire testing. For some tests, the requirement may be less; however, for all testing, the applicant should coordinate the test requirements with the FAA office responsible for the project, submit a detailed calibration and test plan, and verify that all of the needed testing conditions have been covered for the installation to be evaluated.

**NOTE:** The test hardware design should ensure that test hardware sagging or warping does not alter the burner-to-specimen distance resulting in temperature and heat flux density going outside the defined levels. Also the test rig design should preclude significant deposit of specimen debris on the burner.

**8. ENGINE CASE BURNTHROUGH CRITERIA [§ 23.903 (b)(1) and 25.903(d)(1)].** The above discussion on fireproof materials and the test methods and criteria are not appropriate for demonstrating the requirement for minimizing the hazard from engine case burnthrough situations.

**a.** If the installation design provides a burnthrough barrier for deflecting an engine combustion chamber burnthrough and a fire detector installation to provide quick detection of the event, an evaluation is necessary to show that proposed protection is adequate. Although combustion chamber design has continually improved, service experience has shown that turbine engine case burnthroughs have and continue to occur. Burnthroughs have also been caused by other types of failures such as, for example, fuel nozzle malfunctions, turbine vane burnout, and combustion chamber cracking.

**b.** Normally the area of concern is the projection between the forward and aft combustion flange of the engine case, including a 15° cone from the engine flange. This is the section of the engine where the hot, high pressure gas stream from a burnthrough may emerge in the direction of the pylon. A specific engine configuration may be shown to have more or less engine length where burnthrough should be considered. The temperatures (approximately 3000 - 3500°F) and gas pressures (approximately 350 - 550 psi) are considerably higher than the criteria and melting point of the materials used in firewall construction; therefore, conventional firewalls will generally fail in a very localized area and can expose the pylon, fuselage, or wing to a hazardous situation which could go undetected for a considerable length of time. Experience and tests have shown that for a radial distance of approximately 10 burnthrough hole diameters from the engine case surface or burnthrough "hole," the temperatures and pressures do not significantly decay. However, effects of discrete installation considerations (such as fan or full fan ducted airflow) should be individually addressed with respect to the "applied" characteristics of the burnthrough gas stream.

**c.** The test setup and torch configuration required to verify burnthrough protection is a torch with a nominal 1-inch diameter orifice or nozzle, having a torch pressure approximately the same as the maximum

12

Par 7



2/6/90

AC 20-135

burner pressure of the installed engine. The test article (burnthrough barrier) should be located at the same distance and supported similar to the proposed installation. The engine burnthrough criterion requires that under these operating conditions the barrier will maintain its integrity for a minimum of 3 minutes when exposed to a minimum flame temperature of 3000°F.

d. The proposed certification test plan, including the above operating environment, should be submitted to the FAA office responsible for the project for coordination and acceptance prior to conducting the fire testing.

Daniel P. Salvano  
 Acting Director, Aircraft  
 Certification Service

Par 8

13

2/6/90

AC 20-135  
Appendix 1

APPENDIX 1. RELATED FAR SECTIONS

The sections listed below identify requirements that will necessitate the use of the fire testing methods and standards outlined in this AC to show compliance with the applicable powerplant and APU regulations in FAR Parts 1, 23, 25, 27, 29 and 33.

FAR PART	SECTION
1	1.1
23	23.859, 23.863, 23.903, 23.1013, 23.1091, 23.1121, 23.1123, 23.1141, 23.1182, 23.1183, 23.1189, 23.1191, 23.1192, and 23.1193.
25	25.859, 25.863, 25.867, 25.903, 25.1013, 25.1091, 25.1103, 25.1121, 25.1123, 25.1165, 25.1181, 25.1182, 25.1183, 25.1189, 25.1191, 25.1192, 25.1193, 25.1201, 25.1203, and 25.1207.
27	27.859, 27.863, 27.903, 27.1123, 27.1183, 27.1185, 27.1189, 27.1191, 27.1193, 27.1194, and 27.1195.
29	29.859, 29.863, 29.903, 29.1025, 29.1103, 29.1121, 29.1123, 29.1165, 29.1182, 29.1189, 29.1191, 29.1193, 29.1194, 29.1201, and 29.1203.
33	33.17, 33.71.

1 (and 2)

**Project:** Mitigating risks of fire, smoke and fumes  
**Reference ID:** FSS\_P7\_ADS\_D7.9  
**Classification:** Public



### 8.1.3. Annex III: ISO 2685



ISO2685.pdf